R. & M. No. 3618

MINISTRY OF AVIATION SUPPLY

AERONAUTICAL RESEARCH COUNCIL
REPORTS AND MEMORANDA

A New Series of Low-Drag Aerofoils

By T. R. F. NONWEILER, B.Sc., Ph.D.
University of Glasgow

LONDON: HER MAJESTY'S STATIONERY OFFICE
1971
PRICE £2 14*s* 0*d* [£2·70] NET

A New Series of Low-Drag Aerofoils

By T. R. F. NONWEILER, B.Sc., Ph.D.

University of Glasgow

Reports and Memoranda No. 3618*
March, 1968

Summary.

A series of low drag aerofoils, modelled roughly on the NACA 6-series, is described. It appears to offer theoretical advantages over its progenitor, and allows flexibility in the choice of leading-edge thickness and trailing-edge angle. Aerofoils of this series are specified by five parameters, and the aerodynamic and geometrical characteristics of about 1000 of the sections are listed. The mathematical derivation of their shape (by the Lighthill method) is described in detail, and an ALGOL 60 procedure for the computation of their ordinates is included; care has been taken to construct this procedure so that it may be of general use in other applications of the Lighthill method of design.

LIST OF CONTENTS

*Replaces A.R.C. 30 528.

LIST OF APPENDICES

LIST OF ILLUSTRATIONS

1. *Introduction.*

As part of an investigation into the possibilities of designing aerofoils which combine high lift and relatively low drag, the Lighthill method of design[1] has been applied to the derivation of a family of wing sections patterned, generally speaking, on the specification of the well known and well tried NACA 'low-drag' 6-series of aerofoils. That is to say, they have been designed to have uniform velocity over some prescribed forward portion of the chord, either on the lower surface, or else the upper surface, at the two relevant extremes of the 'low-drag' incidence range. This involves use of the concept of 'design at incidence' which was well expounded by Glauert[2].

The original NACA series was derived by an approximate process which does not really bear extrapolation to high camber or thickness, so that the use of an exact method could reasonably be expected to show some improvement in design. Moreover, we have tried to provide a flexibility in design criteria so as to eliminate, if it is felt necessary, regions of reflex curvature and the cusped trailing edge typical of the NACA sections, which can sometimes cause structural complication or conflict with control surface requirements. Further, some degree of selection is provided in the choice of leading edge radius of curvature, as this may be important in relation to the development of high lift.

All that one can assert about the results of such an exercise at this juncture is a satisfaction in the general appearance of the aerofoils so calculated. One single member of the family, of 20 per cent thickness/chord ratio and 7 per cent camber, has been fully tunnel tested, and the results are reported elsewhere[4]; but it is worth noting that at the low Reynolds Number of the tests (0·5 million) a well defined low drag 'bucket' is obtained in its lift-drag polar from $C_L = 0{\cdot}3$ to 1·8 (as compared with a 'theoretical' range of 0·9 to 1·9).

Certainly, a positive result of the study has been an accumulation of data on the inter-dependence of geometric features of the aerofoils on their theoretical aerodynamic characteristics, and these data are discussed below and may prove of interest. The associated calculations are very extensive, and have only been made possible by programming the Lighthill method for digital computer, and some care has been taken to retain a general applicability in the numerical methods, since the computer programme—included here as a procedure written in ALGOL 60—could well be of use in other connections. It has also been judged that its inclusion is the only suitable way of communicating the tabulation of ordinates of aerofoils of the family under discussion, although a fairly comprehensive list of their aerodynamic and geometric features will be found appended to this Report.

2. *Computational Procedure.*

The Lighthill method of design consists of several distinct phases. Firstly, there is the subtle and all-important task of defining the required velocity distribution. In the referenced reports, it is proposed that this may be achieved by stipulating a series of piecewise continuous functions which are added together to provide an expression for lnq_0, where q_0 is the surface velocity at zero lift. The velocity at any other incidence (q_α, say) can subsequently be generated from the relation

$$\frac{q_\alpha}{q_0} = \cos\left(\frac{\theta}{2}-\alpha\right)/\cos\frac{\theta}{2} \tag{1}$$

where α is the incidence relative to the zero lift attitude, and θ is the angular co-ordinate of the point on the unit circle onto which the aerofoil is mapped by conformal transformation.

For the purposes of digital computation, it might be just as convenient to stipulate this velocity distribution in numerical, rather than algebraic, terms. We found no particular advantage in this. Since we were generating a systematic series of velocity distributions, algebraic relations had in any case to be invoked to display the effect of the various parameters of the series.

In prescribing the velocity distribution, it must be ensured that certain geometrical conditions are met: for example, the aerofoil must be a closed contour, which is ensured by making two definite integrals (both involving lnq_0) equate to zero. These conditions again could be computed exclusively in numerical terms—the closure condition being expressed, for instance, by numerical quadrature,—but it happened that the algebraic expression of these conditions presented no special difficulties, and evaluation of the resulting expressions was speedier and more accurate.

Likewise the next step of the process, involving the calculation of the surface slope (χ), which is the complex conjugate of lnq_0 (expressed as a function of θ), can be achieved by using Poisson's integral, and here again numerical quadrature could be used, although we preferred a scheme relying on the computation of algebraic expressions for the various definite integrals involved.

Up to this stage the computation is essentially dependent on the particular aerofoil being designed. Consequently, in the context of an ALGOL programme, it is convenient to regard the values of lnq_0 and χ for any value of θ as being generated by a separate procedure (which in the example given in Appendix IV is given the identifier *dwbydz*). The procedure is called by the main procedure (given the identifier *RM2112*), which latter has, as its primary purpose, the evaluation of the aerofoil contour corresponding to the defined velocity distribution. In other words, in other applications we envisage that the procedure *dwbydz* would be a subroutine used by *RM2112*, to be supplied by the user. Details of the specification and purpose of this procedure *dwbydz* are given by comments in the example of Appendix IV, and the mathematical details of the calculation of lnq_0 and χ for the series of aerofoils to be studied here, are given in Appendix I.

The parent procedure *RM2112* performs tasks which are common and necessary probably to every application of the Lighthill method: and these are more laborious than subtle. The aerofoil shape is derived by numerical quadrature using an adaptive scheme which adjusts the integration accuracy to accord with a prescribed error tolerance (or the storage capacity available for the results). The expression of the shape by ordinates and abscissae relative to the chord line requires a change of axes: the procedure given here allows the possibility either of prescribing the chordwise positions at which these abscissae are to be calculated, or of accepting values corresponding to generally integer values of θ (in degrees) which happen to be found convenient to the computation. Certain aerodynamic properties (such as the aerodynamic-centre position) are evaluated as well as geometric features (such as the thickness and camber). Full details are again given in comments to the procedure in Appendix IV, and the main formulae used are discussed in Appendix II.

The procedures as reproduced here have been used to determine the hundreds of results referred to in the later sections of this Report, and can be regarded as extensively tested. Nonetheless, the root finding techniques used in interpolation could still give trouble in unusual contexts (e.g. the design of suction aerofoils); the comprehensive failure index should, however, help to locate the origin of such troubles.

3. *Specification of the Aerofoil Series.*

We prefer here to specify each member of the family of aerofoils derived by the computation (described above) in terms of parameters of its velocity distribution, rather than (as for the NACA series) by its geometric characteristics. In principle, there would be no difficulty about the latter representation, as an iterative scheme could be envisaged in which the quoted parameters were methodically varied to provide a prescribed set of geometric characteristics. In fact, however, this would add considerably to the computational time, without contributing much to the present purpose, which is to explore precisely this very relationship between the aerodynamic and the geometric properties.

For conciseness, we specify particular aerofoils of the series by the letters GU, followed by a five digit identifier of the particular aerofoil, as follows:

$$GU \quad \mathbf{ab-cde}$$

where **a**, **b**, **c**, **d** and **e** are digits specifying 5 parameters. (We allow the possibility that, where any parameter cannot be correctly represented by a digit, it can be replaced by a bracketed number). The significance of each digit is described below.

'**a**' A measure of the extent of modification of the velocity peak at the leading edge, adopted in order to achieve a larger nose radius of curvature. A zero value denotes no modification, and is valid only for symmetric sections: a value of 2 is a 'normal' figure; values much higher than 4 tend to produce a shape having a flat nose with two 'sharp' shoulders, and are not to be recommended. (This parameter is the value G of Appendix I).

'**b**' A measure of the extent of modification of the velocity distribution at the trailing edge, adopted order to achieve a finite trailing edge angle and reduce regions of reflex curvature. The section will have the same difference in surface slopes (between top and bottom surfaces) at roughly **b** per cent of the chord forward of the trailing edge as at that edge. This produces a more or less wedge shaped trailing edge extending in practise over considerably more than the last **b** per cent of the chord. (In the notation of Appendix I, $\cos \mu = 1{\cdot}0 - 0{\cdot}02\mathbf{b}$).

'**c**' A measure of the extent of the favourable pressure gradient, within the design range of incidence, roughly equal to the fraction of the chord from the leading edge in tenths. (In the notation of Appendix I, $\cos \beta = 0{\cdot}2\mathbf{c} - 1{\cdot}0$).

'**d**' The 'design' incidence in degrees, relative to the zero lift line, this being the middle of the 'low drag' range. (In the notation of Appendix I, $\sigma^{\circ} = 2\mathbf{d}$).

'**e**' The design range of incidence, which therefore extends from $(\mathbf{d} - \frac{1}{2}\mathbf{e})$ to $(\mathbf{d} + \frac{1}{2}\mathbf{e})$ degrees. (In Appendix I, $\alpha_0^{\circ} = 0{\cdot}5\mathbf{e}$).

For thin aerofoils, because the lift curve slope is about 0·11 per degree, the values of **d** and **e** could be interpreted roughly as the design C_L, and the low drag range of C_L, in tenths.

4. *Discussion of Results.*

4.1. *Accuracy and Storage Requirements.*

The accuracy of the numerical evaluations of procedure *RM2112* is determined by the parameter *eps*. Once the calculation is effected, a more realistic estimate of the error in the derived aerofoil shape is obtained by examining the disparity in the closure condition—that is, the difference in the co-ordinates of $\theta = 0$ (the top surface trailing edge) and $\theta = 360°$ (the bottom surface trailing edge), which should of course coincide if the numerical integration process of the procedure could be exact.

It is found that this error (as a fraction of the chord) is given very roughly by $0{\cdot}2\,(eps)^{4/3}$, although individual results are known in which the actual error in the closure condition is up to 5 times larger (or smaller) than this mean figure. In practice, it would seem very unlikely that values smaller than $eps = 10^{-4}$ could ever be justified by constructional accuracy, as this represents generally a closure accuracy better than 1 part in a million.

The computing run time and storage requirements are both roughly proportional to the value of $(eps)^{-1/3}$. The size of the arrays used for storing the results (*x*, *y*, *theta*, *ki* and *qs*) should exceed $10(eps)^{-1/3}$. Thus, with $eps = 10^{-4}$, a size of, say, 224 would be adequate and the total storage requirement, including the local working data space of the procedure, would not exceed about 1,600 words, which is a very modest requirement.

For the computation of the data listed in Tables 1 and 2, it was judged adequate to take $eps = 10^{-2}$. In a few cases it was necessary to reduce *eps* to 10^{-3} in order to discriminate the leading edge (and so avoid the aborted failure exit, coded 100—*see* Appendix IV). The quoted results have a possible 'rounding' error in the least significant figure quoted (with the exception of the quoted relative thickness at 5 per cent chord, which is correct within $\pm 0{\cdot}5$ per cent).

4.2. *Features of Symmetric Sections.*

Uncambered aerofoils of the *GU* series are typified by identifiers of the type *GU* **ab**$-$**c0e**, and their features are listed in the first part of Appendix III. The effect of variation of '**b**' is very local to the trailing-edge region, so that to all intents and purposes the trailing-edge angle can be adjusted at will, by suitable choice of '**b**', without significant effect upon any of the other features. With a far forward maximum thickness, the trailing-edge angle varies roughly in proportion to $\mathbf{b}^{1/2}$, while with the maximum thickness far back the variation is closer to $\mathbf{b}^{1/3}$. These points are exemplified by the following data extracted from Appendix III:

Aerofoil	t_5/t_{max}	δ_{te}	x_{fav}/c	t_{max}/c	x_t/c	$dC_L/d\alpha$	C_{L_2}	x_{ac}/c	Δ_{te}
GU 21–304	0·46	5·2°	0·28	10·5%	0·30	0·118 /°	0·24	0·26	0·61
GU 23–304	0·47	10·4°	0·28	10·6%	0·31	0·118 /°	0·24	0·26	0·98
GU 25–304	0·47	10·4°	0·28	10·7%	0·31	0·118/°	0·24	0·26	1·17
GU 21–704	0·37	14·2°	0·67	13·8%	0·48	0·121/°	0·24	0·28	0·94
GU 23–704	0·36	21·0°	0·68	14·0%	0·48	0·121/°	0·24	0·28	1·35
GU 25–704	0·36	23·5°	0·68	14·2%	0·49	0·122/°	0·24	0·28	1·48

Also included in the above Table is the quantity

$$\Delta_{te} = (c - x_t)\, \delta_{te}/t_{max}$$

which provides a ready impression of the general proportions of the trailing edge. For a wedge shaped section (between maximum thickness and trailing edge) the value of Δ_{te} would be 0·5, and for a biconvex section it would be 1·0.

As is expected, neither the lift curve slope nor the distance of the aerodynamic centre from the leading edge is grossly affected by any parameter, though both quantities tend to increase with increasing thickness, and the aerodynamic centre also tends to move aft as the maximum-thickness position is moved back. The only parameter which has a significant effect upon the low drag range is '**e**', and likewise virtually the only effect upon the extent of favourable pressure gradient—which is very closely correlated with maximum-thickness position—is due to a variation in the parameter '**c**'.

Increase in either of the parameters '**c**' or '**e**', which can therefore be regarded as 'improving' the aerodynamic performance, is only obtained at the expense of increased section thickness, and further the rearward positions of maximum thickness associated with large '**c**' cause a relative sharpening of leading-edge curvature. This latter effect can be controlled to some extent by an increase in the parameter '**a**', but this also causes an increase in thickness—the leading-edge modification being far less localised in its effects upon aerofoil geometry than the trailing-edge modification. The effects of the parameters '**a**', '**c**' and '**e**' upon the leading edge and maximum thickness are graphically illustrated by Figures 2 and 3, and summarised in Figure 4.

This complicated interdependence of the shape parameters and the aerodynamic performance criteria can be exemplified in a number of different ways. For example, t_{max}/c and t_5/c can be kept the same and the extent of the low drag range traded off against the extent of the favourable pressure gradient, as is roughly indicated by the following comparison (extracted from Appendix III):

Aerofoil	t_5/t_{max}	δ_{te}	x_{fav}/c	t_{max}/c	x_t/c	$dC_L/d\alpha$	C_{L_2}	x_{ac}/c
GU 03–308	0·44	12·5°	0·28	15·7%	0·31	0·122/°	0·49	0·27
GU 23–406	0·43	13·5°	0·37	15·5%	0·36	0·122/°	0·37	0·27
GU 41–604	0·43	11·9°	0·57	15·4%	0·43	0·122/°	0·24	0·27

The extent of the favourable pressure gradient is doubled, but it only remains favourable over half the range of C_L. Conversely, an increase of thickness can either be used to increase the extent of the favourable gradient over the same incidence range, as here:

Aerofoil	t_5/t_{max}	δ_{te}	x_{fav}/c	t_{max}/c	x_t/c	$dC_L/d\alpha$	C_{L_2}	x_{ac}/c
GU 25–304	0·47	10·4°	0·29	10·7%	0·31	0·118/°	0·24	0·26
GU 61–704	0·47	20·0°	0·66	20·6%	0·45	0·128/°	0·26	0·28

or to increase the incidence range over which a given extent of the chord has a favourable gradient, as here:

Aerofoil	t_5/t_{max}	δ_{te}	x_{fav}/c	t_{max}/c	x_t/c	$dC_L/d\alpha$	C_{L_2}	x_{ac}/c
GU 45–402	0·44	8·5°	0·39	8·1%	0·36	0·116/°	0·12	0·26
GU 25–408	0·44	19·4°	0·37	19·1%	0·36	0·125/°	0·50	0·28

In either example we see that the variation in x_{fav} or in C_{L_2} with t_{max} is more rapid than a simple linear proportion.

Similarly, a reduction in leading-edge radius of curvative (and consequently, in the value of t_5/t_{max}) with the same maximum thickness, can likewise be used to increase the extent of favourable gradient, as here:

Aerofoil	t_5/t_{max}	δ_{te}	x_{fav}/c	t_{max}/c	x_t/c	$dC_L/d\alpha$	C_{L_2}	x_{ac}/c
GU 45–306	0·53	16·3°	0·27	17·5%	0·30	0·125/°	0·37	0·27
GU 01–706	0·35	17·6°	0·67	17·3%	0·48	0·124/°	0·37	0·28

in which example it would of course be more natural to regard the thinner leading edge as the consequence, rather than the cause, of the rearward movement of maximum thickness; or equally well, it can be used to increase the low drag range with the same extent of favourable gradient, as here:

Aerofoil	t_5/t_{max}	δ_{te}	x_{fav}/c	t_{max}/c	x_t/c	$dC_L/d\alpha$	C_{L_2}	x_{ac}/c
GU 65–504	0·51	21·9°	0·46	19·0%	0·39	0·126/°	0·25	0·27
GU 05–508	0·38	21·9°	0·47	19·2%	0·41	0·125/°	0·50	0·28

To place these figures for (t_5/t_{max}) in their perspective, it can be recalled that 'conservative' wing sections (like, for example, the NACA four-figure series) have values of about 0·60, whereas values of 0·45 or 0·4 are generally associated with low-drag wing sections, and the last quoted example amply illustrates the reason for this. On the other hand, of course, it is generally accepted that the value of t_5/c should be reasonably large (about equal to 0·1) if high sectional maximum lift coefficients (with or without trailing-edge flaps) are to be achieved, but clearly the price paid for this feature is severe.

4.3. *Features of Cambered Sections.*

The effect of the introduction of camber (i.e. $\mathbf{d} \neq 0$) is easy to describe, since it leaves the properties (t_5/c), δ_{te}, (x_t/c), $dC_L/d\alpha$ and (x_{ac}/c) virtually unaltered, and causes only a very slight reduction in (t_{max}/c). Further (x_{fav}/c) is more or less the same—except that the favourable pressure gradient is slightly more extensive on the top surface than the bottom—and the range of C_L over which the favourable pressure gradient exists is also almost the same as without camber.

The dominant effect is of course to increase the design incidence above zero lift by an angle prescribed by the value of '**d**' (in the identifier *GU* **ab**−**cde**), and since the lift-curve slope increases with aerofoil thickness, the corresponding design lift coefficient tends to be rather higher for the thicker aerofoils. A good fit to the values of lift-curve slope is given by

$$dC_L/d\alpha = 2\pi\,[1+0{\cdot}85\,(t_{\max}/c)] \text{ per radian}$$

for the complete range of aerofoils listed in Appendix III.

This however is only one of many influences of the thickness distribution on the effects of camber. These are made all the more apparent by our knowledge of the simple 'first order' effects from thin aerofoil theory, since the camber line adopted is known to have a load distribution which (in this linearised approximation) is uniform over that proportion of the chord where the pressure gradient is favourable (i.e. over a fraction of the chord equal to 0·1 times the parameter **c**), thereafter dropping to zero at the trailing edge linearly with chordwise distance.

Thus, although the design lift coefficient (C_{Li}, say) increases with $(t_{\max}/c)$ for a given design incidence, the maximum geometric camber is in fact reduced. This is exemplified by the following Table. where the characteristics of the cambered arc aerofoil *GU* **a**0—580 are calculated from thin aerofoil theory, although they could be approached by the exact method as a limiting condition.

Aerofoil	$(t_{\max}/c)$	(t_5/c)	C_{Li}	Camber / Chord	Position of max camber	C_{M_0}
GU **a**0–580	0	0	0·88	6·3%	36%	−0·139
GU 23–582	6·9%	2·9%	0·92	6·1%	47%	−0·110
GU 23–588	20·1%	8·4%	1·01	5·1%	47%	−0·092
GU 63–584	18·2%	9·1%	1·00	4·6%	47%	−0·087
GU 63–588	34·0%	17·5%	1·11	1·9%	49%	−0·053

Along with the reduction of camber there is an associated reduction in $(-C_{M_0})$. This latter correlates well with thickness (fig. 5) but still better with the measure (t_5/c) of leading-edge thickness (fig. 6), and presented on the same basis, the values of centreline camber appear to show a consistent reduction as (t_5/c) is increased (fig. 7). This is rather more marked for aerofoils with their maximum thickness well forward than for those with an extensive region of favourable pressure gradient (and therefore of uniform camber loading). This can be seen from the following comparisons:

Aerofoil	$(t_{\max}/c)$	(t_5/c)	C_{Li}	Camber / chord	Position of max camber	C_{M_0}
GU **a**0–380	0	0	0·88	6·1%	29%	−0·093
GU 23–382	6·0%	2·9%	0·92	5·7%	35%	−0·081
GU 23–388	16·7%	8·1%	0·98	4·6%	34%	−0·062
GU 63–384	15·6%	8·7%	0·99	4·0%	36%	−0·057
GU 63–388	28·5%	16·2%	1·07	0·9%	43%	−0·024
GU **a**0–780	0	0	0·88	6·2%	42%	−0·157
GU 23–782	7·7%	3·0%	0·93	5·8%	51%	−0·148
GU 23–788	23·0%	8·6%	1·04	4·9%	55%	−0·134
GU 63–784	20·4%	9·4%	1·02	4·5%	59%	−0·130
GU 63–788	39·3%	19·0%	1·17	2·6%	67%	−0·097

The explanation of this reduction in camber (and consequently in C_{M_0}) would appear to be that, as the aerofoil thickness is increased, so the change of load distribution due to change of incidence becomes less peaked close to the leading edge, and indeed more like that required for the camber line—particularly if the latter has a load line with only a short region of uniform loading. Indeed, for very thick aerofoils, the incremental load distribution due to (small) incidence will tend to resemble that on a circular cylinder (with fixed rear stagnation at $\theta = 0$, say), and this is proportional to $(1-\cos\theta)$. In terms of the same polar co-ordinate θ of the circle onto which the aerofoil is mapped, we demand a distribution which is uniform for some range of $\theta > \beta$, say, but which varies as $(1-\cos\theta)$ for smaller values of θ. The thicker therefore the wing, the greater the proportion of the load distribution that can be accommodated by incidence and the less the camber required. What makes this seem paradoxical perhaps is that one speaks of camber as providing a load distribution, whereas in a truer sense camber merely redistributes the loading due to incidence to conform to that required (at some prescribed C_L).

There is also a noticeable change in shape of the camber line as the thickness increases. As will be seen from the Tables before, the position of the maximum camber moves back, particularly for the load line with a greater extent of uniformity (the *GU* **ab**-7 **de** series). This effect is noticeable even for relatively thin aerofoils—with (t_{max}/c) equal to only 6 or 7 per cent—and it is not sensitive to the amount of camber. A less obvious effect upon the shape of the camber line is the appearance of a reflex curvature and a region of negative camber very close to the leading edge if the parameters '**a**' and '**e**' are large. The effect is only evident from the data Appendix III where this negative camber exceeds the positive; this happens for aerofoils of the *GU* **6b**$-$**cde** series if the 'thickness' parameter '**e**' exceeds the 'camber' parameter '**d**': for example, for the *GU* 63–526, where this negative camber is 1·6 per cent at 0·024 chord from the leading edge, and the positive camber aft is only 0·8 per cent. Strangely, as the positive camber decreases, the negative camber increases, though becoming less extensive.

The effect is due to the definition of what is meant by camber, and to the detailed shape of the leading edge of these thick-nosed sections.

We define the chord line of a section as that straight line through the trailing edge which intersects the aerofoil profile orthogonally. (This accords of course with the accepted convention.) It is also therefore a line of maximum or minimum length and of course the former alternative is intended; however, it may not in fact be the one chosen. For a symmetrical section the chord line is unambiguously the axis of symmetry, and the profile must (by definition) intersect it at right angles. If, for example, the thickness distributions were triangular, with the vertex aft as the trailing edge (Fig. 8a), then by symmetry the line through the vertex bisecting the base (at the leading edge) would be the chord line, although it is a line locally minimum in length (the sides of the triangle being longer). If an infinitesimal camber is added to this section, by which we mean that an infinitesimal assymmetry is produced in the velocity distribution, the actual shape of the profile would not be changed (except by an infinitesimal amount), but the argument of symmetry being lacking, the side of the triangle could now be selected as the chord line (Fig. 8b) if a line of maximum length is looked for. Now the mean line (or centreline) is defined as the locus of points bisecting the ordinates described within the section at right angles to the chord line, and the geometrical (centreline) camber as the maximum ordinate of the mean line (irrespective of sign). Quite clearly in the example of Fig. 8b, the mean line would be the line bisecting the vertex (except near leading edge) and consequently a finite (negative) centreline camber would be ascribed to the section, although the design lift coefficient would be infinitesimal.

Perhaps this only shows the inadequacy of our definitions—although they are the accepted ones. It is to be noted that they do not conform to NACA practice used in formulating their 6-series of sections, where a mean line is postulated *ab initio*, and a chord line is formed by joining its extremities: a thickness distribution is then added by offsets at right angles to this line. This does not guarantee that the end of the chord line is the 'leading edge' as we have defined it.

Although far from triangular, the aerofoils of the *GU* **6b**$-$**cde** series do tend to be flat nosed, with sharply curving corners (*see* for example fig. 17) and the position of the 'leading edge' is very sensitive to camber; there seems no doubt that the effect illustrated by Fig. 8 is an exaggerated, but correct, explanation of their negative camber. As further corroboration we note that the section of Fig. 8b has a positive zero left angle (equal to the semi-vertex angle), and it will be found from Appendix III that increase of the parameter '**a**' produces the very same effect. Thus the *GU* 63–526 develops zero lift at 0·2° incidence, though the *GU* 23–526 has a zero lift incidence of −1·1°.

Clearly all the evidence shows how dangerous it is to treat either the camber load distribution, or the geometric camber line, as linearly superimposed upon the symmetric load or thickness distributions at corresponding abscissae. True, the non linear geometric effects are, in a sense, purely illusory; but there can be no denial of the reality of the aerodynamic non linearities, as evinced for example by the zero lift pitching moment. But the non linearities are mainly connected with the mutual interference of the symmetric and assymmetric terms. The camber effects are linear in the sense that (to the accuracy of the tabulations) properties such as the maximum (positive) geometric camber, and the zero-lift pitching moment, are virtually directly proportional to the value of the parameter **d** (or to the design lift coefficient) if this alone is varied, as for instance in the following set of characteristics for a thick aerofoil:

Aerofoil	t_{max}/c	C_{Li}	$\frac{\text{Camber}}{\text{chord}}$	Position of max. camber	C_{M_0}	α_z	$\frac{x_{ac}}{c}$	$\frac{y_{ac}}{c}$
GU 25–408	19·1%	0	0	—	0	0	27·5%	0
GU 25–408	19·1%	0·25	1·2%	42%	−0·019	−0·9°	27·5%	0·4%
GU 25–448	19·0%	0·50	2·4%	40%	−0·038	−1·9°	27·5%	0·9%
GU 25–468	18·9%	0·75	3·6%	43%	−0·057	−2·9°	27·5%	1·5%
GU 25–488	18·7%	1·00	5·0%	40%	−0·076	−3·9°	27·8%	1·2%

Here α_z is the zero lift incidence. The value of (t_5/c) remains constant for all these sections (and equal to 8·3 per cent), the position of maximum thickness stays at 36 per cent c and the ratio of trailing-edge angle to the thickness/chord ratio is the same in each case.

4.4. *Appearance and Velocity Distributions.*

To illustrates the general appearance of aerofoils of this family, and to bring out pictorially some of the points made in the preceding discussion, a number of the aerofoils mentioned are shown in the appended figures, along with their velocity distributions at one or two incidences.

The first series (Figs. 9 to 14) illustrate some of the comparative pairs of symmetric aerofoils referred to in Section 4.2, and the velocity distributions illustrated are those at the upper limit of design incidence, where the upper surface has a region of constant velocity. In the figures 15 to 20 illustrating some of the cambered sections we have referred to above, the velocity distributions at both extremes of the low drag range are shown. It will be observed that in the condition of large camber and small thickness the velocity rise over the rear portion of the bottom surface due to the camber load distribution can negate the velocity drop at the termination of the designed region of favourable pressure gradient, especially at high C_L; as a result the actual extent of the region of favourable gradient can extend over practically the whole of the undersurface—literally the whole chord if the trailing edge is cusped. (This particular effect is ignored in the tabulations of Appendix III, where it is the designed extent of the region which is listed.) This effect manifests itself whether the reduction in thickness be due to reduction in the 'leading-edge' parameter '**a**' (Fig. 18) or in the design range of incidence (i.e. parameter '**e**' of the identifier *GU* **ab**−**cde**). It is enhanced by a forward movement of the position of maximum thickness, so that (aided by the decrease of thickness involved) it can be brought about by decrease in the parameter '**c**' (Fig. 19).

This effect is the primary reason for choosing the position of the break in the camber load distribution to coincide with the termination of the region of favourable pressure gradient. For if the former were taken further aft, then in this condition of high camber and small (but not zero) thickness, there would exist two successive regions of alternating favourable, then unfavourable, pressure gradient over the undersurface, which does not seem to be a satisfying arrangement. It would of course be nicely avoided by using a uniform load line, but this of course has no reality outside the realm of thin aerofoil theory.

It will be appreciated that no cambered aerofoils of this family exist with a zero parameter '**a**', as the change from top to bottom surface camber load distribution takes place over the region of the surface where the leading edge modification takes place (which has an extent proportional to the parameter '**a**'). If this had to take place discontinuously, there would be a singularity (in fact, a logarithmic spiral) in the surface contour at the leading edge, and the same would happen at the trailing edge if a uniform camber load distribution extended over the whole chord. One can go a long way towards the limit $\mathbf{a} = 0$, however, without distorting the section shape, as is shown in Fig. 21, which also illustrates another aerofoil with a long run of nearly flat undersurface—the *GU* 25–5(11)8 section, which has been the subject of tunnel tests[4].

4.5. *Comparison with the NACA 6-Series of Sections.*

Enough has been said about the cross-coupling of camber and thickness effects to make it clear that there is no basis of comparison available between the theoretical characteristics of the cambered sections of the NACA 6-series and *GU* aerofoils, since the former have mean lines derived from thin aerofoil theory, and there is no exact theoretical calculation readily available of their aerodynamic characteristics.

However a fairly refined method of calculation was adopted for the derivation of the thickness distribution[3], and of the resulting velocity distribution, of the NACA sections, which leads to an estimate of their low drag range of C_L. This is shown in Figure 22. Here we compare it with the low drag range of C_L for a particular family of symmetrical aerofoils of the *GU*-series, these having a cusped trailing edge and the same thickness/chord ratio, the same nominal extent of favourable pressure gradient, and the same 5 per cent chord ordinate as the corresponding NACA section. In all cases, it will be observed, the *GU* series has a larger low drag range (in theory, at least). This disparity grows with increase of thickness (though it is relatively largest for the thinnest aerofoils) and it also is particularly accentuated for the shorter extent of favourable pressure gradient (i.e. in the comparison of the 63-series with *GU* **a**0-30**e** sections).

The 63-series in fact seems the odd one out of the NACA sections, having a thinner leading edge than is consistent with the other members of the NACA family, and a further back position of maximum thickness. This latter usually accords roughly with the position of the maximum thickness of the corresponding members of the *GU* family, but whereas *GU* **a**0-30**e** aerofoils are indeed thickest at about 0·3 chord, the NACA 63-series have their maximum at 0·35 chord.

The NACA sections do not correspond to aerofoils of the *GU* family with a fixed value of the parameter '**a**'; matching on the basis of equal $(t_5/t_{\max})$, produces values of this parameter of between 4 and 5 in the lower range of (t/c)—say, between 6 and 9 per cent—and 2 and 3 at the higher end between 15 and 21 per cent thickness/chord ratio. However, the 63-series correspond to a choice of the parameter '**a**' between 2 and 3 over the complete range of thickness.

Most of the NACA modified A-series of sections (with a finite trailing-edge angle) appear to have a smaller low drag range, though there are exceptions in the middle range of (t/c) between 10 and 12 per cent. We have noted that the addition of a finite trailing-edge angle to the *GU*-series does not substantially alter their low drag range.

The NACA aerofoils have been exhaustively tested in tunnels and flight, and have an excellent record which it is far from our intention—or indeed ability—to disparage on purely theoretical grounds. Rather it is this which encourages us to hope that the added sophistication of the Lighthill design method may reveal like advantages in experiment as well as theory.

5. *Acknowledgments.*

Much of this work was accomplished in part fulfilment of the terms of a D.S.I.R. Contract. The author is greatly indebted to Mrs. B. MacLeod, B.Sc., for the very careful checking of the algebraic and numerical results performed at that time, and to Miss R. Cahill, B.Sc. for subsequent clerical assistance in programming.

LIST OF PRINCIPLE NOTATION

α		Incidence measured relative to zero lift line
α_0	=	$(\alpha_1 - \alpha_2)/2$, half design range of incidence
α_1, α_2		Upper and lower incidences of design range
α_z		Zero lift incidence measured relative to chord line
β		Parameter controlling chordwise extent of favourable pressure gradient
γ		Parameter controlling the leading-edge radius of curvature
δ_{te}		Trailing-edge angle
θ		Angular co-ordinate of the point on the unit circle onto which aerofoil is mapped
μ		Parameter controlling trailing-edge angle
σ	=	$\alpha_1 + \alpha_2$
ϕ		General angular co-ordinate
χ		Direction of surface velocity vector relative to $\theta = 0$
χ'	=	$\chi - \frac{1}{2}\theta$
χ_0	=	$\frac{1}{2}\pi - \alpha_z$, the value of χ satisfying equation (6) of Appendix II
A_n, B_n, C_n		Defined by equation (2) of Appendix I
B_{2n}		Bernoulli Numbers
C_L		Sectional lift coefficient
C_{L2}		C_L at upper limit of design range
C_{Li}		C_L at mid-incidence of design range
C_{Mo}		Sectional pitching-moment coefficient at zero lift
D_n, F_n, G_n		Defined by equation (1) of Appendix I
$E(x)$		Function defined by equation (10) of Appendix I
$F(x)$		Function defined by equation (11) of Appendix I
G	=	χ/α_0
$U(x)$		Function defined by equation (15) of Appendix I
$S(x)$	=	$U(\tan \alpha)$, defined by equation (17) of Appendix I
a_0, a_1, a_2; b_0, b_1, b_2; c_0, c_1, c_2	}	Functions defined in equations (4), (5) and (6) of Appendix I
c		Chord of any section
eps		Tolerance parameter of ALGOL procedure RM2112
f_0, f_1, f_2; g_0, g_1, g_2	}	Functions defined in equations (4), (5) and (6) of Appendix I
q_0		Surface speed at zero-lift incidence
q_0'	=	$q_0 \sec(\theta/2)$

q_α		Surface speed at incidence α
s		Distance measured round aerofoil in direction of increasing θ
t_5		Aerofoil thickness at $0{\cdot}05c$ from leading edge
$t_{\max}$		Maximum aerofoil thickness
x, y		Cartesian axes, origin at nose and x-axis along chordline
x_{ac}		Distance of aerodynamic centre from nose
x_{fav}		Extent of favourable pressure gradient on top surface
x_t		Distance of position of maximum thickness from nose
z	=	$x+iy$, complex co-ordinate
z_0		Complex co-ordinate transformed by equation (8) of Appendix II
$\bar{z}_0$		Complex co-ordinate of aerodynamic centre

REFERENCES

No.	*Author(s)*	*Title, etc.*
1	M. J. Lighthill	A new method of two-dimensional aerodynamic design. A.R.C. R. & M. 2112. April, 1945.
2	M. B. Glauert	The Application of the Exact Method of Aerofoil Deisgn. A.R.C. R. & M. 2683. October, 1947.
3	Ira H. Abbott and Albert E. von Doenhoff	*Theory of Wing Sections.* McGraw Hill Co. 1949.
4	F. Kelling	Experimental investigations of a high-lift low-drag aerofoil. A.R.C. 30 983 September, 1968.

APPENDIX I

Formulation of the Velocity Distribution.

We endeavour here to describe how we construct a formal expression for the complex velocity. This will be composed of a sum of terms, namely

$$\ln q_0 - i\chi = \sum_n D_n (F_n - iG_n), \text{ say,} \tag{1}$$

where D_n is a real constant, and F_n and G_n are functions of θ, such that $G_n(\theta)$ is the complex conjugate of $F_n(\theta)$. Further, we define

$$A_n = \int_{-\pi}^{\pi} F_n(\theta)d\theta, \quad B_n + iC_n = \int_{-\pi}^{\pi} F_n(\theta)e^{i\theta}\, d\theta \tag{2}$$

and we shall have to satisfy the conditions

$$\sum_n A_n = \sum_n B_n = \sum_n C_n = 0 \tag{3}$$

compatible with the boundary conditions and the closure of the contour representing the aerofoil.

We shall form the functions F and G from three basic functions, each of these being expressible as a function of a general angular variable ϕ, say, and a parameter. We suppose that $|\phi| < \pi$, but the analytic extension to other values may be performed in the usual way by supposing they are periodic functions, with period 2π. These basic functions and their conjugates and integrals will be here distinguished by lower-case symbols, and they are listed below.

$$\left.\begin{aligned} f_o(\phi, \beta) &= \tfrac{1}{2}\,\mathrm{sgn}(\phi)(\cos\phi - 1) - \tfrac{1}{2}\,\mathrm{sgn}(\phi - \beta)(\cos\phi - \cos\beta) + (1 - \cos\beta)(\phi/2\pi) \\ g_o(\phi, \beta) &= \tfrac{1}{\pi}(\cos\phi - 1)\ln|\sin\tfrac{1}{2}\phi| - \tfrac{1}{\pi}(\cos\phi - \cos\beta)\ln|\sin\tfrac{1}{2}(\phi - \beta)| + (\beta/2\pi)\sin\phi \\ a_o(\beta) &= \sin\beta - \beta\cos\beta \\ b_o(\beta) + ic_o(\beta) &= \tfrac{1}{2}\beta - \tfrac{1}{4}i\,[\exp(2i\beta) - 1] \end{aligned}\right\} \tag{4}$$

$$\left.\begin{aligned} f_1(\phi, \alpha) &= \ln|2\cos(\tfrac{1}{2}|\phi| - \alpha)| \\ g_1(\phi, \alpha) &= \tfrac{1}{2}\phi - F\,[\tan\alpha\tan(\phi/2)] \\ a_1(\alpha) &= 4\alpha\ln(\cot\alpha) + 2\pi\, U(\tan\alpha) \\ b_1(\alpha) + ic_1(\alpha) &= \pi\cos 2\alpha + 2\sin 2\alpha\ln|\tan\alpha| \end{aligned}\right\} \tag{5}$$

$$\left.\begin{aligned} f_2(\phi, \mu) &= \tfrac{1}{2}[\mathrm{sgn}(\mu + \phi) + \mathrm{sgn}(\mu - \phi)]\ln\left|\cot\frac{\mu}{2}\tan\frac{\phi}{2}\right| \\ \delta_2(\phi, \mu) &= -E\,[\tan(\mu/2)\cot(\phi/2)] \\ a_2(\mu) &= -2\pi\, U\,[\tan(\mu/2)] \\ b_2(\mu) + ic_2(\mu) &= -2\mu \end{aligned}\right\} \tag{6}$$

Before proceeding with the discussion of the use of these functions, a definition of the functions E, F and U is called for, together with some explanation of how they may be computed. They are in fact all related to one function of a complex variable, which in turn is related to the dilogarithm and certain other less familiar transcendental functions; however this is less material in the present context than a knowledge of their specific representations in terms of a real variable. The function $F(x)$ is discussed, and tabulated, by Glauert[2]. It is defined for $x > 0$ by

$$F(x) = -(2/\pi)\int_0^x [(ln t)/(1-t^2)]\, dt, \tag{7}$$

from which we may deduce that, for $x > 0$,

$$F(x)+F(1/x) = \pi/2 \tag{8}$$

and its analytic extension for $x < 0$ appropriate to equation (5) is given by supposing it an odd function of x (that is, replacing $ln\, t$ in the integrand of (7) by $ln|t|$) and so

$$F(x) = -F(-x), \tag{9}$$

For $|x| < 1$, we have, using (9),

$$E(x) = (2/\pi)\, ln\,|x|\, \text{argtanh}\,(x)+F(x) = (2/\pi)\int^x (1/t)\, \text{argtanh}\, t\, dt \tag{10}$$

and there is a series expansion, convergent for $|x| < 1$, given by

$$E(x) = (2/\pi) \sum_{n=0}^{\infty} x^{2n+1}/(2n+1)^2 \tag{11}$$

The appropriate analytic extension to $|x| > 1$, relevant to the context of the use of E in equation (6), is obtained by replacing the argtanh by argcoth in (10), and then, we can deduce, consistent with equations (8) and (9), that

$$\left.\begin{aligned} E(x)+E(1/x) &= (\pi/2)\, \text{sgn}\,(x) \\ E(x) &= -E(-x) \end{aligned}\right\} \tag{12}$$

The series expansion (11) is not sufficiently rapidly convergent for $|x|$ close to unity to be very suitable for numerical work. However, there also exists an expansion about $x = 1$, which is rather troublesome to derive (*see* Appendix IA); it converges for $|ln\, x| < 2\pi$, and is given by

$$E(x) = (\pi/4)+\{1+ln|2/ln\, x|+ \sum_{n=1}^{\infty} [(2^{2n-1}-1)\, B_{2n}/n\,(2n+1)!]\,(ln\, x)^{2n}\}\,(ln\, x)/\pi, \tag{13}$$

Again, another expansion valid for $|x| < 1$ which is rather more rapidly convergent for small x is given by substituting $t = \tanh\,(u/2)$ in the integrand of (10); thus

$$\pi E(x) = \sum_{n=0}^{\infty} [(2-2^{2n}) B_{2n}/(2n+1)\,!\,] (2 \operatorname{argtanh} x)^{2n+1} = \int_0^{2 \operatorname{argtanh} x} u \operatorname{cosech} u \, du . \tag{14}$$

In both (13) and (14), the B_{2n} are the Bernoulli numbers defined in the convention such that $B_0 = 1$ and

$$B_{2n} = (-1)^{n+1}\, 2\,(2n)\,! \sum_{r=1}^{\infty} [1/(2\pi r)^{2n}] \quad (n = 1, 2, \ldots .)$$

In our calculations, we have chosen to cover the interval $0 < x < 1$ by expansions (11) and (13), using (12) to obtain values of $E(x)$ outside this interval; the evaluation of F can then conveniently be made using equation (10). Finally, we note that

$$U(x) = (2/\pi) \int_0^x (1/t) \arctan t \, dt , \tag{15}$$

whence we see that $U(x) = E(ix)/i$, and corresponding to (11) we have the expansion convergent for all x, in the form

$$U(x) = (2/\pi) \sum_{n=0}^{\infty} [(-1)^n x^{2n+1}/(2n+1)^2] . \tag{16}$$

This is a rather slowly converging series, and the expansion corresponding to (14) is to be preferred, namely,

$$S(\alpha) = U\left(\tan \frac{\alpha}{2} \right) = \sum_{n=0}^{\infty} [(-1)^n (2-2^n) B_{2n}/(2n+1)\,!\,] \alpha^{2n+1}/\pi, \quad (|\alpha| < \pi) . \tag{17}$$

We do not have to calculate U for large values of its argument; however, it is not difficult to verify that

$$\left. \begin{aligned} U(x) - U(1/x) &= ln\, x \qquad , \text{for } x > 0 \\ S(\alpha) - S(\pi - \alpha) &= ln \left(\tan \frac{\alpha}{2} \right), \quad \text{for} \quad \pi > \alpha \geq 0 \end{aligned} \right\} \tag{18}$$

whilst clearly $U(x)$ and $S(x)$ are odd functions of x. Thus it is only necessary in numerical work to evaluate sufficient terms of (17) to provide the desired accuracy with $|\alpha| < \pi/2$.

Noting that all other terms of the equations (4), (5) and (6) involve only elementary functions, let us return to the use of the functions f_0, f_1 and f_2 in describing the required form of $ln\, q_0$. Each of these functions is continuous (though not their derivatives) in $|\phi| < \pi$, and moreover their values at $\phi = \pm\pi$ are equal, so that they are continuous periodic functions. The function f_1 in the combination

$$\begin{aligned} f_1(\theta, 0) - f_1\left(\theta - \alpha_1 - \alpha_2, \frac{\alpha_1 - \alpha_2}{2} \right) &= ln \left| \left(\cos \frac{\theta}{2} \right) \Big/ \cos \left(\frac{\theta}{2} - \alpha_1 \right) \right|, \quad \text{for } \alpha_1 + \alpha_2 < \theta < \pi + \alpha_1 + \alpha_2 \\ &= ln \left| \left(\cos \frac{\theta}{2} \right) \Big/ \cos \left(\frac{\theta}{2} - \alpha_2 \right) \right|, \quad \text{for } \alpha_1 + \alpha_2 - \pi < \theta \leq \alpha_1 + \alpha_2 \end{aligned} \tag{19}$$

can be recognised as the fundamental distribution of logarithmic velocity used in the Lighthill method of direct design at incidence, in which the 'upper' surface velocity is prescribed at an incidence α_1, and that of the 'lower' surface at incidence α_2.

The term f_2 is one form of relationship which permits the introduction of a trailing edge angle. Thus, $\tau f_2(\theta, \mu)$ has a conjugate $\chi = \tau g_2(\theta, \mu)$ which (by equation (12)) can be shown to involve a discontinuity $\tau\pi$ in χ at $\theta = 0$, the trailing edge.

The function f_0 is useful in various combinations: thus

$$\left.\begin{aligned} f_0(\theta, -\beta) - f_0(\theta, \beta) &= \operatorname{sgn}(\beta)(\cos\beta - \cos\theta), \text{ for } |\theta| \leqslant |\beta| \\ &= 0 \qquad \text{elsewhere} \end{aligned}\right\} \tag{20}$$

represents (as shown in Figure 1A) a reduction of velocity towards the trailing edge which for thin aerofoils is almost linear with chordwise distance, and has been frequently used in combination with the distribution (19) to produce a 'rooftop' velocity distribution. Again, the periodic function

$$f_0(\theta+\pi-\sigma+\gamma, \gamma)\operatorname{cosec}^2\frac{\gamma}{2} - \tfrac{1}{2}\left[f_0(\theta, \beta) + f_0(\theta, -\beta)\right]\operatorname{cosec}^2\frac{\beta}{2}$$

$$\begin{aligned} &= \quad 1+c & &\text{for } \beta < \theta < \pi+\sigma-\gamma \\ &= \quad 1+c-(\cos\theta-\cos\beta)/(1-\cos\beta) & &\text{for } 0 < \theta < \beta \\ &= -1+c+(\cos\theta-\cos\beta)/(1-\cos\beta) & &\text{for } -\beta < \theta < 0 \\ &= -1+c & &\text{for } -\pi+\sigma < \theta < -\beta \\ &= \quad 1+c-2\left[\cos(\theta-\sigma+\gamma)+1\right]/(1-\cos\gamma) & &\text{for } -\pi+\sigma-\gamma < \theta < -\pi+\sigma \end{aligned} \tag{21}$$

where $c = (\gamma-\sigma)/\pi$,

provides a continuous velocity distribution with a different constant velocity over a region of both upper and lower surfaces (Fig. 1B), corresponding to a camber with a (partly) uniform load line, in the terms of thin aerofoil theory. Finally, we note that the function

$$\left.\begin{aligned} f_0(\phi+\gamma, \gamma) - f_0(\phi-\gamma, -\gamma) &= \operatorname{syn}(\gamma)\left[\cos(|\phi|-|\gamma|)-1\right] + \gamma(1-\cos\gamma)/\pi, \text{ for } |\phi| < |\gamma| \\ &= \gamma(1-\cos\gamma)/\pi \quad \text{for } |\phi| > |\gamma| \end{aligned}\right\} \tag{22}$$

provides a decrement in velocity over a confined region of the aerofoil surface (Fig. 1C) with a discontinuous change in velocity gradient (at $\phi = 0$), and so can be used to eliminate the discontinuity in this gradient which otherwise exists close to the leading edge (due to the form of equation (19)), which in turn would produce a logarithmic singularity in leading-edge curvature.

Accordingly, we compose a distribution of logarithmic velocity in the following form:

$$\left.\begin{aligned} ln\, q_0' = ln\left(q_0/\cos\frac{\theta}{2}\right) \equiv \sum_{n=0}^{6} D_n F_n(\theta) = D_0 f_1(\theta-\sigma, \alpha_0) + D_1 f_0(\theta, \beta) + \\ + D_2 f_0(\theta, -\beta) + D_3 f_0(\theta+\pi-\sigma+\gamma, \gamma) + D_4 f_0(\theta+\pi-\sigma-\gamma, -\gamma) + \\ + D_5 f_2(\theta, \mu) + D_6 \end{aligned}\right\} \tag{23}$$

and the series of conjugates $G_n(\theta)$ will be the value of χ' (say) where

$$\chi' = \chi - \tfrac{1}{2}\theta \equiv \sum_{n=0}^{6} D_n G_n(\theta) = D_0 g_1(\theta-\sigma, \alpha_0) + D_1 g_0(\theta, \beta) \ldots \&\text{c.} \tag{24}$$

If we now place

$$\begin{aligned} D_0 &= -1 \\ D_1 + D_2 &= -[(\sin \tfrac{1}{2}\gamma)/(\sin \tfrac{1}{2}\beta)]^2 (D_3 + D_4) \end{aligned} \tag{25}$$

then we are left with 5 unknown coefficients D_n, describing a velocity distribution compounded of the three functions (20), (21) and (22), the 'trailing edge' term (6), and a constant scaling factor. The equations (3) provide three relations among these constants, which can be expressed, with the help of (4), as

$$\left.\begin{aligned} &a_0(\beta)(D_1 - D_2) + a_0(\gamma)(D_3 - D_4) + a_2(\mu) D_5 = a_1(\alpha_0) + 2\pi(\ln 2 - D_6) \\ &b_0(\beta)(D_1 - D_2) + \tfrac{1}{2}[\sin\gamma \cos\sigma - \gamma\cos(\sigma-\gamma)] D_3 + \tfrac{1}{2}[\gamma\cos(\sigma+\gamma) - \sin\gamma\cos\sigma] D_4 - 2\mu D_5 \\ &\qquad = b_1(\alpha_0)\cos\sigma - \pi \\ &c_0(\beta)(D_1 + D_2) + \tfrac{1}{2}[\sin\gamma\sin\sigma - \gamma\sin(\sigma-\gamma)] D_3 + \tfrac{1}{2}[\gamma\sin(\sigma+\gamma) - \sin\gamma\sin\sigma] D_4 \\ &\qquad = b_1(\alpha_0)\sin\sigma \end{aligned}\right\} \tag{26}$$

The condition that there is no discontunity in velocity gradient at the 'leading edge' $\theta = \pm\pi + \sigma$, gives the equation

$$(D_3 - D_4)\sin\gamma = \cot\alpha_0 \tag{27}$$

and this together with equations (25) and (26) serves to determine 6 of the 7 coefficients D_n. Some condition can therefore finally be invoked to impose a choice of trailing-edge angle, which (as we have seen) is equal to πD_5.

However, allowing D_5 to remain as an independent parameter for the moment, we can observe that the coefficients D_1, D_2, D_3 and D_4 can be calculated from (25), (26) and (27) quite simply by the successive steps:

$$\left.\begin{aligned} (D_3 - D_4) &= \cot\alpha_0 \operatorname{cosec}\gamma \\ (D_3 + D_4) &= X \sin\sigma / \sin^2\frac{\gamma}{2} \\ (D_1 + D_2) &= -X \sin\sigma/\sin^2\frac{\beta}{2} \\ (D_1 - D_2) &= \left\{\left[\gamma\cot\frac{\gamma}{2} + (1+\cos\beta)\cos\sigma\right] X - \pi + 2\mu D_5\right\} \Big/ b_0(\beta) \\ \text{where } X &= [b_1(\alpha_0) - \tfrac{1}{2}\cot\alpha_0(1-\gamma\cot\gamma)] \Big/ \left[1 + \cos\beta + \gamma\left(\cot\frac{\gamma}{2}\right)\cos\sigma\right] \end{aligned}\right\} \tag{28}$$

Finally, the value of D_6 can then be calculated (in terms of D_5) from the first of the equations (26). It will be observed that if the aerofoil is uncambered, then $\sigma = 0$, and $D_1 = -D_2$ and $D_3 = -D_4$ from which it is easily verified from equation (23) that log q_0 is an even function of θ—that is, the same on both top and bottom surfaces.

The value of α_0 is equal to half the design range of incidence (that is, $(\alpha_1-\alpha_2)/2$ in equation (19)) and is generally a small angle, and γ is half the range of angle over which the leading-edge velocity term (equation (22)) is taken to be variable—and this in turn is usually also a small angle. Thus we see from (27) that (D_3-D_4) tends to be large, so that both D_3 and D_4 may be large (compared with unity) but of opposite sign; approximately they equal $\pm 1/2\alpha\gamma$. However, if γ is small, equation (22) shows that the increment to $ln\, q_0$ from this term is approximately

$$-(|\phi|-|\gamma|)^2/(4\,\alpha_0\,\gamma) = -\gamma\,(1-|\phi/\gamma|)^2/(4\,\alpha_0)$$

with a maximum value of $\gamma/4\alpha_0$. Here we have used ϕ in place of $(\theta+\pi-\sigma)$ and in the neighbourhood of $\phi=0$, if α_0 is small, the term $D_0F_0\,(\theta)$ in (23) varies as $-ln\,(2\alpha_0+|\phi|)$ so that in combination, the behaviour of the logarithmic derivative of velocity increment is seen to be described approximately by

$$-(\phi/2\alpha_0)\,[(1/\gamma)-1/(2\alpha_0+|\phi|)] \quad \text{for } |\phi|<\gamma$$

without any discontinuity. In order that the modification introduced should not be disproportionate, we see that (γ/α_0) should be in general of order unity, and so it seems natural to define the extent of the leading-edge modification by a parameter $G=\gamma/\alpha_0$. In particular, for $G=2$ the second derivative in velocity increment is zero at $\phi=0$; for $G>2$ the increment to the velocity distribution becomes double-peaked with maxima at $|\phi|=(G-2)\,\alpha_0$ and a minimum at $\phi=0$. For values of G greater than approximately 5, the minimum at $\phi=0$ is less than the value at $|\phi|=\gamma$. These maxima and minima in the incremental velocity do not show in the total velocity distribution which is dominated by the term $\cos(\theta/2)$.

In considering the magnitude of the trailing-edge angle, and the value of μ in equation (6), we note that the increment in the surface slope (χ) produced by the term $D_5F_5(\theta)$ is exactly halved at $|\phi|=\mu$, since from (12), $E(\pm\infty)=\pi/2$, whereas $E(\pm 1)=\pi/4$. Thus to obtain a trailing edge which is, roughly speaking, wedge shaped, it is convenient to arrange that it has the same slope at $|\theta|=\mu$ as at the trailing edge $(\theta=0)$. On an aerofoil with camber $(\sigma\neq 0)$, the value of $|\chi|$ is different on the top and bottom surfaces at $\theta=\pm\mu$. whereas of course on a symmetric aerofoil, χ is equal and opposite at these two positions.

Consequently, we take

$$\chi|_{\theta=0+}-\chi|_{\theta=0-}=\chi|_{\theta=\mu}-\chi|_{\theta=-\mu} \tag{29}$$

Now, from (28), the introduction of non-zero μ increments D_1 and D_2 by opposite amounts, and from equations (23) and (4), the resulting term in $[g_0\,(\theta,\beta)-g_0\,(\theta,-\beta)]$ is an odd function of θ; further, excluding the trailing-edge term $D_5G_5(\theta)$, the value of χ is continuous through $\theta=0$ (i.e. the trailing edge is cusped). Thus (29) can be rearranged as an explicit expression for the trailing-edge angle (or D_5), namely

$$\left[2\mu\,\{[G_1(-\mu)-G_1(\mu)]/b_0(\beta)\}-\frac{\pi}{2}\right]D_5=\sum_{n=0}^{4} D_n|_{D_5=0}\,[G_n(\mu)-G_n(-\mu)]+\mu \tag{30}$$

where the additional term $\ldots+\mu$ arises from the complex conjugate of $ln\left(\cos\frac{\theta}{2}\right)$, which appears on the left hand side of equation (23). Generally, we would not want the trailing-edge term to interfere with the constant velocity distribution which exists over the lower surface between $\theta=-\beta$ and $-\pi+\sigma+\gamma$ at an incidence α_2, or that which exists over the upper surface for $\beta<\theta<\pi+\sigma-\gamma$ at incidence α_1. Thus, since from (6), the value of $F_5\,(\theta)$ vanishes for $|\phi|>\mu$, it seems pertinent to restrict μ to be less than β. The smaller μ is chosen within this limitation, the smaller will be the corresponding trailing edge angle.

APPENDIX IA

A Derivation of the Expansion of Equation (13) *of Appendix I*

Starting with the identity defining the Bernoulli numbers:

$$(x \coth x - 1)/x = \sum_{k=1}^{\infty} [2^{2k} B_{2k}/(2k)!]\, x^{2k-1} \quad (|x| < 2\pi)$$

we perform a term-by-term integration from $x = 0$ to $x = t$, say. We then obtain

$$f(t) = ln\,[(\sinh t)/t] = \sum_{k=1}^{\infty} [2^{2k-1} B_{2k}/k(2k)!]\, t^{2k} \quad (|t| < 2\pi).$$

If we form $f(t) - 2f(t/2)$, this becomes

$$ln\,[(t/4) \sinh t \operatorname{cosech}^2 (t/2)] = ln\frac{t}{2} + ln \coth\frac{t}{2} = \sum_{k=1}^{\infty} [(2^{2k-1} - 1)\, B_{2k}/k\,(2k)!]\, t^{2k}.$$

But $ln \coth (t/2) = 2 \operatorname{argtanh} (e^t)$, so that if we place $t = ln\, y$, then evidently for $|ln\, y| < 2\pi$ we have

$$(2/\pi y) \operatorname{argtanh} y = (1/\pi y)\, \{ln\,(2/ln\, y) + \sum_{k=1}^{\infty} [(2^{2k-1} - 1)\, B_{2k}/k\,(2k)!]\, (ln\, y)^{2k}\}$$

Performing another term-by-term integration with respect to y from $y = 1$ to x, the result of equation (13) of Appendix I follows, since by equation (10) of that Appendix the integral of the left hand side is then $E(x) - E(1)$, and $E(1) = \pi/4$ by equation (12).

APPENDIX II

Arrangement of the Computation.

1. *Calculation of the Aerofoil Profile.*

In deriving the velocity distribution in Appendix I, it was convenient to regard $|\theta| < \pi$ so that θ varies continuously from $-\pi$ to $+\pi$. In seeking the aerofoil profile, we have to integrate its slope with respect to the distance round the profile, and because of the possible discontinuity in χ at the trailing edge, it is more convenient to start and finish integration at the trailing edge. Thus we henceforward regard θ as defined between 0 and 2π and denote by $[\theta]$ the 'principle part' of θ such that $|[\theta]| < \pi$. As is shown in References 1 and 2, distance round the profile measured in the direction of increasing θ is given by

$$ds = 2|\sin\theta|d\theta/q_0 = 4\left(\sin\frac{\theta}{2}\right)d\theta\left/\left[q_0\left(\sec\frac{\theta}{2}\right)\right]\right. = 4\left(\sin\frac{\theta}{2}\right)d\theta/q_0' \tag{1}$$

Now the direction of the velocity vector, χ, is sensed in the direction of flow (i.e. in the negative s direction) from $\theta = \pi$ to $\theta = 0$ on the top surface, and from $\theta = \pi$ to $\theta = 2\pi$ (in the positive s direction) on the lower surface. Thus

$$dz = dx + idy = -\operatorname{sgn}([\theta])\exp(i\chi)\,ds = -\exp\left[i\left(\chi' + \frac{\theta}{2}\right)\right]ds \tag{2}$$

If the trailing edge is taken as the origin of the z-plane, we find from (1) and (2) upon integration that

$$\frac{1}{4}x = -\int_0^\theta \left(\sin\frac{\theta}{2}\right)\cos\left(\chi' + \frac{\theta}{2}\right)(d\theta/q_0'),\quad \frac{1}{4}y = -\int_0^\theta \left(\sin\frac{\theta}{2}\right)\sin\left(\chi' + \frac{\theta}{2}\right)(d\theta/q_0'), \tag{3}$$

For a thin aerofoil, lnq_0 and χ are both small so that approximately x is equal to $2(\cos\theta - 1)$. As numerical integration in less accurate than function evaluation, it is therefore preferable to evaluate not x, but

$$x/4 + \sin^2\frac{\theta}{2} = \int_0^\theta \left(\sin\frac{\theta}{2}\right)\left[\cos\frac{\theta}{2} - (1/q_0')\cos\left(\chi' + \frac{\theta}{2}\right)\right]d\theta \tag{4}$$

It will be noted that $(1/q_0')$ is non-singular except at the trailing edge where, however, $\sin(\theta/2) = 0$, and the integrand is zero at both $\theta = 0$ and $\theta = 2\pi$.

Generally, the closure of the aerofoil profile (i.e. the return of x and y to zero at $\theta = 2\pi$) is an adequate check on both the accuracy of the integration process, and (at a coarser level) on the correctness of evaluation of the velocity distribution. In the testing phase, it is as well, however, to check numerically that the integrals of lnq_0 and χ, with respect to θ from 0 to 2π, also vanish. The integration of lnq_0 is awkward because of its logarithmic singularities, and it destroys the point of the exercise to extract them. We note however that

$$\int_0^{2\pi} q_0 \exp(\pm i\chi)\,d\theta = 2\pi$$

whence we determine that

$$\int_0^{2\pi} q_0' \cos\frac{\theta}{2}\cos\left(\chi' + \frac{\theta}{2}\right)d\theta = 2\pi \tag{5}$$

This serves to check the evaluation of D_6 in equation (23) of Appendix I, which otherwise could be in error without revealing itself in the closure condition. (*See* also Appendix IV, Para. 2, page 70).

2. *Change of Axes.*

The profile thus calculated has its trailing edge at the origin, and is in the zero-lift attitude for a free stream parallel to the x-axis. For the purpose of tabulating the ordinates it is more convenient to refer them to a chord line joining the leading and trailing edges, the former being defined as that point on the profile most distant from the latter. To find the leading edge, it is necessary to solve the equation.

$$\chi - \arctan(y/x) = \pi/2. \tag{6}$$

This brings us up against the general problem of how best to interpolate the values of (x, y) found by the process of integration. The quadrature process used is an adaptive one, wherein the size of each discrete step of the integration (with respect to θ) is tested by comparing the results of Simpson's rule with a double application of the trapezoidal rule to the same three values of the integrand. If the difference between these two values is outside specified limits, the step size is halved or doubled to bring the difference within limits. At the end of each such step, the values of x and y are recorded along with the corresponding value of θ, (the size of step in θ being arranged where possible to keep θ expressible as an integral number of degrees). Also recorded are the corresponding values of χ, from which (by equation (2)) the derivatives of x and y with respect to θ are immediately calculable. Consideration of the accuracy implicit in various interpolative schemes applied to the data for x and y as functions of θ shows that simple two-point Hermite interpolation (the two values of θ chosen of course to embrace the value at which the interpolate is needed) has an accuracy entirely compatible with the integration process adopted. More sophisticated methods, with a built-in convergence test, can certainly provide apparently better accuracy, but this is of little importance where—as here—the data interpolated are already degraded in accuracy.

Stated more precisely, if $s(\theta)$ is used to mean either $x(\theta)$ or $y(\theta)$, then the integration process is such that the step size $\Delta\theta$, if small, satisfies an inequality of the form

$$\varepsilon/8 < |s'''(\theta)|\,\Delta\theta^3/16 < \varepsilon.$$

The error in the increment $s(\theta+\Delta\theta)-s(\theta)$ is then

$$\Delta\theta^5\, s^V(\theta)/2880$$

and the cumulative error in $s(\theta)$ of order $\varepsilon^{4/3}$, if $s^V(\theta)$ is in general bounded. (A precise size can be determined from the error in the closure condition). Now the additional error introduced by two-point Hermite interpolation of $s(\theta)$ between θ and $\theta+\Delta\theta$ is less than

$$\Delta\theta^4\, s^{IV}(\theta)/384$$

and this is again of order $\varepsilon^{4/3}$, and compatible with the cumulative inaccuracy of $s(\theta)$. The same could be said of four-point Lagrangian interpolation, but clearly Hermite interpolation (which employs the values of $s'(\theta)$, which are evaluated exactly) is in fact preferable.

With values of x and y interpolated in this way, equation (6) can be solved by an interative method. (We use a method based on *Regula Falsi*). The chord of the aerofoil (c) can then be determined, which enables the calculation of the lift coefficient

$$C_L = (8\pi/c)\sin\alpha \tag{7}$$

of the aerofoil at any chosen incidence (α) above zero lift. The axes are then rotated, the origin removed to the leading edge, and the axes scaled down by a factor $(1/c)$, so that the trailing edge is at the point $(1, 0)$. If the original axes are now denoted by subscript 0, the transformation is quite simply

$$z = 1+(z_0/c)\exp(i\alpha_z) \tag{8}$$

where α_z is the zero lift incidence of the transformed profile (and is usually negative for a positively cambered section). It follows further that

$$\chi = \chi_0+\alpha_z \tag{9}$$

where evidently $\chi_0 = \pi/2-\alpha_z$ is the value of χ satisfying equation (6), so that $z_0 = c\exp[i(\pi-\alpha_z)]$ at the leading edge.

If ordinates are to be calculated at prescribed values of x, the same interpolation scheme as suggested above is, in general, employed. Thus the value of θ corresponding to the prescribed value of x is determined iteratively using the Hermite interpolate for x, and the Hermite interpolate of y can be immediately computed. The search for, and calculation of, maximum thickness and camber require the use of similar interpolation techniques, though as these properties are only required for descriptive purposes, accuracy considerations are relatively less important.

3. *Pitching-Moment Characteristics.*

As shown in Reference 1, the pitching-moment coefficient at zero lift is

$$C_{M_0} = -(4/c^2)\int_0^{2\pi} ln\, q_0 \sin 2\theta\, d\theta = (4/c^2)\int_0^{2\pi}\chi_0\cos 2\theta\, d\theta\,. \tag{10}$$

The second (theoretically identical) integral is preferred for numerical work as it avoids the problem of the logarithmic singularities in lnq_0 at the stagnation points. The value of this integral is clearly unaffected by the transformation (5), and it is immaterial whether or not the convention is introduced whereby χ has a discontinuity (of π) at $\theta = \pi$. The co-ordinate of the aerodynamic centre in the original axis system is given by

$$\bar{z}_0 = \frac{1}{2\pi}\int_0^{2\pi}[\bar{z}_0 - 1 + 2ix\exp(2i\theta)]\, d\theta\,.$$

A differentiation by parts, and some rearrangement of the integrand yields the more convenient expression

$$\frac{1}{4}\bar{z}_0 = -\frac{1}{2\pi}\int_0^{2\pi}\theta\frac{d}{d\theta}\left(\frac{1}{4}z+\sin^2\frac{\theta}{2}\right)d\theta+\frac{i}{4\pi}\int_0^{2\pi}\left(\chi'+\frac{\theta}{2}\right)\exp(2i\theta)\, d\theta-\frac{3}{4} \tag{11}$$

which can be integrated along with (3), (4) and (10), and afterwards (8) can be used to find the aerodynamic-centre position in the transformed system of axes. In both (10) and (11) we may observe that

$$\int_0^{2\pi}\chi_0(\cos 2\theta)\, d\theta = \int_0^{2\pi}\left(\chi_0'+\frac{\theta}{2}\right)(\cos 2\theta)\, d\theta = -2\int_0^{2\pi}\chi_0'\sin^2\theta\, d\theta \tag{12}$$

and the latter integrand is preferable for numerical quadrature.

For a symmetric aerofoil, y_0 and of course C_{M_0} vanish, and from (11) we can deduce that

$$\frac{1}{4}(\bar{x}_0 - x_0|_{\theta=\pi}) = \frac{1}{4}-\frac{1}{\pi}\int_0^{\pi}\theta\frac{d}{d\theta}\left(\frac{1}{4}x_0+\sin^2\frac{\theta}{2}\right)d\theta-\frac{1}{\pi}\int_0^{\pi}\left(\chi_0'+\frac{\theta}{2}\right)\cos\theta\sin\theta\, d\theta$$

APPENDIX III

Geometric and Aerodynamic Characteristics of Aerofoils of the GU-Series.

Part 1—Symmetric Sections.

Lists characteristics of 720 aerofoils designated *GU ab—cde* where

a = 0(2)6

b = 1(2)5

c = 3(1)7

e = 2(2)8

Part 2—Cambered Sections.

List characteristics of 720 aerofoils designated *GU* **ab—cde** where

a = 2(2)6

b = 1(2)5

c = 3(1)7

d = 2(2)8

e = 2(2)8

In each part the parameters are in numerical order. In Part 2 the tabulation extends over two facing pages.

APPENDIX III, Part 1

AEROFOIL	THICKNESS AT 0.05c (percent of max.)	T.E. ANGLE (deg)	EXTENT FAV.GRAD. (percent chord)	MAX.THICKNESS (per cent chord)	MAX.THICKNESS POSITION (percent chord)	LIFT CURVE SLOPE (/deg)	LOW DRAG UPPER CL LIMIT	A.C. POSITION (percent chord)
GU 01-302	46.1	3.1	29.0	6.0	30.8	0.114	0.11	25.6
GU 01-304	45.7	4.9	28.4	9.8	30.5	0.117	0.23	25.9
GU 01-306	44.6	6.3	27.9	12.9	30.2	0.119	0.36	26.3
GU 01-308	44.8	7.4	27.5	15.5	29.9	0.121	0.48	26.6
GU 01-402	41.4	3.7	38.7	6.5	36.1	0.114	0.11	25.8
GU 01-404	40.9	6.0	38.0	10.7	35.8	0.118	0.24	26.3
GU 01-406	40.8	7.7	37.4	14.2	35.5	0.120	0.36	26.7
GU 01-408	40.8	9.1	36.8	17.1	35.2	0.122	0.49	27.1
GU 01-502	39.7	4.6	48.5	7.0	40.4	0.115	0.11	26.0
GU 01-504	39.1	7.5	47.6	11.6	40.3	0.118	0.24	26.7
GU 01-506	38.9	9.7	47.0	15.4	40.1	0.121	0.36	27.2
GU 01-508	38.8	11.6	46.4	18.7	39.9	0.124	0.49	27.7
GU 01-602	36.3	6.0	58.4	7.3	44.3	0.115	0.12	26.2
GU 01-604	36.7	9.7	57.5	12.3	44.3	0.119	0.24	27.1
GU 01-606	36.4	12.7	56.7	16.4	44.2	0.122	0.37	27.8
GU 01-608	36.2	15.2	56.1	19.9	44.2	0.125	0.50	28.4
GU 01-702	36.1	8.2	68.4	7.8	47.6	0.116	0.12	26.5
GU 01-704	35.3	13.4	67.5	13.0	47.9	0.120	0.24	27.5
GU 01-706	34.6	17.6	66.7	17.3	48.1	0.124	0.37	28.4
GU 01-708	34.3	21.2	66.2	21.2	48.2	0.127	0.51	29.2
GU 03-302	45.5	5.1	29.1	6.1	31.4	0.114	0.11	25.6
GU 03-304	45.1	8.1	28.5	9.9	31.1	0.117	0.23	26.1
GU 03-306	44.1	10.5	28.1	13.1	30.8	0.120	0.36	26.5
GU 03-308	44.2	12.5	27.7	15.7	30.6	0.122	0.49	26.8
GU 03-402	41.0	6.0	38.8	6.6	36.7	0.115	0.11	25.9
GU 03-404	40.5	9.7	38.1	10.9	36.4	0.118	0.24	26.4
GU 03-406	40.3	12.6	37.6	14.4	36.1	0.121	0.36	26.9
GU 03-408	40.3	15.0	37.1	17.3	35.8	0.123	0.49	27.3
GU 03-502	39.3	7.3	48.6	7.1	41.1	0.115	0.12	26.1
GU 03-504	38.6	11.9	47.8	11.8	41.0	0.119	0.24	26.8
GU 03-506	38.3	15.5	47.2	15.6	40.8	0.122	0.36	27.4
GU 03-508	38.2	18.6	46.7	18.9	40.7	0.124	0.50	28.0
GU 03-602	36.0	9.2	58.6	7.4	45.0	0.116	0.12	26.3
GU 03-604	36.2	15.1	57.7	12.4	45.1	0.119	0.24	27.2
GU 03-606	35.9	19.8	57.1	16.6	45.1	0.123	0.37	28.0
GU 03-608	35.7	23.7	56.5	20.2	45.1	0.126	0.50	28.7
GU 03-702	35.7	12.1	68.6	7.9	48.3	0.116	0.12	26.6
GU 03-704	34.8	20.0	67.8	13.2	48.7	0.120	0.24	27.7
GU 03-706	34.1	26.3	67.2	17.6	49.0	0.124	0.37	28.7
GU 03-708	33.9	31.7	66.7	21.5	49.2	0.128	0.51	29.5

AEROFOIL	THICKNESS AT 0.05c (percent of max.)	T.E. ANGLE (deg)	EXTENT FAV.GRAD. (percent chord)	MAX.THICKNESS (per cent chord)	MAX.THICKNESS POSITION (percent chord)	LIFT CURVE SLOPE (/deg)	LOW DRAG UPPER CL LIMIT	A.C. POSITION (percent chord)
GU 05-302	45.2	6.1	29.1	6.1	31.9	0.114	0.11	25.7
GU 05-304	44.8	9.8	28.6	10.0	31.6	0.118	0.24	26.2
GU 05-306	43.8	12.7	28.2	13.2	31.3	0.120	0.36	26.6
GU 05-308	43.9	15.1	27.8	15.9	31.2	0.122	0.49	27.0
GU 05-402	40.8	7.2	38.9	6.7	37.1	0.115	0.11	25.9
GU 05-404	40.2	11.6	38.2	11.0	36.9	0.118	0.24	26.6
GU 05-406	40.1	15.1	37.7	14.6	36.6	0.121	0.36	27.1
GU 05-408	40.1	18.0	37.3	17.6	36.3	0.123	0.49	27.5
GU 05-502	39.1	8.6	48.7	7.2	41.6	0.115	0.12	26.2
GU 05-504	38.4	14.0	48.0	11.9	41.5	0.119	0.24	26.9
GU 05-506	38.1	18.3	47.4	15.8	41.4	0.122	0.37	27.6
GU 05-508	38.0	21.9	46.9	19.2	41.2	0.125	0.50	28.2
GU 05-602	36.0	10.6	58.7	7.4	45.5	0.116	0.12	26.4
GU 05-604	36.1	17.4	57.9	12.6	45.6	0.120	0.24	27.4
GU 05-606	35.7	22.8	57.3	16.8	45.7	0.123	0.37	28.2
GU 05-608	35.5	27.4	56.8	20.5	45.8	0.126	0.51	28.9
GU 05-702	35.6	13.6	68.7	7.9	48.8	0.116	0.12	26.7
GU 05-704	34.8	22.3	68.0	13.3	49.2	0.121	0.24	27.8
GU 05-706	34.1	29.5	67.5	17.8	49.6	0.125	0.37	28.9
GU 05-708	33.8	35.5	67.0	21.8	49.9	0.128	0.51	29.8
GU 21-302	47.0	3.2	28.9	6.3	30.6	0.114	0.11	25.5
GU 21-304	46.4	5.2	28.2	10.5	30.1	0.118	0.24	25.9
GU 21-306	47.4	6.8	27.6	13.9	29.6	0.120	0.36	26.2
GU 21-308	48.4	8.0	27.0	16.9	29.1	0.123	0.49	26.5
GU 21-402	42.4	3.9	38.6	6.9	35.9	0.115	0.11	25.8
GU 21-404	42.7	6.3	37.7	11.4	35.4	0.118	0.24	26.3
GU 21-406	43.5	8.2	37.0	15.2	35.0	0.121	0.36	26.7
GU 21-408	44.3	9.8	36.3	18.6	34.5	0.124	0.50	27.0
GU 21-502	40.7	4.8	48.4	7.4	40.1	0.115	0.12	26.0
GU 21-504	40.8	7.9	47.4	12.4	39.8	0.119	0.24	26.7
GU 21-506	41.4	10.4	46.6	16.6	39.5	0.122	0.37	27.2
GU 21-508	42.1	12.4	45.8	20.3	39.1	0.125	0.50	27.7
GU 21-602	37.3	6.2	58.3	7.6	44.0	0.116	0.12	26.2
GU 21-604	38.3	10.3	57.2	13.1	43.7	0.120	0.24	27.1
GU 21-606	38.9	13.5	56.4	17.6	43.7	0.124	0.37	27.8
GU 21-608	39.5	16.3	55.6	21.6	43.4	0.127	0.51	28.4
GU 21-702	37.0	8.5	68.3	8.2	47.3	0.116	0.12	26.5
GU 21-704	36.9	14.2	67.3	13.8	47.5	0.121	0.24	27.6
GU 21-706	37.0	18.7	66.4	18.6	47.6	0.125	0.37	28.5
GU 21-708	37.6	22.7	65.7	23.0	47.5	0.129	0.51	29.3

AEROFOIL	THICKNESS AT 0.05c (percent of max.)	T.E. ANGLE (deg)	EXTENT FAV.GRAD. (percent chord)	MAX.THICKNESS (per cent chord)	MAX.THICKNESS POSITION (percent chord)	LIFT CURVE SLOPE (/deg)	LOW DRAG UPPER CL LIMIT	A.C. POSITION (percent chord)
GU 23-302	46.5	5.3	29.0	6.4	31.2	0.115	0.11	25.6
GU 23-304	46.9	8.6	28.3	10.6	30.7	0.118	0.24	26.0
GU 23-306	46.8	11.3	27.7	14.1	30.3	0.121	0.36	26.4
GU 23-308	47.8	13.5	27.2	17.1	29.7	0.123	0.49	26.7
GU 23-402	42.0	6.3	38.7	6.9	36.5	0.115	0.11	25.9
GU 23-404	42.2	10.3	37.9	11.6	35.9	0.119	0.24	26.4
GU 23-406	43.0	13.5	37.2	15.5	35.5	0.122	0.37	26.9
GU 23-408	43.8	16.2	36.5	18.8	35.2	0.125	0.50	27.3
GU 23-502	40.2	7.7	48.5	7.5	40.8	0.115	0.12	26.1
GU 23-504	40.3	12.6	47.6	12.5	40.6	0.119	0.24	26.8
GU 23-506	40.9	16.6	46.8	16.8	40.2	0.123	0.37	27.4
GU 23-508	41.6	19.9	46.2	20.6	39.8	0.126	0.50	28.0
GU 23-602	37.0	9.6	58.5	7.7	44.7	0.116	0.12	26.3
GU 23-604	37.9	15.9	57.5	13.2	44.5	0.120	0.24	27.3
GU 23-606	38.4	21.0	56.7	17.8	44.5	0.124	0.37	28.0
GU 23-608	39.0	25.4	56.1	21.9	44.3	0.128	0.51	28.7
GU 23-702	36.6	12.6	68.5	8.2	48.0	0.116	0.12	26.6
GU 23-704	36.4	21.0	67.6	14.0	48.2	0.121	0.24	27.8
GU 23-706	36.6	27.9	66.9	18.9	48.4	0.126	0.38	28.8
GU 23-708	37.1	33.8	66.3	23.4	48.4	0.130	0.52	29.7
GU 25-302	46.1	6.4	29.0	6.4	31.6	0.115	0.11	25.7
GU 25-304	46.5	10.4	28.4	10.7	31.2	0.118	0.24	26.2
GU 25-306	46.5	13.6	27.8	14.3	30.9	0.121	0.36	26.6
GU 25-308	47.4	16.3	27.3	17.4	30.5	0.124	0.49	26.9
GU 25-402	41.7	7.5	38.8	7.0	36.9	0.115	0.12	25.9
GU 25-404	42.0	12.3	38.0	11.7	36.5	0.119	0.24	26.6
GU 25-406	42.7	16.1	37.4	15.7	36.0	0.122	0.37	27.1
GU 25-408	43.5	19.4	36.8	19.1	35.5	0.125	0.50	27.5
GU 25-502	40.0	9.0	48.6	7.5	41.4	0.116	0.12	26.2
GU 25-504	40.0	14.8	47.8	12.7	41.2	0.120	0.24	27.0
GU 25-506	40.6	19.5	47.1	17.0	40.8	0.123	0.37	27.6
GU 25-508	41.3	23.5	46.4	20.9	40.6	0.127	0.51	28.2
GU 25-602	36.9	11.1	58.6	7.8	45.2	0.116	0.12	26.4
GU 25-604	37.7	18.3	57.7	13.4	45.1	0.121	0.24	27.4
GU 25-606	38.2	24.2	57.0	18.1	45.1	0.125	0.37	28.2
GU 25-608	38.8	29.3	56.4	22.3	44.9	0.128	0.51	29.0
GU 25-702	36.6	14.1	68.6	8.3	48.5	0.117	0.12	26.7
GU 25-704	36.4	23.5	67.8	14.2	48.8	0.122	0.24	27.9
GU 25-706	36.5	31.2	67.2	19.1	49.0	0.126	0.38	29.0
GU 25-708	37.0	37.9	66.7	23.7	49.0	0.130	0.52	29.9

APPENDIX III, Part 1

AEROFOIL	THICKNESS AT 0.05c (percent of max.)	T.E. ANGLE (deg)	EXTENT FAV.GRAD. (percent chord)	MAX.THICKNESS (per cent chord)	POSITION (percent chord)	LIFT CURVE SLOPE (/deg)	LOW DRAG UPPER CL LIMIT	A.C. POSITION (percent chord)
GU 41-302	49.6	3.7	28.6	7.2	30.1	0.115	0.12	25.5
GU 41-304	51.2	6.2	27.5	12.5	29.1	0.120	0.24	25.9
GU 41-306	54.0	8.2	26.5	17.0	28.1	0.123	0.37	26.1
GU 41-308	56.9	10.0	25.5	21.1	27.1	0.127	0.51	26.4
GU 41-402	45.0	4.5	38.3	7.9	35.4	0.116	0.12	25.8
GU 41-404	47.3	7.4	37.0	13.6	34.4	0.120	0.24	26.3
GU 41-406	50.0	9.9	35.8	18.5	33.4	0.125	0.37	26.6
GU 41-408	52.7	12.1	34.7	23.2	32.6	0.129	0.51	27.0
GU 41-502	43.2	5.5	48.1	8.4	39.6	0.116	0.12	26.0
GU 41-504	45.3	9.2	46.7	14.6	38.7	0.121	0.24	26.7
GU 41-506	47.7	12.4	45.5	20.1	37.9	0.126	0.38	27.3
GU 41-508	50.3	15.1	44.3	25.2	37.1	0.130	0.52	27.8
GU 41-602	40.9	7.1	58.0	8.8	43.3	0.117	0.12	26.3
GU 41-604	42.8	11.9	56.5	15.4	42.6	0.122	0.24	27.2
GU 41-606	45.1	16.0	55.3	21.3	42.0	0.127	0.38	28.0
GU 41-608	47.5	19.7	54.1	26.9	41.4	0.133	0.53	28.7
GU 41-702	39.5	9.6	68.0	9.3	46.6	0.117	0.12	26.6
GU 41-704	41.3	16.4	66.7	16.3	46.3	0.123	0.25	27.8
GU 41-706	43.2	22.0	65.5	22.6	45.9	0.129	0.39	28.8
GU 41-708	45.4	27.1	64.4	28.7	45.5	0.135	0.54	29.8
GU 43-302	49.1	6.1	28.7	7.3	30.7	0.116	0.12	25.6
GU 43-304	50.6	10.2	27.7	12.6	29.7	0.120	0.24	26.0
GU 43-306	53.4	13.5	26.7	17.2	28.9	0.124	0.37	26.4
GU 43-308	56.3	16.5	25.8	21.5	27.9	0.128	0.51	26.7
GU 43-402	44.6	7.2	38.4	8.0	35.9	0.116	0.12	25.9
GU 43-404	46.9	12.0	37.2	13.7	35.1	0.121	0.24	26.5
GU 43-406	49.5	16.1	36.1	18.8	34.2	0.125	0.38	26.9
GU 43-408	52.1	19.6	35.0	23.6	33.2	0.130	0.52	27.3
GU 43-502	42.7	8.7	48.2	8.5	40.2	0.116	0.12	26.1
GU 43-504	44.8	14.6	46.9	14.8	39.5	0.122	0.24	26.9
GU 43-506	47.2	19.6	45.8	20.4	38.7	0.127	0.38	27.6
GU 43-508	49.6	24.1	44.7	25.7	37.9	0.131	0.53	28.2
GU 43-602	39.6	10.9	58.1	8.8	44.0	0.117	0.12	26.4
GU 43-604	42.3	18.4	56.9	15.6	43.6	0.123	0.25	27.4
GU 43-606	44.6	24.8	55.7	21.6	43.0	0.128	0.38	28.3
GU 43-608	47.0	30.4	54.7	27.4	42.4	0.134	0.53	29.1
GU 43-702	39.1	14.3	68.2	9.4	47.4	0.118	0.12	26.7
GU 43-704	40.8	24.2	67.0	16.5	47.1	0.124	0.25	28.0
GU 43-706	42.7	32.7	66.0	22.9	46.9	0.130	0.39	29.1
GU 43-708	44.9	40.3	65.2	29.2	46.5	0.136	0.54	30.2

APPENDIX III, Part 1

AEROFOIL	THICKNESS AT 0.05c (percent of max.)	T.E. ANGLE (deg)	EXTENT FAV.GRAD. (percent chord)	MAX.THICKNESS (per cent chord)	MAX.THICKNESS POSITION (percent chord)	LIFT CURVE SLOPE (/deg)	LOW DRAG UPPER CL LIMIT	A.C. POSITION (percent chord)
GU 45-302	48.7	7.3	28.7	7.4	31.2	0.116	0.12	25.7
GU 45-304	50.3	12.2	27.8	12.8	30.3	0.120	0.24	26.2
GU 45-306	53.0	16.3	26.8	17.5	29.5	0.125	0.37	26.6
GU 45-308	55.8	19.9	25.9	21.8	28.5	0.129	0.51	26.9
GU 45-402	44.3	8.5	38.5	8.1	36.3	0.116	0.12	26.0
GU 45-404	46.6	14.3	37.3	13.9	35.5	0.121	0.24	26.6
GU 45-406	49.1	19.2	36.3	19.1	34.6	0.126	0.38	27.1
GU 45-408	51.8	23.5	35.3	23.9	33.8	0.130	0.52	27.6
GU 45-502	42.5	10.2	48.3	8.6	40.7	0.117	0.12	26.2
GU 45-504	44.5	17.2	47.1	15.0	40.0	0.122	0.24	27.1
GU 45-506	46.9	23.1	46.0	20.7	39.5	0.127	0.38	27.8
GU 45-508	49.3	28.3	45.0	26.1	38.7	0.132	0.53	28.5
GU 45-602	39.5	12.5	58.3	8.9	44.6	0.117	0.12	26.5
GU 45-604	42.1	21.2	57.1	15.8	44.1	0.123	0.25	27.6
GU 45-606	44.4	28.6	56.0	22.0	43.6	0.129	0.39	28.5
GU 45-608	46.7	35.1	55.1	27.8	43.0	0.134	0.54	29.4
GU 45-702	39.1	15.9	68.4	9.5	47.9	0.118	0.12	26.8
GU 45-704	40.7	27.1	67.3	16.7	47.7	0.124	0.25	28.2
GU 45-706	42.5	36.6	66.4	23.2	47.5	0.131	0.39	29.4
GU 45-708	44.7	45.1	65.6	29.6	47.3	0.137	0.55	30.6
GU 61-302	53.3	4.5	28.1	8.8	29.3	0.117	0.12	25.5
GU 61-304	57.8	7.8	26.4	15.9	27.5	0.123	0.25	25.8
GU 61-306	62.9	10.6	24.7	22.4	25.8	0.129	0.39	26.0
GU 61-308	67.7	13.2	23.1	28.8	24.2	0.135	0.54	26.3
GU 61-402	48.7	5.4	37.7	9.6	34.4	0.117	0.12	25.8
GU 61-404	53.9	9.3	35.8	17.2	32.8	0.124	0.25	26.2
GU 61-406	58.9	12.7	33.9	24.4	31.2	0.131	0.39	26.6
GU 61-408	63.6	15.8	32.1	31.5	29.3	0.137	0.55	27.1
GU 61-502	46.8	6.6	47.5	10.2	38.3	0.118	0.12	26.1
GU 61-504	51.7	11.5	45.5	18.5	37.1	0.125	0.25	26.8
GU 61-506	56.4	15.7	43.5	26.4	35.5	0.132	0.40	27.5
GU 61-508	61.0	19.6	41.7	34.3	34.0	0.140	0.56	28.2
GU 61-602	44.5	8.5	57.4	10.7	42.2	0.119	0.12	26.4
GU 61-604	49.2	14.7	55.4	19.5	41.0	0.126	0.25	27.4
GU 61-606	53.7	20.2	53.5	28.0	39.5	0.134	0.40	28.3
GU 61-608	58.3	25.3	51.6	36.6	38.3	0.143	0.57	29.4
GU 61-702	43.0	11.5	67.5	11.2	45.3	0.119	0.12	26.8
GU 61-704	47.2	20.0	65.6	20.6	44.7	0.128	0.26	28.1
GU 61-706	51.6	27.6	63.9	29.8	43.4	0.137	0.41	29.4
GU 61-708	56.0	34.5	62.3	39.2	42.6	0.146	0.59	30.8

APPENDIX III, Part 1

AEROFOIL	THICKNESS AT 0.05c (percent of max.)	T.E. ANGLE (deg)	EXTENT FAV.GRAD. (percent chord)	MAX.THICKNESS (per cent chord)	MAX.THICKNESS POSITION (percent chord)	LIFT CURVE SLOPE (/deg)	LOW DRAG UPPER CL LIMIT	A.C. POSITION (percent chord)
GU 63-302	52.7	7.3	28.2	8.9	29.7	0.117	0.12	25.6
GU 63-304	57.2	12.7	26.5	16.1	28.3	0.124	0.25	26.0
GU 63-306	62.3	17.3	24.9	22.8	26.6	0.130	0.39	26.3
GU 63-308	67.1	21.6	23.3	29.3	25.0	0.136	0.54	26.7
GU 63-402	48.2	8.6	37.9	9.7	34.8	0.118	0.12	25.9
GU 63-404	53.4	14.9	36.0	17.4	33.4	0.125	0.25	26.5
GU 63-406	58.3	20.5	34.2	24.8	31.6	0.131	0.39	27.0
GU 63-408	63.0	25.5	32.5	32.1	30.1	0.138	0.55	27.6
GU 63-502	46.3	10.4	47.7	10.3	39.1	0.118	0.12	26.2
GU 63-504	51.1	18.1	45.8	18.8	37.9	0.126	0.25	27.0
GU 63-506	55.8	24.8	43.9	26.8	36.3	0.133	0.40	27.8
GU 63-508	60.4	31.0	42.2	34.9	34.8	0.141	0.56	28.7
GU 63-602	44.0	13.0	57.6	10.8	43.0	0.119	0.12	26.5
GU 63-604	48.6	22.6	55.8	19.8	41.8	0.127	0.25	27.7
GU 63-606	53.1	31.1	54.0	28.5	40.6	0.136	0.41	28.7
GU 63-608	57.6	38.9	52.4	37.4	39.5	0.144	0.58	29.9
GU 63-702	42.6	16.9	67.8	11.4	46.1	0.120	0.12	26.9
GU 63-704	46.7	29.6	66.1	20.8	45.5	0.129	0.26	28.4
GU 63-706	51.1	40.8	64.6	30.3	44.5	0.138	0.41	29.9
GU 63-708	55.4	51.1	63.3	40.0	43.7	0.148	0.59	31.5
GU 65-302	52.4	8.8	28.3	9.0	30.1	0.117	0.12	25.7
GU 65-304	56.8	15.2	26.7	16.3	28.7	0.124	0.25	26.2
GU 65-306	61.9	20.8	25.1	23.1	27.0	0.130	0.39	26.6
GU 65-308	66.6	26.0	23.5	29.8	25.8	0.137	0.55	27.0
GU 65-402	48.0	10.2	38.0	9.8	35.5	0.118	0.12	26.0
GU 65-404	53.0	17.7	36.2	17.7	34.0	0.125	0.25	26.7
GU 65-406	57.9	24.3	34.5	25.2	32.4	0.132	0.40	27.3
GU 65-408	62.6	30.3	32.8	32.7	30.9	0.139	0.56	27.9
GU 65-502	46.1	12.2	47.8	10.5	39.8	0.118	0.12	26.3
GU 65-504	50.8	21.2	46.0	19.0	38.5	0.126	0.25	27.2
GU 65-506	55.4	29.1	44.3	27.3	37.1	0.134	0.40	28.1
GU 65-508	60.0	36.3	42.6	35.6	35.5	0.142	0.57	29.1
GU 65-602	43.8	14.9	57.8	10.9	43.4	0.119	0.12	26.7
GU 65-604	48.4	26.0	56.0	20.0	42.6	0.128	0.26	27.9
GU 65-606	52.9	35.8	54.4	29.0	41.4	0.136	0.41	29.1
GU 65-608	57.3	44.8	52.9	38.1	40.2	0.146	0.58	30.4
GU 65-702	42.5	18.9	68.0	11.5	46.9	0.120	0.12	27.0
GU 65-704	46.6	33.1	66.4	21.1	46.1	0.129	0.26	28.6
GU 65-706	50.9	45.6	65.1	30.7	45.3	0.139	0.42	30.2
GU 65-708	55.1	57.2	64.0	40.7	44.5	0.150	0.60	31.9

AEROFOIL	THICKNESS AT 0.05c (percent of max.)	T.E. ANGLE (deg)	EXTENT OF FAV. PRESSURE GRAD. (percent c) TOP	BOTTOM	MAX. CAMBER (per cent chord)	POSITION (percent chord)	MAX. THICKNESS (per cent chord)	POSITION (percent chord)
GU 21-322	46.5	3.2	29.8	27.9	1.4	35.6	6.2	30.8
GU 21-324	46.6	5.2	29.0	27.3	1.3	34.7	10.4	30.2
GU 21-326	47.4	6.8	28.3	26.8	1.2	34.3	13.8	29.7
GU 21-328	48.5	8.1	27.7	26.3	1.1	34.5	16.8	29.2
GU 21-342	46.4	3.2	30.7	26.8	2.9	34.8	6.2	31.2
GU 21-344	46.8	5.3	29.8	26.3	2.6	34.2	10.3	30.5
GU 21-346	47.6	6.9	29.1	25.9	2.4	34.2	13.8	29.9
GU 21-348	48.5	8.2	28.4	25.5	2.2	34.2	16.7	29.4
GU 21-362	47.2	3.2	31.4	25.6	4.3	34.4	6.1	31.7
GU 21-364	47.4	5.4	30.5	25.3	4.0	34.2	10.3	30.8
GU 21-366	48.0	7.1	29.8	25.0	3.7	34.1	13.7	30.2
GU 21-368	48.7	8.6	29.1	24.7	3.4	34.1	16.6	29.7
GU 21-382	48.2	3.1	32.2	24.3	5.7	34.5	5.9	32.4
GU 21-384	48.3	5.4	31.2	24.1	5.4	34.2	10.1	31.3
GU 21-386	48.6	7.2	30.5	24.0	5.0	34.0	13.5	30.6
GU 21-388	49.1	8.8	29.8	23.8	4.6	34.0	16.5	30.0
GU 21-422	42.7	3.9	39.5	37.7	1.5	39.5	6.8	36.0
GU 21-424	43.0	6.3	38.5	36.9	1.4	42.8	11.4	35.5
GU 21-426	43.7	8.3	37.7	36.2	1.3	41.9	15.2	35.0
GU 21-428	44.6	9.9	37.0	35.6	1.2	41.2	18.6	34.5
GU 21-442	43.2	3.9	40.3	36.7	3.0	39.6	6.8	36.3
GU 21-444	43.4	6.4	39.3	36.0	2.7	43.5	11.4	35.6
GU 21-446	43.9	8.3	38.5	35.3	2.6	42.6	15.2	35.1
GU 21-448	44.6	10.0	37.8	34.8	2.4	41.8	18.5	34.6
GU 21-462	44.1	3.9	41.0	35.6	4.5	39.5	6.6	37.2
GU 21-464	44.0	6.5	40.0	35.0	4.2	39.6	11.2	35.9
GU 21-466	44.3	8.6	39.2	34.5	3.9	43.2	15.0	35.2
GU 21-468	44.9	10.4	38.5	34.0	3.6	42.5	18.4	34.6
GU 21-482	45.2	3.8	41.7	34.5	6.0	39.4	6.4	38.5
GU 21-484	44.8	6.5	40.7	33.9	5.6	39.6	11.0	36.5
GU 21-486	44.9	8.8	39.9	33.5	5.2	43.9	14.9	35.5
GU 21-488	45.3	10.7	39.2	33.1	4.9	43.1	18.2	34.9
GU 21-522	40.3	4.8	49.2	47.6	1.5	44.8	7.3	40.3
GU 21-524	40.4	7.9	48.2	46.6	1.4	46.0	12.3	40.0
GU 21-526	40.9	10.4	47.3	45.8	1.3	47.3	16.4	39.6
GU 21-528	41.6	12.5	46.6	45.1	1.3	47.0	20.1	39.3
GU 21-542	40.8	4.8	50.0	46.7	3.0	45.2	7.2	40.5
GU 21-544	40.8	8.0	48.9	45.8	2.8	45.7	12.2	40.1
GU 21-546	41.2	10.5	48.1	45.0	2.7	47.0	16.4	39.7
GU 21-548	41.8	12.6	47.3	44.3	2.5	47.2	20.1	39.4

AEROFOIL	ZERO LIFT INCIDENCE (deg)	LIFT CURVE SLOPE (/deg)	LOW DRAG RANGE OF LIFT COEFFICIENT LOWER LIMIT	DESIGN	UPPER LIMIT	AERODYNAMIC CENTRE POSN. (percent c) x	y	PITCHING MOMENT COEF.
GU 21-322	-1.0	0.115	0.11	0.23	0.34	25.5	0.5	-0.020
GU 21-324	-1.0	0.118	0.00	0.24	0.47	25.9	0.5	-0.018
GU 21-326	-0.9	0.120	-0.12	0.24	0.60	26.2	0.5	-0.017
GU 21-328	-0.8	0.123	-0.25	0.25	0.74	26.5	0.4	-0.015
GU 21-342	-2.1	0.115	0.34	0.46	0.57	25.5	1.1	-0.040
GU 21-344	-2.0	0.118	0.24	0.47	0.71	25.9	1.0	-0.036
GU 21-346	-1.8	0.120	0.12	0.48	0.84	26.2	1.0	-0.033
GU 21-348	-1.7	0.123	0.00	0.49	0.98	26.5	0.9	-0.030
GU 21-362	-3.2	0.115	0.57	0.69	0.80	25.5	1.6	-0.060
GU 21-364	-3.0	0.118	0.47	0.71	0.94	25.9	1.6	-0.054
GU 21-366	-2.7	0.120	0.36	0.72	1.08	26.2	1.6	-0.050
GU 21-368	-2.5	0.123	0.25	0.74	1.22	26.5	1.5	-0.046
GU 21-382	-4.2	0.115	0.80	0.92	1.03	25.5	2.2	-0.081
GU 21-384	-4.0	0.118	0.71	0.94	1.17	25.9	2.2	-0.073
GU 21-386	-3.7	0.121	0.60	0.96	1.32	26.2	2.1	-0.066
GU 21-388	-3.5	0.123	0.49	0.98	1.46	26.5	2.1	-0.061
GU 21-422	-1.2	0.115	0.11	0.23	0.34	25.8	0.5	-0.024
GU 21-424	-1.1	0.118	0.00	0.24	0.47	26.3	0.5	-0.022
GU 21-426	-1.0	0.121	-0.12	0.24	0.61	26.7	0.5	-0.020
GU 21-428	-0.9	0.124	-0.25	0.25	0.74	27.0	0.5	-0.019
GU 21-442	-2.3	0.115	0.34	0.46	0.57	25.8	1.0	-0.047
GU 21-444	-2.2	0.118	0.24	0.47	0.71	26.3	1.0	-0.043
GU 21-446	-2.0	0.121	0.12	0.49	0.85	26.7	1.0	-0.040
GU 21-448	-1.9	0.124	0.00	0.50	0.99	27.0	0.9	-0.038
GU 21-462	-3.5	0.115	0.57	0.69	0.80	25.8	1.5	-0.071
GU 21-464	-3.3	0.119	0.47	0.71	0.95	26.3	1.6	-0.065
GU 21-466	-3.1	0.122	0.36	0.73	1.09	26.7	1.5	-0.060
GU 21-468	-2.9	0.124	0.25	0.74	1.24	27.0	1.5	-0.056
GU 21-482	-4.6	0.115	0.81	0.92	1.03	25.7	2.1	-0.095
GU 21-484	-4.4	0.119	0.71	0.95	1.18	26.2	2.1	-0.087
GU 21-486	-4.1	0.122	0.61	0.97	1.33	26.7	2.1	-0.081
GU 21-488	-3.9	0.124	0.50	0.99	1.48	27.1	2.0	-0.075
GU 21-522	-1.2	0.115	0.12	0.23	0.35	26.0	0.4	-0.027
GU 21-524	-1.2	0.119	0.00	0.24	0.48	26.6	0.4	-0.025
GU 21-526	-1.1	0.122	-0.12	0.24	0.61	27.2	0.4	-0.023
GU 21-528	-1.0	0.125	-0.25	0.25	0.75	27.6	0.4	-0.022
GU 21-542	-2.5	0.115	0.35	0.46	0.58	26.0	0.9	-0.054
GU 21-544	-2.3	0.119	0.24	0.48	0.71	26.6	0.9	-0.051
GU 21-546	-2.2	0.123	0.12	0.49	0.86	27.2	0.9	-0.047
GU 21-548	-2.1	0.126	0.00	0.50	1.00	27.7	0.8	-0.045

AEROFOIL	THICKNESS AT 0.05c (percent of max.)	T.E. ANGLE (deg)	EXTENT OF FAV. PRESSURE GRAD. (percent c) TOP	BOTTOM	MAX.CAMBER (per cent chord)	POSITION (percent chord)	MAX. THICKNESS (per cent chord)	POSITION (percent chord)
GU 21-562	41.7	4.8	50.7	45.8	4.5	46.1	7.1	40.9
GU 21-564	41.3	8.1	49.6	44.9	4.3	45.4	12.1	40.3
GU 21-566	41.5	10.8	48.8	44.2	4.0	46.5	16.3	39.8
GU 21-568	42.0	13.0	48.1	43.5	3.8	47.1	20.0	39.5
GU 21-582	42.8	4.8	51.4	44.8	6.1	46.7	6.8	41.8
GU 21-584	42.1	8.2	50.4	44.0	5.7	45.8	11.9	40.6
GU 21-586	42.1	10.9	49.5	43.3	5.4	46.0	16.1	40.1
GU 21-588	42.4	13.3	48.8	42.7	5.1	46.8	19.8	39.6
GU 21-622	38.5	6.2	59.0	57.6	1.5	49.4	7.7	44.0
GU 21-624	38.4	10.3	57.9	56.5	1.4	49.3	13.0	43.9
GU 21-626	38.8	13.6	57.1	55.6	1.3	50.9	17.5	43.7
GU 21-628	39.4	16.4	56.3	54.8	1.3	56.1	21.5	43.5
GU 21-642	39.0	6.2	59.7	56.8	3.0	48.4	7.6	44.2
GU 21-644	38.8	10.3	58.7	55.7	2.8	49.1	13.0	44.0
GU 21-646	39.1	13.7	57.8	54.8	2.6	50.5	17.5	43.8
GU 21-648	39.6	16.5	57.1	54.1	2.5	56.0	21.5	43.6
GU 21-662	39.7	6.3	60.4	56.0	4.5	48.1	7.5	44.5
GU 21-664	39.2	10.5	59.4	54.9	4.2	49.0	12.8	44.2
GU 21-666	39.3	14.0	58.6	54.1	4.0	50.3	17.3	43.9
GU 21-668	39.7	16.9	57.8	53.3	3.8	56.8	21.4	43.7
GU 21-682	40.7	6.2	61.0	55.2	6.0	48.0	7.3	45.1
GU 21-684	39.9	10.6	60.1	54.1	5.7	48.8	12.6	44.5
GU 21-686	39.8	14.1	59.3	53.3	5.4	50.1	17.2	44.2
GU 21-688	40.0	17.2	58.6	52.5	5.1	52.3	21.2	43.9
GU 21-722	36.8	8.5	68.9	67.7	1.5	51.1	8.1	47.4
GU 21-724	36.7	14.2	67.9	66.6	1.4	52.2	13.7	47.5
GU 21-726	36.9	18.8	67.1	65.7	1.3	57.1	18.6	47.6
GU 21-728	37.5	22.7	66.4	65.0	1.2	60.8	22.9	47.6
GU 21-742	37.2	8.5	69.5	67.0	2.9	51.0	8.0	47.5
GU 21-744	37.0	14.2	68.6	65.9	2.7	52.2	13.7	47.7
GU 21-746	37.2	18.9	67.8	65.0	2.6	58.1	18.5	47.7
GU 21-748	37.6	22.9	67.2	64.3	2.4	57.6	22.9	47.6
GU 21-762	38.0	8.6	70.2	66.4	4.4	50.9	7.9	47.8
GU 21-764	37.4	14.4	69.3	65.3	4.1	52.0	13.5	47.8
GU 21-766	37.5	19.1	68.5	64.3	3.9	59.1	18.4	47.8
GU 21-768	37.8	23.3	67.9	63.6	3.7	58.6	22.8	47.8
GU 21-782	38.9	8.6	70.8	65.8	5.8	50.8	7.6	48.3
GU 21-784	38.0	14.5	69.9	64.6	5.5	51.9	13.4	48.1
GU 21-786	37.8	19.3	69.3	63.6	5.2	53.4	18.2	48.0
GU 21-788	38.0	23.6	68.7	62.8	5.0	58.3	22.6	47.9

AEROFOIL	ZERO LIFT INCIDENCE (deg)	LIFT CURVE SLOPE (/deg)	LOW DRAG RANGE OF LIFT COEFFICIENT LOWER LIMIT	DESIGN	UPPER LIMIT	AERODYNAMIC CENTRE POSN. (percent c) x	y	PITCHING MOMENT COEF.
GU 21-562	-3.7	0.116	0.58	0.69	0.81	26.0	1.3	-0.082
GU 21-564	-3.5	0.119	0.48	0.71	0.95	26.7	1.4	-0.076
GU 21-566	-3.3	0.123	0.37	0.73	1.10	27.2	1.4	-0.071
GU 21-568	-3.2	0.126	0.25	0.75	1.25	27.7	1.3	-0.067
GU 21-582	-5.0	0.116	0.81	0.92	1.04	26.0	1.8	-0.110
GU 21-584	-4.7	0.120	0.72	0.95	1.19	26.7	1.9	-0.102
GU 21-586	-4.5	0.123	0.61	0.98	1.34	27.2	1.9	-0.095
GU 21-588	-4.3	0.126	0.50	1.00	1.50	27.7	1.8	-0.090
GU 21-622	-1.4	0.116	0.12	0.23	0.35	26.3	0.4	-0.032
GU 21-624	-1.3	0.120	0.00	0.24	0.48	27.1	0.4	-0.030
GU 21-626	-1.2	0.124	-0.12	0.25	0.62	27.8	0.4	-0.028
GU 21-628	-1.2	0.127	-0.25	0.25	0.76	28.5	0.4	-0.027
GU 21-642	-2.7	0.116	0.35	0.46	0.58	26.3	0.8	-0.064
GU 21-644	-2.6	0.120	0.24	0.48	0.72	27.1	0.8	-0.060
GU 21-646	-2.5	0.124	0.12	0.49	0.86	27.9	0.8	-0.057
GU 21-648	-2.3	0.127	0.00	0.51	1.01	28.5	0.8	-0.054
GU 21-662	-4.1	0.116	0.58	0.69	0.81	26.3	1.1	-0.096
GU 21-664	-3.9	0.120	0.48	0.72	0.96	27.2	1.2	-0.090
GU 21-666	-3.7	0.124	0.37	0.74	1.11	27.9	1.2	-0.086
GU 21-668	-3.6	0.127	0.25	0.76	1.26	28.6	1.2	-0.082
GU 21-682	-5.4	0.116	0.81	0.93	1.04	26.3	1.5	-0.128
GU 21-684	-5.2	0.120	0.72	0.96	1.20	27.2	1.6	-0.121
GU 21-686	-5.0	0.124	0.62	0.99	1.36	28.0	1.7	-0.115
GU 21-688	-4.8	0.127	0.51	1.01	1.52	28.6	1.7	-0.109
GU 21-722	-1.5	0.116	0.12	0.23	0.35	26.6	0.2	-0.037
GU 21-724	-1.4	0.121	0.00	0.24	0.48	27.6	0.2	-0.036
GU 21-726	-1.4	0.125	-0.13	0.25	0.62	28.5	0.2	-0.035
GU 21-728	-1.3	0.129	-0.26	0.26	0.77	29.4	0.2	-0.034
GU 21-742	-2.9	0.116	0.35	0.46	0.58	26.6	0.5	-0.074
GU 21-744	-2.8	0.121	0.24	0.48	0.72	27.6	0.6	-0.071
GU 21-746	-2.7	0.125	0.13	0.50	0.87	28.6	0.6	-0.069
GU 21-748	-2.6	0.129	0.00	0.52	1.03	29.4	0.5	-0.067
GU 21-762	-4.4	0.116	0.58	0.70	0.81	26.6	0.9	-0.111
GU 21-764	-4.3	0.121	0.48	0.73	0.97	27.7	0.9	-0.106
GU 21-766	-4.1	0.125	0.38	0.75	1.12	28.6	0.9	-0.103
GU 21-768	-4.0	0.129	0.26	0.77	1.28	29.5	0.9	-0.100
GU 21-782	-5.9	0.117	0.81	0.93	1.05	26.6	1.2	-0.147
GU 21-784	-5.7	0.121	0.73	0.97	1.21	27.7	1.2	-0.141
GU 21-786	-5.5	0.125	0.63	1.00	1.37	28.7	1.3	-0.137
GU 21-788	-5.3	0.129	0.52	1.03	1.54	29.5	1.2	-0.132

AEROFOIL	THICKNESS AT 0.05c (percent of max.)	T.E. ANGLE (deg)	EXTENT OF FAV. PRESSURE GRAD. (percent c) TOP	BOTTOM	MAX.CAMBER (per cent chord)	POSITION (percent chord)	MAX. THICKNESS (per cent chord)	POSITION (percent chord)
GU 23-322	46.0	5.3	29.9	28.0	1.4	35.7	6.3	31.3
GU 23-324	46.1	8.6	29.1	27.4	1.3	34.9	10.6	30.8
GU 23-326	46.9	11.3	28.5	26.9	1.2	34.4	14.0	30.3
GU 23-328	47.9	13.5	27.9	26.4	1.1	34.6	17.1	29.9
GU 23-342	46.0	5.2	30.7	26.9	2.9	34.8	6.3	31.7
GU 23-344	46.3	8.5	29.9	26.4	2.6	34.3	10.5	31.0
GU 23-346	47.1	11.2	29.2	26.0	2.4	34.2	14.0	30.5
GU 23-348	47.9	13.4	28.6	25.7	2.2	34.4	17.0	30.1
GU 23-362	46.8	5.0	31.5	25.7	4.3	34.4	6.2	32.2
GU 23-364	46.9	8.4	30.7	25.4	4.0	34.3	10.4	31.3
GU 23-366	47.4	11.1	29.9	25.1	3.7	34.2	13.9	30.8
GU 23-368	48.1	13.4	29.3	24.8	3.4	34.2	16.9	30.3
GU 23-382	47.7	4.8	32.2	24.4	5.7	34.5	6.0	32.7
GU 23-384	47.7	8.2	31.3	24.2	5.3	34.3	10.2	31.8
GU 23-386	48.0	11.0	30.6	24.1	5.0	34.1	13.7	31.1
GU 23-388	48.5	13.4	30.0	23.9	4.6	34.1	16.7	30.6
GU 23-422	42.2	6.3	39.6	37.8	1.5	39.5	6.9	36.6
GU 23-424	42.6	10.3	38.7	37.0	1.4	43.0	11.6	36.1
GU 23-426	43.2	13.5	37.9	36.4	1.3	42.2	15.5	35.6
GU 23-428	44.1	16.2	37.3	35.8	1.2	41.4	18.9	35.2
GU 23-442	42.7	6.2	40.4	36.8	3.0	39.6	6.8	36.9
GU 23-444	42.9	10.2	39.5	36.1	2.7	43.7	11.5	36.1
GU 23-446	43.5	13.4	38.7	35.5	2.6	42.8	15.4	35.6
GU 23-448	44.1	16.1	38.0	35.0	2.4	42.1	18.8	35.2
GU 23-462	43.6	6.0	41.1	35.7	4.5	39.5	6.7	37.8
GU 23-464	43.5	10.1	40.2	35.1	4.2	39.7	11.4	36.5
GU 23-466	43.8	13.4	39.4	34.6	3.9	43.5	15.3	35.8
GU 23-468	44.3	16.1	38.7	34.2	3.6	42.7	18.7	35.3
GU 23-482	44.6	5.8	41.8	34.5	6.0	39.3	6.5	39.1
GU 23-484	44.3	10.0	40.9	34.1	5.6	39.7	11.2	37.2
GU 23-486	44.4	13.3	40.1	33.7	5.3	39.8	15.1	36.3
GU 23-488	44.7	16.2	39.4	33.3	4.9	43.4	18.5	35.6
GU 23-522	39.9	7.6	49.3	47.7	1.5	44.7	7.4	40.9
GU 23-524	39.9	12.6	48.4	46.8	1.4	45.8	12.4	40.7
GU 23-526	40.5	16.5	47.6	46.1	1.3	47.4	16.7	40.4
GU 23-528	41.3	19.9	46.9	45.4	1.2	47.2	20.5	40.1
GU 23-542	40.3	7.6	50.1	46.8	3.0	45.3	7.3	41.2
GU 23-544	40.4	12.5	49.1	46.0	2.8	45.5	12.4	40.8
GU 23-546	40.7	16.5	48.4	45.3	2.6	47.0	16.6	40.5
GU 23-548	41.3	19.9	47.7	44.7	2.5	47.4	20.4	40.1

AEROFOIL	ZERO LIFT INCIDENCE (deg)	LIFT CURVE SLOPE (/deg)	LOW DRAG RANGE OF LIFT COEFFICIENT LOWER LIMIT	DESIGN	UPPER LIMIT	AERODYNAMIC CENTRE POSN. (percent c) x	y	PITCHING MOMENT COEF.
GU 23-322	-1.0	0.115	0.11	0.23	0.34	25.6	0.5	-0.020
GU 23-324	-1.0	0.118	0.00	0.24	0.47	26.1	0.5	-0.018
GU 23-326	-0.9	0.121	-0.12	0.24	0.60	26.4	0.5	-0.017
GU 23-328	-0.8	0.123	-0.25	0.25	0.74	26.7	0.4	-0.015
GU 23-342	-2.1	0.115	0.34	0.46	0.57	25.6	1.1	-0.040
GU 23-344	-2.0	0.118	0.24	0.47	0.71	26.1	1.0	-0.036
GU 23-346	-1.8	0.121	0.12	0.48	0.84	26.4	1.0	-0.033
GU 23-348	-1.7	0.123	0.00	0.49	0.98	26.7	0.9	-0.031
GU 23-362	-3.2	0.115	0.57	0.69	0.80	25.6	1.6	-0.060
GU 23-364	-3.0	0.118	0.47	0.71	0.94	26.1	1.6	-0.055
GU 23-366	-2.8	0.121	0.36	0.72	1.08	26.4	1.6	-0.050
GU 23-368	-2.6	0.123	0.25	0.74	1.23	26.7	1.5	-0.046
GU 23-382	-4.2	0.115	0.80	0.92	1.03	25.5	2.2	-0.081
GU 23-384	-4.0	0.118	0.71	0.94	1.18	26.0	2.2	-0.073
GU 23-386	-3.7	0.121	0.60	0.96	1.32	26.4	2.1	-0.067
GU 23-388	-3.5	0.123	0.49	0.98	1.47	26.7	2.1	-0.062
GU 23-422	-1.2	0.115	0.11	0.23	0.34	25.9	0.5	-0.024
GU 23-424	-1.1	0.119	0.00	0.24	0.47	26.5	0.5	-0.022
GU 23-426	-1.0	0.122	-0.12	0.24	0.61	26.9	0.5	-0.021
GU 23-428	-0.9	0.125	-0.25	0.25	0.75	27.3	0.4	-0.019
GU 23-442	-2.3	0.115	0.34	0.46	0.57	25.9	1.0	-0.047
GU 23-444	-2.2	0.119	0.24	0.47	0.71	26.5	1.0	-0.043
GU 23-446	-2.0	0.122	0.12	0.49	0.85	26.9	1.0	-0.041
GU 23-448	-1.9	0.125	0.00	0.50	0.99	27.3	0.9	-0.038
GU 23-462	-3.5	0.115	0.58	0.69	0.80	25.9	1.5	-0.071
GU 23-464	-3.3	0.119	0.48	0.71	0.95	26.4	1.6	-0.065
GU 23-466	-3.1	0.122	0.37	0.73	1.09	26.9	1.5	-0.061
GU 23-468	-2.9	0.125	0.25	0.75	1.24	27.3	1.5	-0.057
GU 23-482	-4.6	0.115	0.81	0.92	1.03	25.9	2.0	-0.095
GU 23-484	-4.4	0.119	0.71	0.95	1.18	26.4	2.1	-0.087
GU 23-486	-4.2	0.122	0.61	0.97	1.33	26.9	2.1	-0.081
GU 23-488	-3.9	0.125	0.50	1.00	1.49	27.3	2.0	-0.076
GU 23-522	-1.2	0.115	0.12	0.23	0.35	26.1	0.4	-0.027
GU 23-524	-1.2	0.119	0.00	0.24	0.48	26.8	0.4	-0.025
GU 23-526	-1.1	0.123	-0.12	0.25	0.61	27.4	0.4	-0.024
GU 23-528	-1.0	0.126	-0.25	0.25	0.76	27.9	0.4	-0.022
GU 23-542	-2.5	0.115	0.35	0.46	0.58	26.1	0.9	-0.055
GU 23-544	-2.4	0.120	0.24	0.48	0.72	26.8	0.9	-0.051
GU 23-546	-2.2	0.123	0.12	0.49	0.86	27.4	0.9	-0.048
GU 23-548	-2.1	0.126	0.00	0.50	1.01	28.0	0.8	-0.045

APPENDIX III, Part 2

AEROFOIL	THICKNESS AT 0.05c (percent of max.)	T.E. ANGLE (deg)	EXTENT OF FAV. PRESSURE GRAD. (percent c) TOP	BOTTOM	MAX. CAMBER (per cent chord)	POSITION (percent chord)	MAX. THICKNESS (per cent chord)	POSITION (percent chord)
GU 23-562	41.3	7.4	50.8	45.9	4.5	46.2	7.1	41.7
GU 23-564	40.9	12.4	49.9	45.1	4.3	45.4	12.2	41.0
GU 23-566	41.1	16.5	49.1	44.4	4.0	46.5	16.5	40.6
GU 23-568	41.5	19.9	48.4	43.9	3.8	47.2	20.3	40.3
GU 23-582	42.4	7.3	51.5	44.9	6.1	46.8	6.9	42.7
GU 23-584	41.6	12.4	50.6	44.1	5.7	46.0	12.0	41.5
GU 23-586	41.6	16.5	49.8	43.5	5.4	45.9	16.3	40.9
GU 23-588	41.8	20.0	49.2	43.0	5.1	46.8	20.1	40.4
GU 23-622	38.2	9.6	59.2	57.7	1.5	49.6	7.8	44.7
GU 23-624	38.1	15.9	58.2	56.7	1.4	49.2	13.2	44.7
GU 23-626	38.5	21.0	57.5	55.9	1.3	50.6	17.8	44.6
GU 23-628	39.1	25.4	56.8	55.3	1.2	56.4	21.9	44.4
GU 23-642	38.6	9.5	59.9	57.0	3.0	48.5	7.7	44.9
GU 23-644	38.4	15.9	58.9	56.0	2.8	49.1	13.1	44.8
GU 23-646	38.6	21.0	58.2	55.2	2.6	50.4	17.7	44.7
GU 23-648	39.1	25.4	57.6	54.5	2.5	56.4	21.9	44.5
GU 23-662	39.3	9.4	60.5	56.2	4.5	48.0	7.6	45.3
GU 23-664	38.8	15.8	59.6	55.2	4.2	48.9	13.0	45.0
GU 23-666	38.9	21.0	58.9	54.4	4.0	50.2	17.6	44.8
GU 23-668	39.3	25.4	58.3	53.7	3.7	57.2	21.7	44.6
GU 23-682	40.3	9.3	61.2	55.4	6.0	48.1	7.3	45.9
GU 23-684	39.4	15.7	60.4	54.4	5.7	48.8	12.8	45.3
GU 23-686	39.3	21.0	59.7	53.6	5.4	49.9	17.4	45.1
GU 23-688	39.5	25.5	59.1	53.0	5.1	51.7	21.6	44.8
GU 23-722	36.5	12.6	69.1	67.8	1.5	51.1	8.2	48.1
GU 23-724	36.3	21.0	68.3	66.9	1.4	52.1	13.9	48.3
GU 23-726	36.5	27.9	67.6	66.2	1.3	57.5	18.8	48.4
GU 23-728	37.0	33.8	67.0	65.6	1.2	57.1	23.3	48.5
GU 23-742	36.9	12.6	69.7	67.2	2.9	50.9	8.1	48.3
GU 23-744	36.6	21.0	68.9	66.2	2.7	52.1	13.8	48.5
GU 23-746	36.8	27.9	68.3	65.5	2.5	58.5	18.8	48.6
GU 23-748	37.2	33.8	67.8	64.8	2.4	58.1	23.3	48.6
GU 23-762	37.6	12.5	70.4	66.6	4.4	50.9	7.9	48.6
GU 23-764	37.0	21.0	69.6	65.6	4.1	52.0	13.7	48.7
GU 23-766	37.0	27.9	69.0	64.8	3.9	53.4	18.7	48.7
GU 23-768	37.3	33.9	68.5	64.1	3.7	59.1	23.2	48.7
GU 23-782	38.5	12.4	71.0	65.9	5.8	50.8	7.7	49.1
GU 23-784	37.6	20.9	70.3	64.9	5.5	51.8	13.5	49.0
GU 23-786	37.4	27.9	69.7	64.1	5.2	53.2	18.5	49.0
GU 23-788	37.5	34.0	69.3	63.4	4.9	58.8	23.0	49.0

AEROFOIL	ZERO LIFT INCIDENCE (deg)	LIFT CURVE SLOPE (/deg)	LOW DRAG RANGE OF LIFT COEFFICIENT LOWER LIMIT	DESIGN	UPPER LIMIT	AERODYNAMIC CENTRE POSN. (percent c) x	y	PITCHING MOMENT COEF.
GU 23-562	-3.7	0.116	0.58	0.69	0.81	26.1	1.3	-0.082
GU 23-564	-3.6	0.120	0.48	0.72	0.95	26.8	1.4	-0.077
GU 23-566	-3.4	0.123	0.37	0.74	1.10	27.4	1.4	-0.072
GU 23-568	-3.2	0.126	0.25	0.76	1.26	28.0	1.3	-0.068
GU 23-582	-5.0	0.116	0.81	0.92	1.04	26.1	1.8	-0.110
GU 23-584	-4.8	0.120	0.72	0.96	1.19	26.8	1.9	-0.102
GU 23-586	-4.5	0.123	0.62	0.98	1.35	27.5	1.9	-0.096
GU 23-588	-4.3	0.126	0.51	1.01	1.51	28.0	1.8	-0.091
GU 23-622	-1.4	0.116	0.12	0.23	0.35	26.4	0.4	-0.032
GU 23-624	-1.3	0.120	0.00	0.24	0.48	27.3	0.4	-0.030
GU 23-626	-1.2	0.124	-0.12	0.25	0.62	28.1	0.4	-0.029
GU 23-628	-1.2	0.128	-0.26	0.26	0.77	28.8	0.4	-0.027
GU 23-642	-2.7	0.116	0.35	0.46	0.58	26.4	0.8	-0.064
GU 23-644	-2.6	0.120	0.24	0.48	0.72	27.3	0.8	-0.060
GU 23-646	-2.5	0.124	0.12	0.50	0.87	28.1	0.8	-0.058
GU 23-648	-2.4	0.128	0.00	0.51	1.02	28.8	0.8	-0.055
GU 23-662	-4.1	0.116	0.58	0.70	0.81	26.4	1.1	-0.096
GU 23-664	-3.9	0.121	0.48	0.72	0.96	27.3	1.2	-0.091
GU 23-666	-3.8	0.124	0.37	0.74	1.11	28.2	1.2	-0.087
GU 23-668	-3.6	0.128	0.26	0.77	1.27	28.9	1.2	-0.083
GU 23-682	-5.4	0.116	0.81	0.93	1.04	26.4	1.5	-0.128
GU 23-684	-5.2	0.121	0.72	0.96	1.20	27.4	1.6	-0.121
GU 23-686	-5.0	0.125	0.62	0.99	1.36	28.2	1.6	-0.116
GU 23-688	-4.8	0.128	0.51	1.02	1.53	28.9	1.6	-0.111
GU 23-722	-1.5	0.116	0.12	0.23	0.35	26.7	0.2	-0.037
GU 23-724	-1.4	0.121	0.00	0.24	0.48	27.8	0.2	-0.036
GU 23-726	-1.4	0.126	-0.13	0.25	0.63	28.8	0.2	-0.035
GU 23-728	-1.3	0.130	-0.26	0.26	0.78	29.7	0.2	-0.034
GU 23-742	-2.9	0.116	0.35	0.47	0.58	26.7	0.5	-0.074
GU 23-744	-2.9	0.121	0.24	0.49	0.73	27.8	0.6	-0.072
GU 23-746	-2.8	0.126	0.13	0.50	0.88	28.9	0.5	-0.069
GU 23-748	-2.6	0.130	0.00	0.52	1.04	29.8	0.5	-0.068
GU 23-762	-4.4	0.117	0.58	0.70	0.81	26.7	0.8	-0.111
GU 23-764	-4.3	0.122	0.49	0.73	0.97	27.9	0.9	-0.107
GU 23-766	-4.2	0.126	0.38	0.75	1.13	28.9	0.9	-0.104
GU 23-768	-4.0	0.130	0.26	0.78	1.29	29.8	0.8	-0.101
GU 23-782	-5.9	0.117	0.82	0.93	1.05	26.8	1.1	-0.148
GU 23-784	-5.8	0.122	0.73	0.97	1.21	27.9	1.2	-0.142
GU 23-786	-5.6	0.126	0.63	1.00	1.38	29.0	1.2	-0.138
GU 23-788	-5.4	0.130	0.52	1.04	1.55	29.9	1.2	-0.134

AEROFOIL	THICKNESS AT 0.05c (percent of max.)	T.E. ANGLE (deg)	EXTENT OF FAV. PRESSURE GRAD. (percent c) TOP	BOTTOM	MAX.CAMBER (per cent chord)	POSITION (percent chord)	MAX. THICKNESS (per cent chord)	POSITION (percent chord)
GU 25-322	45.6	6.4	29.9	28.1	1.4	35.8	6.4	31.8
GU 25-324	45.7	10.4	29.2	27.5	1.3	35.0	10.7	31.4
GU 25-326	46.5	13.6	28.6	27.0	1.2	34.6	14.2	30.9
GU 25-328	47.4	16.3	28.1	26.6	1.1	34.7	17.3	30.5
GU 25-342	45.6	6.2	30.8	26.9	2.9	34.9	6.4	32.1
GU 25-344	45.9	10.3	30.0	26.5	2.7	34.3	10.6	31.5
GU 25-346	46.7	13.5	29.4	26.2	2.4	34.4	14.2	31.1
GU 25-348	47.4	16.2	28.8	25.8	2.2	34.5	17.2	30.6
GU 25-362	46.4	6.0	31.6	25.8	4.3	34.5	6.2	32.6
GU 25-364	46.5	10.1	30.7	25.5	4.0	34.3	10.5	31.8
GU 25-366	47.0	13.4	30.1	25.2	3.7	34.3	14.0	31.3
GU 25-368	47.7	16.1	29.5	25.0	3.4	34.3	17.1	30.8
GU 25-382	47.3	5.7	32.3	24.4	5.7	34.5	6.1	33.1
GU 25-384	47.3	9.8	31.4	24.3	5.4	34.3	10.3	32.2
GU 25-386	47.6	13.2	30.7	24.2	5.0	34.2	13.9	31.6
GU 25-388	48.0	16.0	30.1	24.0	4.7	34.2	17.0	31.1
GU 25-422	41.9	7.5	39.6	37.9	1.5	39.6	7.0	37.0
GU 25-424	42.2	12.2	38.8	37.1	1.4	43.2	11.7	36.5
GU 25-426	42.8	16.1	38.1	36.5	1.3	42.4	15.7	36.1
GU 25-428	43.7	19.3	37.5	36.0	1.2	41.7	19.1	35.7
GU 25-442	42.4	7.3	40.4	36.9	3.0	39.6	6.9	37.4
GU 25-444	42.5	12.2	39.6	36.2	2.7	43.8	11.6	36.6
GU 25-446	43.1	16.0	38.9	35.7	2.6	43.0	15.6	36.1
GU 25-448	43.7	19.3	38.2	35.2	2.4	42.3	19.0	35.7
GU 25-462	43.2	7.2	41.2	35.8	4.5	39.5	6.8	38.4
GU 25-464	43.1	12.0	40.3	35.3	4.2	39.7	11.5	37.1
GU 25-466	43.4	15.9	39.6	34.8	3.9	43.7	15.4	36.4
GU 25-468	44.0	19.2	38.9	34.4	3.6	43.0	18.9	35.9
GU 25-482	44.2	6.9	41.9	34.6	6.0	39.4	6.6	39.6
GU 25-484	43.9	11.8	41.0	34.2	5.6	39.7	11.3	37.8
GU 25-486	44.0	15.7	40.3	33.8	5.3	39.9	15.3	36.9
GU 25-488	44.3	19.1	39.7	33.5	4.9	43.6	18.7	36.3
GU 25-522	39.6	9.0	49.4	47.8	1.5	44.8	7.4	41.5
GU 25-524	39.7	14.8	48.5	46.9	1.4	45.9	12.6	41.2
GU 25-526	40.2	19.5	47.8	46.3	1.3	47.6	16.9	41.0
GU 25-528	40.9	23.5	47.2	45.7	1.2	47.3	20.7	40.7
GU 25-542	40.0	8.9	50.2	46.9	3.0	45.4	7.4	41.7
GU 25-544	40.0	14.7	49.3	46.1	2.8	45.5	12.5	41.4
GU 25-546	40.4	19.4	48.6	45.5	2.7	47.2	16.8	41.1
GU 25-548	40.9	23.5	47.9	44.9	2.5	47.5	20.7	40.8

AEROFOIL	ZERO LIFT INCIDENCE (deg)	LIFT CURVE SLOPE (/deg)	LOW DRAG RANGE OF LIFT COEFFICIENT LOWER LIMIT	DESIGN	UPPER LIMIT	AERODYNAMIC CENTRE POSN. (percent c) x	y	PITCHING MOMENT COEF.
GU 25-322	-1.0	0.115	0.11	0.23	0.34	25.7	0.5	-0.020
GU 25-324	-1.0	0.118	0.00	0.24	0.47	26.2	0.5	-0.018
GU 25-326	-0.9	0.121	-0.12	0.24	0.61	26.6	0.5	-0.017
GU 25-328	-0.8	0.124	-0.25	0.25	0.74	26.9	0.4	-0.015
GU 25-342	-2.1	0.115	0.34	0.46	0.57	25.7	1.1	-0.040
GU 25-344	-2.0	0.118	0.24	0.47	0.71	26.2	1.0	-0.036
GU 25-346	-1.8	0.121	0.12	0.48	0.85	26.6	1.0	-0.033
GU 25-348	-1.7	0.124	0.00	0.49	0.99	26.9	0.9	-0.031
GU 25-362	-3.2	0.115	0.57	0.69	0.80	25.7	1.6	-0.061
GU 25-364	-3.0	0.118	0.47	0.71	0.94	26.2	1.6	-0.055
GU 25-366	-2.8	0.121	0.36	0.73	1.09	26.6	1.6	-0.050
GU 25-368	-2.6	0.124	0.25	0.74	1.23	26.9	1.5	-0.046
GU 25-382	-4.2	0.115	0.80	0.92	1.03	25.6	2.2	-0.081
GU 25-384	-4.0	0.119	0.71	0.94	1.18	26.1	2.2	-0.073
GU 25-386	-3.7	0.121	0.61	0.97	1.33	26.5	2.1	-0.067
GU 25-388	-3.5	0.124	0.50	0.99	1.48	26.9	2.1	-0.062
GU 25-422	-1.2	0.115	0.12	0.23	0.35	26.0	0.5	-0.024
GU 25-424	-1.1	0.119	0.00	0.24	0.48	26.6	0.5	-0.022
GU 25-426	-1.0	0.122	-0.12	0.24	0.61	27.1	0.5	-0.020
GU 25-428	-0.9	0.125	-0.25	0.25	0.75	27.5	0.4	-0.019
GU 25-442	-2.3	0.115	0.35	0.46	0.58	25.9	1.0	-0.047
GU 25-444	-2.2	0.119	0.24	0.48	0.71	26.6	1.0	-0.043
GU 25-446	-2.0	0.122	0.12	0.49	0.85	27.0	1.0	-0.041
GU 25-448	-1.9	0.125	0.00	0.50	1.00	27.5	0.9	-0.038
GU 25-462	-3.5	0.115	0.58	0.69	0.81	26.0	1.5	-0.071
GU 25-464	-3.3	0.119	0.48	0.71	0.95	26.5	1.6	-0.065
GU 25-466	-3.1	0.122	0.37	0.73	1.10	27.1	1.5	-0.061
GU 25-468	-2.9	0.125	0.25	0.75	1.25	27.5	1.5	-0.057
GU 25-482	-4.6	0.116	0.81	0.92	1.04	25.9	2.0	-0.095
GU 25-484	-4.4	0.119	0.71	0.95	1.19	26.5	2.1	-0.087
GU 25-486	-4.2	0.122	0.61	0.98	1.34	27.1	2.1	-0.082
GU 25-488	-3.9	0.125	0.50	1.00	1.49	27.5	2.0	-0.076
GU 25-522	-1.2	0.116	0.12	0.23	0.35	26.2	0.4	-0.027
GU 25-524	-1.2	0.120	0.00	0.24	0.48	27.0	0.4	-0.025
GU 25-526	-1.1	0.123	-0.12	0.25	0.62	27.6	0.4	-0.024
GU 25-528	-1.0	0.127	-0.25	0.25	0.76	28.2	0.4	-0.022
GU 25-542	-2.5	0.116	0.35	0.46	0.58	26.2	0.9	-0.055
GU 25-544	-2.4	0.120	0.24	0.48	0.72	26.9	0.9	-0.051
GU 25-546	-2.2	0.123	0.12	0.49	0.86	27.6	0.9	-0.048
GU 25-548	-2.1	0.127	0.00	0.51	1.01	28.2	0.8	-0.045

AEROFOIL	THICKNESS AT 0.05c (percent of max.)	T.E. ANGLE (deg)	EXTENT OF FAV. PRESSURE GRAD. (percent c) TOP	BOTTOM	MAX.CAMBER (per cent chord)	POSITION (percent chord)	MAX. THICKNESS (per cent chord)	POSITION (percent chord)
GU 25-562	41.0	8.7	50.9	46.0	4.5	46.3	7.2	42.2
GU 25-564	40.5	14.6	50.0	45.2	4.3	45.5	12.4	41.7
GU 25-566	40.7	19.3	49.3	44.6	4.0	46.4	16.7	41.3
GU 25-568	41.1	23.4	48.7	44.1	3.8	47.3	20.5	40.9
GU 25-582	42.0	8.5	51.6	45.0	6.1	46.9	7.0	43.4
GU 25-584	41.3	14.4	50.7	44.3	5.7	46.1	12.2	42.1
GU 25-586	41.2	19.2	50.0	43.7	5.4	45.9	16.5	41.6
GU 25-588	41.4	23.3	49.4	43.2	5.1	46.8	20.4	41.1
GU 25-622	37.9	11.0	59.3	57.8	1.5	49.6	7.9	45.3
GU 25-624	37.8	18.3	58.4	56.9	1.4	49.3	13.3	45.3
GU 25-626	38.1	24.2	57.7	56.2	1.3	50.8	18.0	45.2
GU 25-628	38.7	29.3	57.1	55.6	1.2	56.5	22.2	45.1
GU 25-642	38.3	11.0	60.0	57.1	3.0	48.6	7.8	45.5
GU 25-644	38.0	18.3	59.1	56.2	2.8	49.1	13.3	45.4
GU 25-646	38.3	24.2	58.5	55.4	2.6	50.4	17.9	45.3
GU 25-648	38.7	29.3	57.9	54.8	2.5	56.8	22.1	45.2
GU 25-662	39.0	10.8	60.6	56.3	4.5	48.1	7.6	45.9
GU 25-664	38.5	18.2	59.8	55.4	4.2	49.0	13.1	45.7
GU 25-666	38.5	24.1	59.2	54.7	4.0	50.2	17.8	45.5
GU 25-668	38.9	29.3	58.6	54.1	3.8	52.0	22.0	45.3
GU 25-682	40.0	10.7	61.3	55.5	6.0	48.2	7.4	46.6
GU 25-684	39.1	18.0	60.5	54.6	5.7	48.8	12.9	46.0
GU 25-686	39.0	24.0	59.9	53.9	5.4	49.9	17.6	45.8
GU 25-688	39.2	29.2	59.4	53.3	5.1	51.5	21.8	45.6
GU 25-722	36.3	14.1	69.2	68.0	1.5	51.2	8.2	48.6
GU 25-724	36.0	23.5	68.5	67.1	1.4	52.3	14.0	48.9
GU 25-726	36.3	31.2	67.9	66.5	1.3	57.8	19.0	49.0
GU 25-728	36.7	37.9	67.4	65.9	1.2	57.4	23.6	49.2
GU 25-742	36.6	14.1	69.9	67.3	2.9	51.0	8.1	48.8
GU 25-744	36.4	23.5	69.1	66.5	2.7	52.1	14.0	49.0
GU 25-746	36.5	31.2	68.6	65.8	2.5	58.7	19.0	49.2
GU 25-748	36.9	37.9	68.2	65.2	2.4	58.4	23.5	49.3
GU 25-762	37.4	14.0	70.5	66.7	4.4	50.9	8.0	49.1
GU 25-764	36.8	23.4	69.8	65.8	4.1	52.0	13.8	49.3
GU 25-766	36.8	31.2	69.3	65.1	3.9	53.5	18.9	49.4
GU 25-768	37.0	37.9	68.9	64.5	3.7	59.5	23.4	49.5
GU 25-782	38.3	13.8	71.1	66.0	5.8	50.9	7.8	49.7
GU 25-784	37.3	23.3	70.5	65.1	5.5	51.9	13.7	49.6
GU 25-786	37.1	31.1	70.1	64.3	5.2	53.2	18.7	49.6
GU 25-788	37.2	37.9	69.7	63.7	4.9	59.1	23.3	49.7

AEROFOIL	ZERO LIFT INCIDENCE (deg)	LIFT CURVE SLOPE (/deg)	LOW DRAG RANGE OF LIFT COEFFICIENT LOWER LIMIT	DESIGN	UPPER LIMIT	AERODYNAMIC CENTRE POSN. (percent c) x	y	PITCHING MOMENT COEF.
GU 25-562	-3.7	0.116	0.58	0.69	0.81	26.2	1.3	-0.082
GU 25-564	-3.6	0.120	0.48	0.72	0.96	26.9	1.4	-0.077
GU 25-566	-3.4	0.124	0.37	0.74	1.11	27.6	1.4	-0.072
GU 25-568	-3.2	0.127	0.25	0.76	1.26	28.2	1.3	-0.068
GU 25-582	-5.0	0.116	0.81	0.93	1.04	26.1	1.8	-0.110
GU 25-584	-4.8	0.120	0.72	0.96	1.20	27.0	1.9	-0.103
GU 25-586	-4.6	0.124	0.62	0.99	1.35	27.6	1.9	-0.097
GU 25-588	-4.3	0.127	0.51	1.01	1.51	28.2	1.8	-0.092
GU 25-622	-1.4	0.116	0.12	0.23	0.35	26.4	0.4	-0.032
GU 25-624	-1.3	0.121	0.00	0.24	0.48	27.4	0.4	-0.030
GU 25-626	-1.2	0.125	-0.12	0.25	0.62	28.3	0.4	-0.029
GU 25-628	-1.2	0.128	-0.26	0.26	0.77	29.0	0.4	-0.027
GU 25-642	-2.7	0.116	0.35	0.46	0.58	26.4	0.8	-0.064
GU 25-644	-2.6	0.121	0.24	0.48	0.72	27.4	0.8	-0.061
GU 25-646	-2.5	0.125	0.12	0.50	0.87	28.3	0.8	-0.058
GU 25-648	-2.4	0.128	0.00	0.51	1.02	29.0	0.8	-0.055
GU 25-662	-4.1	0.116	0.58	0.70	0.81	26.5	1.1	-0.096
GU 25-664	-3.9	0.121	0.48	0.72	0.96	27.5	1.2	-0.091
GU 25-666	-3.8	0.125	0.37	0.75	1.12	28.3	1.2	-0.087
GU 25-668	-3.6	0.128	0.26	0.77	1.28	29.1	1.2	-0.083
GU 25-682	-5.5	0.117	0.81	0.93	1.04	26.5	1.5	-0.129
GU 25-684	-5.3	0.121	0.72	0.96	1.20	27.5	1.6	-0.122
GU 25-686	-5.1	0.125	0.62	1.00	1.37	28.4	1.6	-0.116
GU 25-688	-4.9	0.129	0.51	1.03	1.53	29.1	1.6	-0.112
GU 25-722	-1.5	0.117	0.12	0.23	0.35	26.7	0.2	-0.037
GU 25-724	-1.4	0.122	0.00	0.24	0.49	27.9	0.2	-0.036
GU 25-726	-1.4	0.126	-0.13	0.25	0.63	29.0	0.2	-0.035
GU 25-728	-1.3	0.130	-0.26	0.26	0.78	29.9	0.2	-0.034
GU 25-742	-2.9	0.117	0.35	0.47	0.58	26.7	0.5	-0.074
GU 25-744	-2.9	0.122	0.24	0.49	0.73	27.9	0.6	-0.072
GU 25-746	-2.8	0.126	0.13	0.50	0.88	29.0	0.5	-0.070
GU 25-748	-2.6	0.130	0.00	0.52	1.04	30.0	0.5	-0.068
GU 25-762	-4.4	0.117	0.58	0.70	0.82	26.8	0.8	-0.111
GU 25-764	-4.3	0.122	0.49	0.73	0.97	28.0	0.9	-0.107
GU 25-766	-4.2	0.126	0.38	0.76	1.13	29.1	0.9	-0.104
GU 25-768	-4.0	0.130	0.26	0.78	1.30	30.0	0.8	-0.102
GU 25-782	-5.9	0.117	0.82	0.93	1.05	26.9	1.1	-0.148
GU 25-784	-5.8	0.122	0.73	0.97	1.21	28.0	1.2	-0.143
GU 25-786	-5.6	0.126	0.63	1.01	1.38	29.1	1.2	-0.139
GU 25-788	-5.4	0.131	0.52	1.04	1.56	30.1	1.2	-0.135

AEROFOIL	THICKNESS AT 0.05c (percent of max.)	T.E. ANGLE (deg)	EXTENT OF FAV. PRESSURE GRAD. (percent c) TOP	BOTTOM	MAX. CAMBER (per cent chord)	POSITION (percent chord)	MAX. THICKNESS (per cent chord)	POSITION (percent chord)
GU 41-322	49.2	3.7	29.5	27.7	1.3	35.3	7.2	30.2
GU 41-324	51.2	6.2	28.3	26.7	1.1	35.5	12.4	29.3
GU 41-326	53.9	8.2	27.2	25.8	0.8	40.3	16.9	28.3
GU 41-328	56.6	10.0	26.1	25.0	0.5	40.1	21.1	27.4
GU 41-342	49.0	3.7	30.3	26.6	2.7	34.6	7.1	30.6
GU 41-344	51.2	6.2	29.1	25.9	2.3	35.0	12.3	29.5
GU 41-346	53.7	8.3	27.9	25.1	1.8	35.8	16.9	28.5
GU 41-348	56.0	10.1	26.8	24.5	1.3	39.5	21.0	27.6
GU 41-362	49.8	3.7	31.1	25.5	4.1	34.5	7.0	31.2
GU 41-364	51.6	6.3	29.8	24.9	3.6	34.6	12.2	29.9
GU 41-366	53.5	8.6	28.6	24.4	2.9	35.2	16.7	28.8
GU 41-368	55.6	10.5	27.5	23.9	2.3	40.0	20.8	27.9
GU 41-382	50.7	3.6	31.8	24.2	5.6	34.5	6.9	31.8
GU 41-384	52.1	6.3	30.5	23.9	4.9	34.5	12.0	30.4
GU 41-386	53.7	8.7	29.3	23.6	4.1	34.8	16.5	29.2
GU 41-388	55.1	10.7	28.1	23.3	3.3	40.5	20.7	28.2
GU 41-422	45.3	4.4	39.1	37.4	1.4	43.6	7.9	35.4
GU 41-424	47.5	7.5	37.8	36.2	1.2	42.1	13.6	34.5
GU 41-426	50.0	9.9	36.5	35.2	0.9	40.7	18.6	33.6
GU 41-428	52.6	12.1	35.4	34.2	0.6	44.9	23.2	32.7
GU 41-442	45.6	4.4	39.9	36.4	2.9	39.7	7.7	35.6
GU 41-444	47.7	7.5	38.5	35.4	2.4	42.7	13.5	34.6
GU 41-446	49.9	10.0	37.3	34.5	2.0	41.4	18.5	33.6
GU 41-448	52.2	12.2	36.0	33.6	1.6	40.8	23.1	32.8
GU 41-462	46.5	4.4	40.7	35.4	4.3	39.6	7.6	36.3
GU 41-464	48.0	7.6	39.3	34.5	3.8	43.4	13.3	34.7
GU 41-466	49.8	10.3	38.0	33.7	3.2	42.0	18.3	33.7
GU 41-468	51.8	12.6	36.8	33.0	2.6	40.7	23.0	32.8
GU 41-482	47.6	4.4	41.4	34.3	5.8	39.5	7.4	37.4
GU 41-484	48.6	7.7	40.0	33.5	5.1	39.8	13.1	35.2
GU 41-486	50.0	10.4	38.7	32.9	4.5	42.7	18.1	33.9
GU 41-488	51.4	12.9	37.5	32.3	3.8	41.4	22.7	32.9
GU 41-522	42.8	5.5	48.9	47.2	1.5	45.4	8.3	39.6
GU 41-524	44.8	9.3	47.4	45.9	1.3	47.6	14.5	38.9
GU 41-526	47.1	12.4	46.1	44.8	1.0	47.4	19.9	38.1
GU 41-528	49.5	15.1	44.9	43.7	0.8	48.2	25.0	37.2
GU 41-542	43.2	5.5	49.6	46.4	2.9	45.0	8.2	39.8
GU 41-544	45.0	9.3	48.2	45.2	2.6	47.0	14.4	39.0
GU 41-546	47.2	12.5	46.9	44.1	2.2	47.1	19.9	38.2
GU 41-548	49.3	15.3	45.6	43.1	1.8	47.3	25.0	37.4

AEROFOIL	ZERO LIFT INCIDENCE (deg)	LIFT CURVE SLOPE (/deg)	LOW DRAG RANGE OF LIFT COEFFICIENT LOWER LIMIT	DESIGN	UPPER LIMIT	AERODYNAMIC CENTRE POSN. (percent c) x	y	PITCHING MOMENT COEF.
GU 41-322	-1.0	0.115	0.12	0.23	0.35	25.5	0.4	-0.019
GU 41-324	-0.8	0.120	0.00	0.24	0.48	25.9	0.3	-0.017
GU 41-326	-0.5	0.123	-0.12	0.25	0.62	26.2	0.1	-0.014
GU 41-328	-0.3	0.127	-0.25	0.25	0.76	26.4	-0.1	-0.012
GU 41-342	-2.0	0.115	0.35	0.46	0.58	25.5	1.0	-0.039
GU 41-344	-1.7	0.120	0.24	0.48	0.72	25.9	0.8	-0.033
GU 41-346	-1.3	0.123	0.12	0.49	0.86	26.2	0.6	-0.028
GU 41-348	-0.9	0.127	0.00	0.51	1.01	26.5	0.2	-0.024
GU 41-362	-3.0	0.115	0.58	0.69	0.81	25.5	1.5	-0.058
GU 41-364	-2.6	0.120	0.48	0.72	0.95	25.9	1.4	-0.050
GU 41-366	-2.1	0.123	0.37	0.74	1.11	26.3	1.0	-0.043
GU 41-368	-1.6	0.127	0.25	0.76	1.26	26.6	0.7	-0.036
GU 41-382	-4.1	0.116	0.81	0.92	1.04	25.5	2.1	-0.078
GU 41-384	-3.5	0.120	0.72	0.95	1.19	25.9	1.9	-0.067
GU 41-386	-3.0	0.123	0.62	0.98	1.35	26.3	1.6	-0.057
GU 41-388	-2.4	0.127	0.51	1.01	1.51	26.6	1.2	-0.048
GU 41-422	-1.1	0.116	0.12	0.23	0.35	25.8	0.5	-0.023
GU 41-424	-0.9	0.120	0.00	0.24	0.48	26.3	0.3	-0.020
GU 41-426	-0.7	0.125	-0.12	0.25	0.62	26.7	0.2	-0.018
GU 41-428	-0.4	0.129	-0.26	0.26	0.77	27.0	-0.0	-0.016
GU 41-442	-2.2	0.116	0.35	0.46	0.58	25.8	0.9	-0.046
GU 41-444	-1.9	0.120	0.24	0.48	0.72	26.3	0.8	-0.041
GU 41-446	-1.5	0.125	0.12	0.50	0.87	26.7	0.6	-0.036
GU 41-448	-1.1	0.129	0.00	0.51	1.03	27.1	0.2	-0.031
GU 41-462	-3.3	0.116	0.58	0.69	0.81	25.8	1.5	-0.069
GU 41-464	-2.9	0.120	0.48	0.72	0.96	26.3	1.3	-0.061
GU 41-466	-2.4	0.125	0.37	0.75	1.12	26.8	1.0	-0.054
GU 41-468	-1.9	0.128	0.26	0.77	1.28	27.2	0.7	-0.046
GU 41-482	-4.5	0.116	0.81	0.93	1.04	25.8	2.0	-0.092
GU 41-484	-4.0	0.121	0.72	0.96	1.20	26.3	1.8	-0.081
GU 41-486	-3.4	0.125	0.62	0.99	1.36	26.8	1.6	-0.072
GU 41-488	-2.8	0.128	0.51	1.02	1.53	27.3	1.2	-0.063
GU 41-522	-1.2	0.116	0.12	0.23	0.35	26.1	0.4	-0.026
GU 41-524	-1.0	0.121	0.00	0.24	0.48	26.7	0.2	-0.024
GU 41-526	-0.7	0.126	-0.13	0.25	0.63	27.2	0.1	-0.021
GU 41-528	-0.5	0.131	-0.26	0.26	0.78	27.8	-0.2	-0.019
GU 41-542	-2.4	0.116	0.35	0.46	0.58	26.1	0.8	-0.053
GU 41-544	-2.1	0.121	0.24	0.48	0.73	26.7	0.7	-0.048
GU 41-546	-1.7	0.126	0.13	0.50	0.88	27.3	0.5	-0.043
GU 41-548	-1.3	0.130	0.00	0.52	1.04	27.9	0.2	-0.038

AEROFOIL	THICKNESS AT 0.05c (percent of max.)	T.E. ANGLE (deg)	EXTENT OF FAV. PRESSURE GRAD. (percent c) TOP	BOTTOM	MAX.CAMBER (per cent chord)	POSITION (percent chord)	MAX. THICKNESS (per cent chord)	POSITION (percent chord)
GU 41-562	44.1	5.5	50.3	45.5	4.4	45.8	8.1	40.2
GU 41-564	45.4	9.4	48.9	44.3	3.9	46.4	14.3	39.1
GU 41-566	47.1	12.8	47.6	43.3	3.4	47.2	19.8	38.3
GU 41-568	48.9	15.7	46.4	42.4	2.9	47.8	24.9	37.5
GU 41-582	45.2	5.5	51.1	44.5	5.9	46.4	7.9	40.8
GU 41-584	45.9	9.5	49.6	43.4	5.3	45.8	14.1	39.4
GU 41-586	47.2	12.9	48.4	42.5	4.7	47.0	19.6	38.4
GU 41-588	48.5	16.0	47.1	41.7	4.1	47.1	24.7	37.6
GU 41-622	41.0	7.1	58.7	57.2	1.4	49.1	8.8	43.3
GU 41-624	42.7	12.0	57.2	55.8	1.3	51.8	15.3	42.8
GU 41-626	44.8	16.1	56.0	54.6	1.1	56.0	21.2	42.1
GU 41-628	47.1	19.7	54.8	53.5	0.9	56.0	26.8	41.5
GU 41-642	41.5	7.1	59.4	56.5	2.9	48.7	8.7	43.5
GU 41-644	42.9	12.0	58.0	55.1	2.6	51.0	15.3	42.8
GU 41-646	44.9	16.2	56.7	53.9	2.2	55.7	21.2	42.2
GU 41-648	46.9	19.8	55.5	52.8	1.9	55.7	26.8	41.6
GU 41-662	42.1	7.1	60.1	55.7	4.4	48.5	8.6	43.7
GU 41-664	43.2	12.2	58.7	54.3	3.9	50.5	15.2	43.0
GU 41-666	44.8	16.4	57.5	53.2	3.5	56.4	21.1	42.3
GU 41-668	46.6	20.3	56.3	52.2	3.1	55.9	26.6	41.7
GU 41-682	43.0	7.1	60.7	54.9	5.9	48.4	8.4	44.1
GU 41-684	43.7	12.2	59.4	53.5	5.3	50.1	15.0	43.2
GU 41-686	44.9	16.6	58.2	52.4	4.7	57.1	20.9	42.5
GU 41-688	46.3	20.5	57.1	51.5	4.2	56.0	26.4	41.8
GU 41-722	39.3	9.6	68.6	67.4	1.4	52.0	9.2	46.7
GU 41-724	40.9	16.4	67.3	66.0	1.2	57.1	16.2	46.4
GU 41-726	42.9	22.1	66.2	64.8	1.1	60.6	22.5	46.0
GU 41-728	45.1	27.1	65.1	63.8	0.9	65.5	28.5	45.6
GU 41-742	39.6	9.6	69.3	66.7	2.8	51.7	9.1	46.8
GU 41-744	41.1	16.4	68.0	65.3	2.5	58.1	16.1	46.5
GU 41-746	43.0	22.2	66.9	64.1	2.2	59.8	22.5	46.1
GU 41-748	44.9	27.3	65.8	63.1	1.9	65.6	28.5	45.7
GU 41-762	40.3	9.7	69.9	66.1	4.2	51.4	9.0	47.0
GU 41-764	41.4	16.6	68.7	64.7	3.8	59.0	16.0	46.6
GU 41-766	42.9	22.5	67.6	63.5	3.4	58.1	22.3	46.2
GU 41-768	44.6	27.7	66.6	62.5	3.1	65.3	28.4	45.8
GU 41-782	41.2	9.7	70.5	65.5	5.7	51.3	8.8	47.4
GU 41-784	41.7	16.7	69.4	64.0	5.2	53.6	15.8	46.8
GU 41-786	43.0	22.6	68.4	62.8	4.7	58.1	22.2	46.3
GU 41-788	44.3	28.0	67.4	61.8	4.3	64.5	28.2	45.9

AEROFOIL	ZERO LIFT INCIDENCE (deg)	LIFT CURVE SLOPE (/deg)	LOW DRAG RANGE OF LIFT COEFFICIENT LOWER LIMIT	DESIGN	UPPER LIMIT	AERODYNAMIC CENTRE POSN. (percent c) x	y	PITCHING MOMENT COEF.
GU 41-562	-3.6	0.116	0.58	0.70	0.81	26.0	1.3	-0.080
GU 41-564	-3.2	0.121	0.49	0.73	0.97	26.8	1.1	-0.072
GU 41-566	-2.7	0.126	0.38	0.75	1.13	27.4	0.9	-0.065
GU 41-568	-2.3	0.130	0.26	0.78	1.30	28.0	0.6	-0.058
GU 41-582	-4.8	0.117	0.81	0.93	1.05	26.1	1.7	-0.107
GU 41-584	-4.3	0.121	0.73	0.97	1.21	26.8	1.6	-0.096
GU 41-586	-3.8	0.126	0.63	1.00	1.38	27.5	1.4	-0.087
GU 41-588	-3.2	0.130	0.52	1.04	1.55	28.1	1.1	-0.077
GU 41-622	-1.3	0.117	0.12	0.23	0.35	26.3	0.4	-0.031
GU 41-624	-1.1	0.122	0.00	0.24	0.49	27.2	0.2	-0.029
GU 41-626	-0.9	0.127	-0.13	0.25	0.64	28.0	0.1	-0.026
GU 41-628	-0.7	0.132	-0.26	0.26	0.79	28.8	-0.1	-0.024
GU 41-642	-2.6	0.117	0.35	0.47	0.58	26.3	0.7	-0.063
GU 41-644	-2.3	0.122	0.24	0.49	0.73	27.3	0.6	-0.058
GU 41-646	-2.0	0.127	0.13	0.51	0.89	28.1	0.4	-0.053
GU 41-648	-1.6	0.132	0.00	0.53	1.06	28.9	0.2	-0.048
GU 41-662	-3.9	0.117	0.58	0.70	0.82	26.4	1.1	-0.094
GU 41-664	-3.6	0.122	0.49	0.73	0.98	27.3	1.0	-0.087
GU 41-666	-3.1	0.127	0.38	0.76	1.14	28.2	0.8	-0.079
GU 41-668	-2.6	0.132	0.26	0.79	1.32	28.9	0.4	-0.073
GU 41-682	-5.3	0.117	0.82	0.93	1.05	26.4	1.4	-0.126
GU 41-684	-4.8	0.122	0.73	0.98	1.22	27.4	1.4	-0.116
GU 41-686	-4.3	0.127	0.64	1.02	1.39	28.3	1.2	-0.106
GU 41-688	-3.7	0.132	0.53	1.05	1.58	29.1	0.9	-0.097
GU 41-722	-1.4	0.117	0.12	0.23	0.35	26.7	0.2	-0.037
GU 41-724	-1.2	0.123	0.00	0.25	0.49	27.8	0.1	-0.035
GU 41-726	-1.0	0.129	-0.13	0.26	0.65	28.9	-0.1	-0.033
GU 41-728	-0.8	0.135	-0.27	0.27	0.81	29.8	-0.2	-0.030
GU 41-742	-2.8	0.117	0.35	0.47	0.59	26.7	0.5	-0.073
GU 41-744	-2.6	0.123	0.25	0.49	0.74	27.9	0.4	-0.069
GU 41-746	-2.3	0.129	0.13	0.52	0.90	28.9	0.2	-0.065
GU 41-748	-1.9	0.135	0.00	0.54	1.08	29.9	-0.0	-0.060
GU 41-762	-4.3	0.118	0.59	0.70	0.82	26.7	0.8	-0.109
GU 41-764	-4.0	0.124	0.49	0.74	0.98	27.9	0.7	-0.103
GU 41-766	-3.5	0.129	0.39	0.77	1.16	29.0	0.4	-0.097
GU 41-768	-3.1	0.135	0.27	0.81	1.34	30.1	0.2	-0.091
GU 41-782	-5.8	0.118	0.82	0.94	1.06	26.8	1.1	-0.146
GU 41-784	-5.3	0.124	0.74	0.99	1.23	28.0	1.0	-0.137
GU 41-786	-4.9	0.129	0.65	1.03	1.41	29.1	0.8	-0.129
GU 41-788	-4.3	0.135	0.54	1.07	1.60	30.2	0.5	-0.121

AEROFOIL	THICKNESS AT 0.05c (percent of max.)	T.E. ANGLE (deg)	EXTENT OF FAV. PRESSURE GRAD. (percent c) TOP	BOTTOM	MAX. CAMBER (per cent chord)	POSITION (percent chord)	MAX. THICKNESS (per cent chord)	POSITION (percent chord)
GU 43-322	48.7	6.0	29.6	27.7	1.3	35.4	7.3	30.8
GU 43-324	50.7	10.1	28.4	26.8	1.1	35.6	12.6	29.9
GU 43-326	53.3	13.5	27.4	26.0	0.8	40.6	17.2	29.0
GU 43-328	56.0	16.5	26.3	25.2	0.5	40.3	21.4	28.1
GU 43-342	48.5	5.9	30.4	26.7	2.7	34.6	7.2	31.1
GU 43-344	50.7	10.1	29.2	26.0	2.3	35.0	12.5	30.1
GU 43-346	53.1	13.5	28.1	25.3	1.8	35.9	17.1	29.1
GU 43-348	55.5	16.5	27.0	24.7	1.3	39.8	21.3	28.2
GU 43-362	49.3	5.8	31.2	25.5	4.1	34.6	7.1	31.6
GU 43-364	51.0	9.9	29.9	25.0	3.6	34.7	12.4	30.4
GU 43-366	53.0	13.4	28.8	24.5	2.9	35.3	17.0	29.4
GU 43-368	55.0	16.4	27.7	24.1	2.3	40.3	21.2	28.5
GU 43-382	50.2	5.5	31.9	24.3	5.6	34.6	6.9	32.2
GU 43-384	51.6	9.8	30.6	24.0	4.9	34.6	12.2	30.8
GU 43-386	53.1	13.3	29.5	23.7	4.1	34.9	16.8	29.7
GU 43-388	54.5	16.4	28.4	23.5	3.3	40.8	21.0	28.8
GU 43-422	44.9	7.1	39.2	37.5	1.4	43.7	7.9	36.0
GU 43-424	47.1	12.0	38.0	36.4	1.2	42.3	13.7	35.1
GU 43-426	49.5	16.1	36.8	35.4	0.9	41.0	18.8	34.2
GU 43-428	52.0	19.6	35.7	34.5	0.6	45.2	23.6	33.3
GU 43-442	45.2	7.0	40.0	36.5	2.9	39.7	7.8	36.3
GU 43-444	47.2	11.9	38.7	35.6	2.4	42.9	13.6	35.2
GU 43-446	49.4	16.0	37.5	34.7	2.0	41.6	18.8	34.3
GU 43-448	51.6	19.6	36.4	33.9	1.6	41.0	23.5	33.4
GU 43-462	46.0	6.9	40.8	35.5	4.3	39.6	7.7	37.0
GU 43-464	47.6	11.9	39.5	34.7	3.7	43.6	13.5	35.4
GU 43-466	49.3	16.0	38.2	33.9	3.2	42.3	18.6	34.4
GU 43-468	51.2	19.6	37.1	33.3	2.6	41.1	23.3	33.5
GU 43-482	47.1	6.7	41.5	34.4	5.8	39.5	7.5	38.1
GU 43-484	48.1	11.7	40.2	33.7	5.1	39.9	13.3	35.9
GU 43-486	49.5	15.9	39.0	33.1	4.4	42.9	18.4	34.6
GU 43-488	50.8	19.7	37.8	32.6	3.8	41.7	23.1	33.7
GU 43-522	42.4	8.7	49.0	47.4	1.5	45.3	8.4	40.3
GU 43-524	44.5	14.6	47.7	46.2	1.2	47.8	14.7	39.6
GU 43-526	46.7	19.6	46.5	45.1	1.0	47.6	20.3	38.9
GU 43-528	49.1	24.1	45.3	44.1	0.7	48.5	25.5	38.1
GU 43-542	42.8	8.6	49.8	46.5	2.9	45.0	8.3	40.5
GU 43-544	44.6	14.6	48.4	45.4	2.5	47.1	14.6	39.7
GU 43-546	46.6	19.6	47.2	44.4	2.2	47.3	20.2	39.0
GU 43-548	48.6	24.1	46.1	43.5	1.8	47.6	25.4	38.2

AEROFOIL	ZERO LIFT INCIDENCE (deg)	LIFT CURVE SLOPE (/deg)	LOW DRAG RANGE OF LIFT COEFFICIENT LOWER LIMIT	DESIGN	UPPER LIMIT	AERODYNAMIC CENTRE POSN. (percent c) x	y	PITCHING MOMENT COEF.
GU 43-322	-1.0	0.116	0.12	0.23	0.35	25.6	0.4	-0.019
GU 43-324	-0.8	0.120	0.00	0.24	0.48	26.1	0.3	-0.017
GU 43-326	-0.5	0.124	-0.12	0.25	0.62	26.4	0.1	-0.014
GU 43-328	-0.3	0.128	-0.26	0.26	0.77	26.7	-0.1	-0.012
GU 43-342	-2.0	0.116	0.35	0.46	0.58	25.6	1.0	-0.039
GU 43-344	-1.7	0.120	0.24	0.48	0.72	26.1	0.8	-0.034
GU 43-346	-1.3	0.124	0.12	0.50	0.87	26.5	0.6	-0.029
GU 43-348	-0.9	0.128	0.00	0.51	1.02	26.8	0.2	-0.024
GU 43-362	-3.0	0.116	0.58	0.69	0.81	25.6	1.5	-0.059
GU 43-364	-2.6	0.120	0.48	0.72	0.96	26.1	1.4	-0.050
GU 43-366	-2.1	0.124	0.37	0.74	1.11	26.5	1.0	-0.043
GU 43-368	-1.6	0.127	0.25	0.76	1.27	26.9	0.7	-0.036
GU 43-382	-4.1	0.116	0.81	0.92	1.04	25.6	2.1	-0.078
GU 43-384	-3.6	0.120	0.72	0.96	1.19	26.1	1.9	-0.068
GU 43-386	-3.0	0.124	0.62	0.99	1.35	26.5	1.6	-0.058
GU 43-388	-2.4	0.127	0.51	1.02	1.52	26.9	1.2	-0.049
GU 43-422	-1.1	0.116	0.12	0.23	0.35	25.9	0.5	-0.023
GU 43-424	-0.9	0.121	0.00	0.24	0.48	26.5	0.3	-0.020
GU 43-426	-0.7	0.125	-0.13	0.25	0.63	26.9	0.2	-0.018
GU 43-428	-0.4	0.130	-0.26	0.26	0.78	27.4	-0.1	-0.016
GU 43-442	-2.2	0.116	0.35	0.46	0.58	25.9	0.9	-0.046
GU 43-444	-1.9	0.121	0.24	0.48	0.72	26.5	0.8	-0.041
GU 43-446	-1.5	0.125	0.13	0.50	0.87	27.0	0.6	-0.036
GU 43-448	-1.1	0.129	0.00	0.52	1.03	27.4	0.2	-0.032
GU 43-462	-3.3	0.116	0.58	0.70	0.81	25.9	1.5	-0.069
GU 43-464	-2.9	0.121	0.48	0.72	0.96	26.5	1.3	-0.061
GU 43-466	-2.5	0.125	0.38	0.75	1.12	27.0	1.0	-0.054
GU 43-468	-2.0	0.129	0.26	0.77	1.29	27.5	0.7	-0.047
GU 43-482	-4.5	0.116	0.81	0.93	1.04	25.9	2.0	-0.092
GU 43-484	-4.0	0.121	0.72	0.96	1.20	26.5	1.8	-0.082
GU 43-486	-3.4	0.125	0.62	1.00	1.37	27.1	1.6	-0.072
GU 43-488	-2.8	0.129	0.52	1.03	1.54	27.6	1.2	-0.063
GU 43-522	-1.2	0.116	0.12	0.23	0.35	26.2	0.4	-0.026
GU 43-524	-1.0	0.122	0.00	0.24	0.49	26.9	0.3	-0.024
GU 43-526	-0.8	0.127	-0.13	0.25	0.63	27.5	0.1	-0.021
GU 43-528	-0.5	0.131	-0.26	0.26	0.79	28.2	-0.1	-0.019
GU 43-542	-2.4	0.116	0.35	0.47	0.58	26.2	0.8	-0.053
GU 43-544	-2.1	0.122	0.24	0.49	0.73	26.9	0.7	-0.048
GU 43-546	-1.7	0.127	0.13	0.51	0.88	27.6	0.4	-0.043
GU 43-548	-1.3	0.131	0.00	0.52	1.05	28.2	0.1	-0.039

AEROFOIL	THICKNESS AT 0.05c (percent of max.)	T.E. ANGLE (deg)	EXTENT OF FAV. PRESSURE GRAD. (percent c) TOP	BOTTOM	MAX.CAMBER (per cent chord)	POSITION (percent chord)	MAX. THICKNESS (per cent chord)	POSITION (percent chord)
GU 43-562	43.7	8.5	50.5	45.6	4.4	45.9	8.2	40.9
GU 43-564	44.9	14.5	49.2	44.5	3.9	46.3	14.5	39.9
GU 43-566	46.5	19.6	48.0	43.6	3.4	47.4	20.1	39.1
GU 43-568	48.4	24.1	46.8	42.8	2.9	47.4	25.3	38.3
GU 43-582	44.7	8.3	51.2	44.7	5.9	46.6	8.0	41.6
GU 43-584	45.4	14.4	49.9	43.7	5.3	45.8	14.3	40.2
GU 43-586	46.7	19.6	48.7	42.8	4.7	47.1	19.9	39.3
GU 43-588	48.0	24.1	47.6	42.1	4.1	47.5	25.1	38.5
GU 43-622	40.6	10.9	58.9	57.4	1.4	49.3	8.9	44.0
GU 43-624	42.4	18.4	57.6	56.1	1.2	51.6	15.6	43.6
GU 43-626	44.5	24.8	56.4	55.0	1.0	56.4	21.6	43.0
GU 43-628	46.6	30.4	55.4	54.0	0.9	56.3	27.3	42.4
GU 43-642	41.1	10.8	59.6	56.7	2.9	48.6	8.8	44.2
GU 43-644	42.5	18.4	58.3	55.4	2.5	50.9	15.5	43.7
GU 43-646	44.4	24.8	57.2	54.3	2.2	56.0	21.6	43.1
GU 43-648	46.4	30.4	56.1	53.4	1.9	56.1	27.3	42.5
GU 43-662	41.7	10.7	60.2	55.9	4.4	48.5	8.7	44.5
GU 43-664	42.8	18.3	59.0	54.6	3.9	50.4	15.4	43.8
GU 43-666	44.3	24.8	57.9	53.6	3.4	56.8	21.4	43.3
GU 43-668	46.1	30.5	56.9	52.7	3.0	56.2	27.1	42.7
GU 43-682	42.6	10.6	60.9	55.1	5.9	48.3	8.5	45.0
GU 43-684	43.2	18.3	59.7	53.8	5.3	50.0	15.2	44.1
GU 43-686	44.4	24.8	58.7	52.8	4.7	57.6	21.2	43.4
GU 43-688	45.7	30.6	57.6	52.0	4.2	56.6	26.9	42.8
GU 43-722	38.9	14.2	68.9	67.6	1.4	52.0	9.3	47.4
GU 43-724	40.5	24.2	67.7	66.4	1.2	57.4	16.4	47.2
GU 43-726	42.5	32.7	66.7	65.4	1.1	61.1	22.8	47.0
GU 43-728	44.6	40.3	65.8	64.5	0.9	66.1	29.1	46.6
GU 43-742	39.2	14.2	69.5	66.9	2.8	51.6	9.2	47.6
GU 43-744	40.7	24.2	68.4	65.7	2.5	58.4	16.3	47.3
GU 43-746	42.6	32.7	67.4	64.7	2.2	60.3	22.9	47.0
GU 43-748	44.4	40.3	66.6	63.8	1.9	66.1	29.1	46.7
GU 43-762	40.0	14.1	70.1	66.3	4.3	51.5	9.1	47.8
GU 43-764	40.9	24.2	69.1	65.0	3.8	59.4	16.2	47.5
GU 43-766	42.4	32.7	68.2	64.0	3.4	58.6	22.7	47.2
GU 43-768	44.1	40.3	67.4	63.2	3.0	65.4	28.9	46.8
GU 43-782	40.8	14.0	70.7	65.7	5.7	51.3	8.9	48.2
GU 43-784	41.3	24.1	69.8	64.3	5.1	53.5	16.0	47.8
GU 43-786	42.5	32.7	68.9	63.3	4.6	58.6	22.5	47.4
GU 43-788	43.8	40.4	68.2	62.4	4.2	64.3	28.7	47.0

APPENDIX III, Part 2

AEROFOIL	ZERO LIFT INCIDENCE (deg)	LIFT CURVE SLOPE (/deg)	LOW DRAG RANGE OF LIFT COEFFICIENT LOWER LIMIT	DESIGN	UPPER LIMIT	AERODYNAMIC CENTRE POSN. (percent c) x	y	PITCHING MOMENT COEF.
GU 43-562	-3.6	0.117	0.58	0.70	0.81	26.1	1.3	-0.081
GU 43-564	-3.2	0.122	0.49	0.73	0.97	27.0	1.1	-0.073
GU 43-566	-2.7	0.127	0.38	0.76	1.13	27.7	0.9	-0.065
GU 43-568	-2.2	0.131	0.26	0.79	1.31	28.3	0.6	-0.058
GU 43-582	-4.8	0.117	0.82	0.93	1.05	26.2	1.7	-0.108
GU 43-584	-4.4	0.122	0.73	0.97	1.21	27.0	1.6	-0.097
GU 43-586	-3.8	0.127	0.63	1.01	1.38	27.7	1.4	-0.087
GU 43-588	-3.2	0.131	0.52	1.05	1.56	28.4	1.0	-0.078
GU 43-622	-1.3	0.117	0.12	0.23	0.35	26.4	0.3	-0.031
GU 43-624	-1.1	0.123	0.00	0.25	0.49	27.5	0.3	-0.029
GU 43-626	-0.9	0.128	-0.13	0.26	0.64	28.3	0.1	-0.026
GU 43-628	-0.7	0.134	-0.27	0.27	0.80	29.2	0.1	-0.024
GU 43-642	-2.6	0.117	0.35	0.47	0.58	26.5	0.7	-0.063
GU 43-644	-2.3	0.123	0.25	0.49	0.74	27.5	0.6	-0.058
GU 43-646	-2.0	0.128	0.13	0.51	0.90	28.4	0.4	-0.053
GU 43-648	-1.6	0.133	0.00	0.53	1.06	29.3	0.1	-0.049
GU 43-662	-4.0	0.117	0.59	0.70	0.82	26.5	1.1	-0.095
GU 43-664	-3.6	0.123	0.49	0.74	0.98	27.6	1.0	-0.087
GU 43-666	-3.1	0.128	0.38	0.77	1.15	28.5	0.8	-0.080
GU 43-668	-2.7	0.133	0.27	0.80	1.33	29.4	0.4	-0.074
GU 43-682	-5.3	0.117	0.82	0.94	1.05	26.5	1.4	-0.126
GU 43-684	-4.9	0.123	0.74	0.98	1.22	27.6	1.4	-0.117
GU 43-686	-4.3	0.128	0.64	1.02	1.40	28.6	1.2	-0.107
GU 43-688	-3.8	0.133	0.53	1.06	1.59	29.5	0.9	-0.099
GU 43-722	-1.4	0.118	0.12	0.24	0.35	26.8	0.2	-0.037
GU 43-724	-1.3	0.124	0.00	0.25	0.50	28.0	0.1	-0.035
GU 43-726	-1.1	0.130	-0.13	0.26	0.65	29.2	-0.1	-0.034
GU 43-728	-0.8	0.136	-0.27	0.27	0.82	30.4	-0.3	-0.032
GU 43-742	-2.9	0.118	0.35	0.47	0.59	26.8	0.5	-0.073
GU 43-744	-2.6	0.124	0.25	0.50	0.74	28.1	0.4	-0.070
GU 43-746	-2.3	0.130	0.13	0.52	0.91	29.3	0.1	-0.066
GU 43-748	-1.9	0.136	0.00	0.54	1.08	30.4	-0.1	-0.062
GU 43-762	-4.3	0.118	0.59	0.71	0.82	26.9	0.8	-0.110
GU 43-764	-4.0	0.124	0.50	0.74	0.99	28.2	0.7	-0.104
GU 43-766	-3.6	0.130	0.39	0.78	1.17	29.4	0.4	-0.098
GU 43-768	-3.1	0.136	0.27	0.81	1.35	30.6	0.1	-0.093
GU 43-782	-5.8	0.118	0.82	0.94	1.06	26.9	1.1	-0.146
GU 43-784	-5.4	0.124	0.74	0.99	1.24	28.3	1.0	-0.138
GU 43-786	-4.9	0.130	0.65	1.04	1.42	29.5	0.8	-0.131
GU 43-788	-4.4	0.136	0.54	1.08	1.62	30.7	0.5	-0.123

AEROFOIL	THICKNESS AT 0.05c (percent of max.)	T.E. ANGLE (deg)	EXTENT OF FAV. PRESSURE GRAD. (percent c) TOP	BOTTOM	MAX.CAMBER (per cent chord)	POSITION (percent chord)	MAX. THICKNESS (per cent chord)	POSITION (percent chord)
GU 45-322	48.3	7.3	29.6	27.8	1.3	35.5	7.3	31.3
GU 45-324	50.2	12.2	28.5	26.9	1.1	35.7	12.7	30.4
GU 45-326	52.8	16.3	27.5	26.2	0.8	40.8	17.4	29.5
GU 45-328	55.5	19.9	26.5	25.4	0.5	40.7	21.7	28.7
GU 45-342	48.1	7.1	30.5	26.7	2.7	34.7	7.3	31.6
GU 45-344	50.3	12.1	29.3	26.1	2.3	35.1	12.6	30.6
GU 45-346	52.7	16.2	28.2	25.5	1.8	36.1	17.3	29.7
GU 45-348	55.0	19.8	27.2	24.9	1.3	40.0	21.6	28.8
GU 45-362	48.9	6.9	31.3	25.6	4.1	34.6	7.2	32.0
GU 45-364	50.6	11.9	30.1	25.1	3.6	34.8	12.5	30.9
GU 45-366	52.5	16.1	28.9	24.7	3.0	35.4	17.2	29.9
GU 45-368	54.5	19.7	27.9	24.3	2.3	40.6	21.5	29.1
GU 45-382	49.8	6.6	32.0	24.3	5.6	34.6	7.0	32.5
GU 45-384	51.1	11.6	30.8	24.1	4.9	34.7	12.3	31.2
GU 45-386	52.6	15.9	29.6	23.8	4.1	35.0	17.0	30.2
GU 45-388	54.0	19.6	28.5	23.6	3.4	35.7	21.3	29.3
GU 45-422	44.6	8.5	39.3	37.6	1.4	43.8	8.0	36.5
GU 45-424	46.7	14.3	38.1	36.5	1.2	42.5	13.9	35.6
GU 45-426	49.1	19.2	37.0	35.6	0.9	41.2	19.1	34.8
GU 45-428	51.6	23.4	35.9	34.8	0.6	45.5	23.9	33.9
GU 45-442	44.8	8.4	40.1	36.6	2.9	39.8	7.9	36.8
GU 45-444	46.8	14.2	38.9	35.7	2.4	43.1	13.8	35.7
GU 45-446	49.0	19.1	37.7	34.9	2.0	41.9	19.0	34.8
GU 45-448	51.1	23.4	36.6	34.2	1.6	41.3	23.8	34.0
GU 45-462	45.7	8.2	40.9	35.6	4.3	39.7	7.8	37.5
GU 45-464	47.1	14.1	39.6	34.8	3.7	43.7	13.7	36.0
GU 45-466	48.9	19.0	38.5	34.1	3.2	42.5	18.8	34.9
GU 45-468	50.8	23.3	37.3	33.5	2.6	41.3	23.7	34.1
GU 45-482	46.7	7.9	41.6	34.5	5.8	39.6	7.6	38.7
GU 45-484	47.7	13.8	40.3	33.8	5.1	39.9	13.5	36.5
GU 45-486	49.0	18.8	39.2	33.3	4.4	43.2	18.7	35.3
GU 45-488	50.4	23.2	38.0	32.8	3.8	42.0	23.5	34.3
GU 45-522	42.1	10.1	49.1	47.5	1.5	45.4	8.5	40.8
GU 45-524	44.1	17.2	47.9	46.4	1.2	48.0	14.9	40.2
GU 45-526	46.3	23.1	46.7	45.4	1.0	47.8	20.5	39.5
GU 45-528	48.7	28.3	45.7	44.5	0.7	48.8	25.9	38.8
GU 45-542	42.5	10.1	49.9	46.6	2.9	45.1	8.4	41.0
GU 45-544	44.2	17.1	48.6	45.6	2.5	47.3	14.8	40.3
GU 45-546	46.2	23.0	47.5	44.6	2.2	47.5	20.5	39.6
GU 45-548	48.2	28.3	46.4	43.8	1.8	47.9	25.7	38.9

AEROFOIL	ZERO LIFT INCIDENCE (deg)	LIFT CURVE SLOPE (/deg)	LOW DRAG RANGE OF LIFT COEFFICIENT LOWER LIMIT	DESIGN	UPPER LIMIT	AERODYNAMIC CENTRE POSN. (percent c) x	y	PITCHING MOMENT COEF.
GU 45-322	-1.0	0.116	0.12	0.23	0.35	25.7	0.4	-0.019
GU 45-324	-0.8	0.120	0.00	0.24	0.48	26.2	0.3	-0.017
GU 45-326	-0.5	0.124	-0.12	0.25	0.62	26.6	0.1	-0.014
GU 45-328	-0.3	0.128	-0.26	0.26	0.77	26.9	-0.1	-0.012
GU 45-342	-2.0	0.116	0.35	0.46	0.58	25.7	1.0	-0.039
GU 45-344	-1.7	0.120	0.24	0.48	0.72	26.2	0.8	-0.034
GU 45-346	-1.3	0.124	0.12	0.50	0.87	26.6	0.6	-0.029
GU 45-348	-0.9	0.128	0.00	0.51	1.02	27.0	0.2	-0.024
GU 45-362	-3.0	0.116	0.58	0.69	0.81	25.7	1.5	-0.059
GU 45-364	-2.6	0.120	0.48	0.72	0.96	26.2	1.4	-0.051
GU 45-366	-2.1	0.124	0.37	0.74	1.11	26.7	1.0	-0.043
GU 45-368	-1.6	0.128	0.26	0.77	1.27	27.1	0.7	-0.036
GU 45-382	-4.1	0.116	0.81	0.92	1.04	25.7	2.1	-0.079
GU 45-384	-3.6	0.120	0.72	0.96	1.20	26.2	1.9	-0.068
GU 45-386	-3.0	0.124	0.62	0.99	1.36	26.7	1.6	-0.058
GU 45-388	-2.4	0.128	0.51	1.02	1.52	27.1	1.2	-0.049
GU 45-422	-1.1	0.116	0.12	0.23	0.35	26.0	0.5	-0.023
GU 45-424	-0.9	0.121	0.00	0.24	0.48	26.6	0.3	-0.020
GU 45-426	-0.7	0.126	-0.13	0.25	0.63	27.1	0.1	-0.018
GU 45-428	-0.4	0.130	-0.26	0.26	0.78	27.6	-0.1	-0.016
GU 45-442	-2.2	0.116	0.35	0.46	0.58	26.0	0.9	-0.046
GU 45-444	-1.9	0.121	0.24	0.48	0.73	26.6	0.8	-0.041
GU 45-446	-1.5	0.126	0.13	0.50	0.88	27.2	0.5	-0.036
GU 45-448	-1.1	0.130	0.00	0.52	1.04	27.7	0.2	-0.032
GU 45-462	-3.3	0.116	0.58	0.70	0.81	26.0	1.5	-0.069
GU 45-464	-2.9	0.121	0.48	0.73	0.97	26.6	1.3	-0.061
GU 45-466	-2.5	0.126	0.38	0.75	1.13	27.2	1.0	-0.054
GU 45-468	-2.0	0.130	0.26	0.78	1.29	27.8	0.7	-0.048
GU 45-482	-4.5	0.116	0.81	0.93	1.04	25.9	2.0	-0.093
GU 45-484	-4.0	0.121	0.73	0.97	1.21	26.7	1.8	-0.082
GU 45-486	-3.4	0.126	0.63	1.00	1.37	27.3	1.6	-0.073
GU 45-488	-2.8	0.130	0.52	1.03	1.55	27.8	1.2	-0.064
GU 45-522	-1.2	0.117	0.12	0.23	0.35	26.2	0.4	-0.026
GU 45-524	-1.0	0.122	0.00	0.24	0.49	27.0	0.3	-0.024
GU 45-526	-0.7	0.127	-0.13	0.25	0.64	27.7	0.1	-0.021
GU 45-528	-0.5	0.132	-0.26	0.26	0.79	28.4	-0.1	-0.019
GU 45-542	-2.4	0.117	0.35	0.47	0.58	26.3	0.8	-0.053
GU 45-544	-2.1	0.122	0.24	0.49	0.73	27.1	0.7	-0.048
GU 45-546	-1.7	0.127	0.13	0.51	0.89	27.8	0.4	-0.044
GU 45-548	-1.3	0.132	0.00	0.53	1.05	28.5	0.1	-0.039

AEROFOIL	THICKNESS AT 0.05c (percent of max.)	T.E. ANGLE (deg)	EXTENT OF FAV. PRESSURE GRAD. (percent c) TOP	BOTTOM	MAX.CAMBER (per cent chord)	POSITION (percent chord)	MAX. THICKNESS (per cent chord)	POSITION (percent chord)
GU 45-562	43.3	9.9	50.6	45.7	4.4	46.0	8.3	41.5
GU 45-564	44.5	17.0	49.4	44.7	3.9	46.5	14.6	40.5
GU 45-566	46.1	22.9	48.2	43.9	3.4	47.5	20.3	39.7
GU 45-568	47.9	28.2	47.1	43.1	2.9	47.6	25.7	39.0
GU 45-582	44.3	9.7	51.3	44.8	5.9	46.7	8.1	42.3
GU 45-584	45.0	16.8	50.1	43.8	5.3	45.8	14.4	40.8
GU 45-586	46.3	22.8	49.0	43.1	4.7	47.2	20.1	39.9
GU 45-588	47.5	28.1	47.9	42.4	4.1	47.7	25.4	39.2
GU 45-622	40.4	12.5	59.0	57.5	1.4	49.4	9.0	44.6
GU 45-624	42.1	21.2	57.8	56.3	1.2	51.7	15.8	44.2
GU 45-626	44.1	28.5	56.7	55.3	1.0	56.6	21.9	43.7
GU 45-628	46.2	35.1	55.8	54.4	0.9	56.7	27.6	43.2
GU 45-642	40.8	12.4	59.7	56.8	2.9	48.7	8.9	44.8
GU 45-644	42.2	21.1	58.5	55.6	2.6	50.9	15.7	44.3
GU 45-646	44.1	28.5	57.5	54.6	2.2	56.3	21.8	43.8
GU 45-648	46.0	35.1	56.5	53.8	1.9	56.5	27.6	43.3
GU 45-662	41.3	12.3	60.4	56.0	4.4	48.5	8.7	45.1
GU 45-664	42.4	21.0	59.2	54.8	3.9	50.4	15.5	44.5
GU 45-666	44.0	28.4	58.2	53.9	3.4	57.1	21.7	44.0
GU 45-668	45.7	35.0	57.3	53.1	3.0	56.4	27.5	43.4
GU 45-682	42.3	12.1	61.1	55.2	5.9	48.4	8.5	45.6
GU 45-684	42.9	20.9	60.0	54.1	5.3	50.0	15.3	44.8
GU 45-686	44.1	28.4	59.0	53.1	4.7	57.9	21.5	44.2
GU 45-688	45.3	35.0	58.0	52.4	4.2	57.0	27.3	43.6
GU 45-722	38.8	15.9	69.0	67.7	1.4	51.9	9.4	47.9
GU 45-724	40.2	27.1	68.0	66.6	1.2	57.6	16.5	47.8
GU 45-726	42.1	36.6	67.1	65.7	1.1	61.4	23.1	47.6
GU 45-728	44.2	45.1	66.3	65.0	1.0	66.4	29.4	47.4
GU 45-742	39.0	15.9	69.6	67.1	2.8	51.7	9.3	48.0
GU 45-744	40.4	27.1	68.6	65.9	2.5	58.6	16.5	47.9
GU 45-746	42.2	36.6	67.8	65.0	2.2	58.4	23.1	47.7
GU 45-748	44.1	45.1	67.1	64.3	1.9	66.4	29.4	47.5
GU 45-762	39.7	15.8	70.3	66.4	4.3	51.5	9.2	48.3
GU 45-764	40.7	27.0	69.3	65.3	3.8	59.6	16.4	48.1
GU 45-766	42.1	36.5	68.6	64.3	3.4	58.9	22.9	47.9
GU 45-768	43.8	45.1	67.8	63.6	3.0	65.4	29.3	47.6
GU 45-782	40.5	15.6	70.9	65.8	5.7	51.3	9.0	48.8
GU 45-784	41.0	26.9	70.0	64.6	5.1	53.5	16.2	48.4
GU 45-786	42.2	36.5	69.3	63.6	4.6	58.9	22.8	48.1
GU 45-788	43.4	45.1	68.6	62.9	4.2	61.9	29.1	47.8

AEROFOIL	ZERO LIFT INCIDENCE (deg)	LIFT CURVE SLOPE (/deg)	LOW DRAG RANGE OF LIFT COEFFICIENT LOWER LIMIT	DESIGN	UPPER LIMIT	AERODYNAMIC CENTRE POSN. (percent c) x	y	PITCHING MOMENT COEF.
GU 45-562	-3.6	0.117	0.58	0.70	0.82	26.2	1.3	-0.081
GU 45-564	-3.2	0.122	0.49	0.73	0.97	27.1	1.1	-0.073
GU 45-566	-2.8	0.127	0.38	0.76	1.14	27.9	0.9	-0.066
GU 45-568	-2.3	0.132	0.26	0.79	1.31	28.6	0.6	-0.059
GU 45-582	-4.8	0.117	0.82	0.93	1.05	26.2	1.7	-0.108
GU 45-584	-4.4	0.122	0.73	0.97	1.22	27.1	1.6	-0.098
GU 45-586	-3.8	0.127	0.63	1.01	1.39	27.9	1.4	-0.088
GU 45-588	-3.3	0.132	0.53	1.05	1.57	28.7	1.0	-0.079
GU 45-622	-1.3	0.117	0.12	0.23	0.35	26.5	0.3	-0.031
GU 45-624	-1.1	0.123	0.00	0.25	0.49	27.6	0.3	-0.029
GU 45-626	-0.9	0.129	-0.13	0.26	0.64	28.5	0.1	-0.027
GU 45-628	-0.7	0.134	-0.27	0.27	0.80	29.5	-0.1	-0.024
GU 45-642	-2.6	0.117	0.35	0.47	0.59	26.5	0.7	-0.063
GU 45-644	-2.3	0.123	0.25	0.49	0.74	27.6	0.6	-0.058
GU 45-646	-2.0	0.129	0.13	0.51	0.90	28.6	0.4	-0.054
GU 45-648	-1.6	0.134	0.00	0.54	1.07	29.5	0.1	-0.049
GU 45-662	-4.0	0.117	0.59	0.70	0.82	26.6	1.1	-0.095
GU 45-664	-3.6	0.123	0.49	0.74	0.98	27.7	1.0	-0.088
GU 45-666	-3.1	0.129	0.39	0.77	1.15	28.7	0.7	-0.081
GU 45-668	-2.7	0.134	0.27	0.80	1.33	29.6	0.4	-0.075
GU 45-682	-5.3	0.118	0.82	0.94	1.05	26.6	1.4	-0.127
GU 45-684	-4.9	0.123	0.74	0.98	1.23	27.7	1.4	-0.117
GU 45-686	-4.4	0.129	0.64	1.03	1.41	28.8	1.2	-0.108
GU 45-688	-3.8	0.134	0.54	1.07	1.60	29.8	0.9	-0.099
GU 45-722	-1.4	0.118	0.12	0.24	0.35	26.8	0.2	-0.037
GU 45-724	-1.3	0.124	0.00	0.25	0.50	28.2	0.1	-0.035
GU 45-726	-1.0	0.131	-0.13	0.26	0.65	29.4	-0.1	-0.034
GU 45-728	-0.8	0.137	-0.27	0.27	0.82	30.6	-0.3	-0.032
GU 45-742	-2.9	0.118	0.35	0.47	0.59	26.9	0.5	-0.073
GU 45-744	-2.6	0.124	0.25	0.50	0.74	28.2	0.3	-0.070
GU 45-746	-2.3	0.131	0.13	0.52	0.91	29.5	0.1	-0.066
GU 45-748	-1.9	0.137	0.00	0.55	1.09	30.7	-0.2	-0.063
GU 45-762	-4.3	0.118	0.59	0.71	0.82	27.0	0.8	-0.110
GU 45-764	-4.0	0.124	0.50	0.75	0.99	28.3	0.7	-0.104
GU 45-766	-3.6	0.131	0.39	0.78	1.17	29.6	0.4	-0.099
GU 45-768	-3.1	0.137	0.27	0.82	1.36	30.8	0.1	-0.094
GU 45-782	-5.8	0.118	0.83	0.94	1.06	27.0	1.1	-0.147
GU 45-784	-5.4	0.125	0.75	0.99	1.24	28.4	1.0	-0.139
GU 45-786	-4.9	0.131	0.65	1.04	1.43	29.7	0.8	-0.132
GU 45-788	-4.4	0.137	0.55	1.09	1.63	30.9	0.4	-0.124

AEROFOIL	THICKNESS AT 0.05c (percent of max.)	T.E. ANGLE (deg)	EXTENT OF FAV. PRESSURE GRAD. (percent c) TOP	BOTTOM	MAX.CAMBER (per cent chord)	POSITION (percent chord)	MAX. THICKNESS (per cent chord)	POSITION (percent chord)
GU 61-322	52.3	4.5	29.0	27.2	1.2	35.8	8.8	29.5
GU 61-324	57.3	7.8	27.1	25.8	-0.7	1.1	15.8	27.8
GU 61-326	62.0	10.6	25.2	24.5	-1.5	2.4	22.3	26.2
GU 61-328	66.1	13.2	23.3	23.4	-2.5	4.1	28.6	24.8
GU 61-342	52.3	4.5	29.8	26.2	2.5	35.1	8.7	29.8
GU 61-344	56.9	7.8	27.8	25.1	1.6	40.9	15.7	28.1
GU 61-346	60.9	10.7	25.9	24.1	-1.3	3.0	22.2	26.5
GU 61-348	64.0	13.3	24.0	23.3	-2.3	5.1	28.5	25.1
GU 61-362	53.1	4.5	30.6	25.2	3.8	34.8	8.6	30.4
GU 61-364	56.6	7.9	28.6	24.4	2.8	36.0	15.5	28.5
GU 61-366	59.7	11.0	26.6	23.7	1.5	39.2	22.0	26.8
GU 61-368	61.2	13.7	24.7	23.2	-1.8	6.0	28.2	25.4
GU 61-382	53.9	4.4	31.3	24.0	5.2	34.7	8.4	31.0
GU 61-384	56.6	8.0	29.3	23.6	4.0	35.3	15.4	28.9
GU 61-386	58.3	11.1	27.4	23.2	2.5	39.8	21.8	27.2
GU 61-388	57.7	14.0	25.4	23.0	-1.2	6.8	27.9	25.8
GU 61-422	48.9	5.4	38.6	36.9	1.2	43.0	9.5	34.6
GU 61-424	53.6	9.3	36.5	35.2	-0.7	1.1	17.2	33.0
GU 61-426	58.2	12.7	34.4	33.7	-1.5	2.4	24.4	31.4
GU 61-428	62.1	15.8	32.3	32.4	-2.5	4.0	31.3	29.9
GU 61-442	48.9	5.3	39.4	36.0	2.6	43.7	9.4	34.7
GU 61-444	53.1	9.3	37.3	34.5	1.9	41.4	17.0	33.1
GU 61-446	57.2	12.8	35.2	33.2	-1.4	3.0	24.3	31.5
GU 61-448	60.4	16.0	33.1	32.2	-2.4	5.1	31.3	30.2
GU 61-462	49.8	5.4	40.1	35.0	4.1	39.8	9.3	35.1
GU 61-464	53.1	9.5	38.0	33.8	3.0	42.1	16.9	33.2
GU 61-466	56.2	13.1	35.9	32.7	1.8	43.7	24.1	31.7
GU 61-468	57.8	16.4	33.8	31.9	-2.0	5.9	31.0	30.4
GU 61-482	50.7	5.3	40.8	34.0	5.5	39.7	9.1	36.0
GU 61-484	53.1	9.5	38.7	33.0	4.3	42.7	16.7	33.4
GU 61-486	55.0	13.2	36.7	32.1	3.0	40.8	23.8	31.9
GU 61-488	54.7	16.7	34.6	31.6	1.4	43.8	30.8	30.7
GU 61-522	46.5	6.6	48.3	46.7	1.3	47.4	10.1	38.7
GU 61-524	50.7	11.5	46.2	44.9	0.8	48.9	18.3	37.2
GU 61-526	55.2	15.7	44.0	43.2	-1.5	2.3	26.1	35.7
GU 61-528	59.2	19.6	41.9	41.9	-2.6	4.0	33.9	34.4
GU 61-542	46.7	6.6	49.1	45.9	2.7	46.0	10.0	38.8
GU 61-544	50.7	11.5	46.9	44.2	2.0	47.5	18.3	37.4
GU 61-546	54.5	15.8	44.8	42.7	-1.4	3.0	26.1	35.9
GU 61-548	57.6	19.8	42.6	41.5	-2.5	5.0	33.8	34.6

APPENDIX III, Part 2

AEROFOIL	ZERO LIFT INCIDENCE (deg)	LIFT CURVE SLOPE (/deg)	LOW DRAG RANGE OF LIFT COEFFICIENT LOWER LIMIT	DESIGN	UPPER LIMIT	AERODYNAMIC CENTRE POSN. (percent c) x	y	PITCHING MOMENT COEF.
GU 61-322	-0.8	0.117	0.12	0.23	0.35	25.6	0.3	-0.018
GU 61-324	-0.3	0.123	0.00	0.25	0.49	25.9	-0.2	-0.014
GU 61-326	0.4	0.129	-0.13	0.26	0.64	26.2	-0.9	-0.010
GU 61-328	1.3	0.134	-0.27	0.27	0.80	26.6	-1.9	-0.006
GU 61-342	-1.8	0.117	0.35	0.47	0.58	25.6	0.8	-0.037
GU 61-344	-1.1	0.123	0.25	0.49	0.73	26.0	0.3	-0.028
GU 61-346	-0.2	0.128	0.13	0.51	0.90	26.4	-0.5	-0.020
GU 61-348	0.9	0.134	0.00	0.53	1.07	26.8	-1.5	-0.011
GU 61-362	-2.8	0.117	0.58	0.70	0.82	25.6	1.4	-0.055
GU 61-364	-1.9	0.123	0.49	0.73	0.98	26.1	0.8	-0.042
GU 61-366	-0.9	0.128	0.38	0.77	1.15	26.5	0.0	-0.030
GU 61-368	0.3	0.133	0.27	0.80	1.33	27.0	-1.0	-0.017
GU 61-382	-3.8	0.117	0.82	0.93	1.05	25.6	1.9	-0.074
GU 61-384	-2.8	0.122	0.73	0.98	1.22	26.1	1.4	-0.057
GU 61-386	-1.6	0.128	0.64	1.02	1.40	26.6	0.6	-0.040
GU 61-388	-0.4	0.133	0.53	1.06	1.58	27.2	-0.4	-0.023
GU 61-422	-0.9	0.117	0.12	0.23	0.35	25.8	0.3	-0.022
GU 61-424	-0.4	0.124	0.00	0.25	0.50	26.3	-0.2	-0.018
GU 61-426	0.3	0.130	-0.13	0.26	0.65	26.8	-0.9	-0.014
GU 61-428	1.2	0.137	-0.27	0.27	0.82	27.4	-1.9	-0.010
GU 61-442	-2.0	0.117	0.35	0.47	0.59	25.9	0.8	-0.044
GU 61-444	-1.3	0.124	0.25	0.49	0.74	26.4	0.2	-0.036
GU 61-446	-0.4	0.130	0.13	0.52	0.91	27.0	-0.5	-0.027
GU 61-448	0.7	0.136	0.00	0.54	1.09	27.6	-1.5	-0.017
GU 61-462	-3.1	0.117	0.59	0.70	0.82	25.9	1.3	-0.065
GU 61-464	-2.2	0.124	0.49	0.74	0.99	26.5	0.8	-0.053
GU 61-466	-1.2	0.130	0.39	0.78	1.16	27.1	-0.0	-0.041
GU 61-468	0.0	0.136	0.27	0.81	1.35	27.8	-1.0	-0.027
GU 61-482	-4.2	0.118	0.82	0.94	1.05	25.9	1.8	-0.088
GU 61-484	-3.2	0.124	0.74	0.99	1.23	26.5	1.4	-0.071
GU 61-486	-2.0	0.129	0.65	1.03	1.41	27.3	0.6	-0.055
GU 61-488	-0.7	0.135	0.54	1.08	1.61	28.0	-0.4	-0.037
GU 61-522	-1.0	0.118	0.12	0.24	0.35	26.1	0.2	-0.025
GU 61-524	-0.5	0.125	0.00	0.25	0.50	26.8	-0.3	-0.021
GU 61-526	0.3	0.132	-0.13	0.26	0.66	27.5	-1.0	-0.017
GU 61-528	1.2	0.139	-0.28	0.28	0.83	28.3	-2.0	-0.012
GU 61-542	-2.2	0.118	0.35	0.47	0.59	26.1	0.7	-0.051
GU 61-544	-1.5	0.125	0.25	0.50	0.75	26.9	0.2	-0.043
GU 61-546	-0.5	0.132	0.13	0.53	0.92	27.7	-0.6	-0.034
GU 61-548	0.6	0.139	0.00	0.55	1.11	28.6	-1.6	-0.025

AEROFOIL	THICKNESS AT 0.05c (percent of max.)	T.E. ANGLE (deg)	EXTENT OF FAV. PRESSURE GRAD. (percent c) TOP	BOTTOM	MAX.CAMBER (per cent chord)	POSITION (percent chord)	MAX. THICKNESS (per cent chord)	POSITION (percent chord)
GU 61-562	47.3	6.6	49.8	45.1	4.2	45.4	9.9	39.1
GU 61-564	50.4	11.7	47.7	43.4	3.3	47.3	18.1	37.5
GU 61-566	53.5	16.1	45.6	42.1	2.2	47.8	25.9	36.1
GU 61-568	55.3	20.2	43.4	41.1	-2.1	5.9	33.6	34.8
GU 61-582	48.2	6.6	50.5	44.1	5.6	46.0	9.7	39.5
GU 61-584	50.5	11.7	48.4	42.7	4.6	47.0	17.9	37.6
GU 61-586	52.5	16.3	46.3	41.5	3.3	47.3	25.7	36.3
GU 61-588	52.5	20.5	44.2	40.6	2.0	48.6	33.2	35.0
GU 61-622	44.3	8.5	58.1	56.7	1.3	50.9	10.6	42.3
GU 61-624	48.6	14.7	56.0	54.7	0.9	56.5	19.4	41.1
GU 61-626	52.9	20.2	54.0	53.1	-1.6	2.3	27.8	39.8
GU 61-628	56.7	25.3	51.9	51.7	-2.7	4.1	36.4	38.6
GU 61-642	44.7	8.4	58.8	56.0	2.7	49.9	10.6	42.5
GU 61-644	48.5	14.8	56.8	54.1	2.0	55.9	19.4	41.2
GU 61-646	52.2	20.3	54.7	52.5	-1.5	3.0	27.8	39.9
GU 61-648	55.3	25.4	52.6	51.3	-2.6	5.0	36.3	38.8
GU 61-662	45.2	8.5	59.5	55.2	4.1	49.4	10.4	42.6
GU 61-664	48.3	14.9	57.5	53.4	3.3	56.4	19.2	41.3
GU 61-666	51.3	20.6	55.5	51.9	2.4	57.1	27.7	40.1
GU 61-668	53.2	25.9	53.4	50.8	-2.3	5.9	36.1	39.0
GU 61-682	46.0	8.4	60.2	54.4	5.6	49.1	10.2	42.9
GU 61-684	48.3	15.0	58.3	52.7	4.6	57.2	19.0	41.5
GU 61-686	50.4	20.8	56.3	51.2	3.6	55.9	27.4	40.3
GU 61-688	50.6	26.2	54.3	50.2	2.3	55.9	35.8	39.2
GU 61-722	42.8	11.5	68.2	66.9	1.3	54.6	11.2	45.7
GU 61-724	46.7	20.0	66.2	65.0	0.9	66.0	20.4	44.7
GU 61-726	50.9	27.6	64.4	63.5	-1.6	2.3	29.6	43.7
GU 61-728	54.6	34.5	62.5	62.3	-2.8	4.2	38.9	42.8
GU 61-742	43.0	11.5	68.8	66.3	2.6	53.1	11.1	45.8
GU 61-744	46.7	20.1	66.9	64.4	2.0	60.0	20.4	44.8
GU 61-746	50.3	27.7	65.1	62.9	-1.6	3.0	29.6	43.9
GU 61-748	53.3	34.7	63.3	61.8	-2.8	5.1	38.9	43.0
GU 61-762	43.4	11.5	69.4	65.6	4.0	52.6	10.9	45.9
GU 61-764	46.4	20.3	67.7	63.7	3.3	58.1	20.3	45.0
GU 61-766	49.5	28.0	65.9	62.2	2.6	65.5	29.4	44.0
GU 61-768	51.3	35.1	64.1	61.1	-2.4	5.8	38.5	43.1
GU 61-782	44.1	11.5	70.1	65.0	5.5	52.3	10.7	46.2
GU 61-784	46.4	20.3	68.4	63.1	4.5	58.3	20.1	45.1
GU 61-786	48.6	28.2	66.7	61.6	3.7	65.1	29.2	44.2
GU 61-788	49.0	35.4	65.0	60.5	2.8	65.3	38.3	43.3

AEROFOIL	ZERO LIFT INCIDENCE (deg)	LIFT CURVE SLOPE (/deg)	LOW DRAG RANGE OF LIFT COEFFICIENT LOWER LIMIT	DESIGN	UPPER LIMIT	AERODYNAMIC CENTRE POSN. (percent c) x	y	PITCHING MOMENT COEF.
GU 61-562	-3.4	0.118	0.59	0.71	0.82	26.1	1.1	-0.077
GU 61-564	-2.5	0.125	0.50	0.75	1.00	27.0	0.6	-0.065
GU 61-566	-1.4	0.132	0.39	0.79	1.18	27.9	-0.1	-0.051
GU 61-568	-0.2	0.138	0.28	0.83	1.38	28.8	-1.1	-0.037
GU 61-582	-4.6	0.118	0.83	0.94	1.06	26.2	1.6	-0.103
GU 61-584	-3.6	0.125	0.75	1.00	1.24	27.1	1.1	-0.086
GU 61-586	-2.4	0.131	0.66	1.05	1.44	28.0	0.4	-0.069
GU 61-588	-1.1	0.138	0.55	1.10	1.64	29.0	-0.6	-0.052
GU 61-622	-1.1	0.119	0.12	0.24	0.36	26.4	0.2	-0.030
GU 61-624	-0.6	0.126	0.00	0.25	0.50	27.5	-0.3	-0.026
GU 61-626	0.1	0.134	-0.13	0.27	0.67	28.5	-1.0	-0.022
GU 61-628	1.1	0.142	-0.28	0.28	0.85	29.6	-2.1	-0.018
GU 61-642	-2.4	0.119	0.36	0.47	0.59	26.5	0.6	-0.061
GU 61-644	-1.7	0.126	0.25	0.50	0.76	27.6	0.1	-0.053
GU 61-646	-0.8	0.134	0.13	0.54	0.94	28.7	-0.6	-0.044
GU 61-648	0.4	0.142	0.00	0.57	1.13	29.9	-1.7	-0.035
GU 61-662	-3.7	0.119	0.59	0.71	0.83	26.5	0.9	-0.091
GU 61-664	-2.9	0.126	0.50	0.76	1.01	27.7	0.5	-0.079
GU 61-666	-1.8	0.134	0.40	0.80	1.20	28.9	-0.2	-0.066
GU 61-668	-0.5	0.141	0.28	0.85	1.41	30.1	-1.2	-0.052
GU 61-682	-5.0	0.119	0.83	0.95	1.06	26.6	1.3	-0.122
GU 61-684	-4.1	0.126	0.76	1.01	1.25	27.8	1.0	-0.106
GU 61-686	-2.9	0.133	0.67	1.06	1.46	29.0	0.3	-0.089
GU 61-688	-1.5	0.141	0.56	1.12	1.68	30.3	-0.6	-0.070
GU 61-722	-1.2	0.119	0.12	0.24	0.36	26.9	0.0	-0.036
GU 61-724	-0.7	0.128	0.00	0.26	0.51	28.2	-0.5	-0.033
GU 61-726	0.0	0.137	-0.14	0.27	0.68	29.6	-1.1	-0.028
GU 61-728	1.0	0.146	-0.29	0.29	0.87	31.1	-2.2	-0.024
GU 61-742	-2.7	0.119	0.36	0.48	0.60	26.9	0.3	-0.071
GU 61-744	-2.0	0.128	0.26	0.51	0.77	28.3	-0.1	-0.065
GU 61-746	-1.1	0.136	0.14	0.55	0.95	29.7	-0.8	-0.056
GU 61-748	0.1	0.146	0.00	0.58	1.16	31.3	-1.9	-0.047
GU 61-762	-4.1	0.119	0.60	0.71	0.83	26.9	0.6	-0.107
GU 61-764	-3.3	0.128	0.51	0.76	1.02	28.5	0.2	-0.097
GU 61-766	-2.2	0.136	0.41	0.82	1.22	30.0	-0.6	-0.086
GU 61-768	-0.9	0.145	0.29	0.87	1.44	31.5	-1.6	-0.071
GU 61-782	-5.5	0.120	0.83	0.95	1.07	27.0	1.0	-0.142
GU 61-784	-4.6	0.128	0.76	1.02	1.27	28.6	0.5	-0.129
GU 61-786	-3.5	0.136	0.68	1.08	1.49	30.1	-0.2	-0.114
GU 61-788	-2.1	0.145	0.58	1.15	1.72	31.7	-1.1	-0.095

AEROFOIL	THICKNESS AT 0.05c (percent of max.)	T.E. ANGLE (deg)	EXTENT OF FAV. PRESSURE GRAD. (percent c) TOP	BOTTOM	MAX.CAMBER (per cent chord)	POSITION (percent chord)	MAX. THICKNESS (per cent chord)	POSITION (percent chord)
GU 63-322	51.8	7.3	29.1	27.3	1.2	35.9	8.9	30.0
GU 63-324	56.8	12.7	27.2	25.9	-0.7	1.1	16.0	28.4
GU 63-326	61.5	17.3	25.4	24.7	-1.5	2.4	22.7	26.9
GU 63-328	65.5	21.6	23.6	23.7	-2.5	4.1	29.2	25.5
GU 63-342	51.8	7.2	29.9	26.3	2.5	35.1	8.8	30.3
GU 63-344	56.3	12.6	28.0	25.3	1.6	41.1	15.9	28.7
GU 63-346	60.3	17.3	26.1	24.3	-1.3	3.1	22.6	27.1
GU 63-348	63.3	21.6	24.2	23.6	-2.3	5.2	29.0	25.8
GU 63-362	52.6	7.0	30.6	25.3	3.8	34.8	8.7	30.8
GU 63-364	56.0	12.5	28.8	24.5	2.8	36.1	15.8	29.0
GU 63-366	59.1	17.2	26.9	23.9	1.5	39.5	22.4	27.4
GU 63-368	60.6	21.6	24.9	23.4	-1.8	6.1	28.7	26.1
GU 63-382	53.3	6.8	31.4	24.1	5.2	34.7	8.5	31.4
GU 63-384	56.0	12.3	29.5	23.7	4.0	35.4	15.6	29.4
GU 63-386	57.7	17.1	27.6	23.4	2.5	40.1	22.1	27.8
GU 63-388	57.0	21.6	25.7	23.2	-1.2	6.9	28.5	26.4
GU 63-422	48.4	8.6	38.7	37.0	1.2	43.1	9.7	35.2
GU 63-424	53.1	14.9	36.7	35.4	-0.7	1.1	17.4	33.6
GU 63-426	57.6	20.4	34.7	34.0	-1.5	2.4	24.8	32.1
GU 63-428	61.6	25.5	32.7	32.8	-2.6	4.1	32.1	30.7
GU 63-442	48.5	8.5	39.5	36.1	2.6	43.8	9.5	35.4
GU 63-444	52.8	14.9	37.5	34.7	1.8	41.7	17.3	33.7
GU 63-446	56.7	20.4	35.5	33.5	-1.4	3.0	24.7	32.3
GU 63-448	59.7	25.5	33.4	32.6	-2.4	5.1	31.9	30.9
GU 63-462	49.3	8.4	40.3	35.1	4.0	39.8	9.4	35.8
GU 63-464	52.5	14.8	38.2	34.0	3.0	42.3	17.1	33.9
GU 63-466	55.5	20.4	36.2	32.9	1.9	44.0	24.4	32.4
GU 63-468	57.2	25.5	34.2	32.2	-1.9	5.9	31.5	31.1
GU 63-482	50.2	8.2	41.0	34.1	5.5	39.8	9.2	36.7
GU 63-484	52.6	14.6	39.0	33.2	4.3	43.0	17.0	34.1
GU 63-486	54.4	20.3	37.0	32.4	2.9	41.0	24.2	32.6
GU 63-488	54.1	25.6	34.9	31.9	1.5	44.3	31.2	31.3
GU 63-522	46.0	10.4	48.5	46.9	1.3	47.4	10.3	39.4
GU 63-524	50.4	18.1	46.5	45.2	0.7	49.2	18.6	38.0
GU 63-526	54.8	24.8	44.5	43.7	-1.6	2.4	26.7	36.7
GU 63-528	58.5	31.0	42.4	42.4	-2.7	4.0	34.6	35.2
GU 63-542	46.1	10.3	49.2	46.0	2.7	45.9	10.1	39.5
GU 63-544	50.0	18.0	47.2	44.4	2.0	47.6	18.5	38.1
GU 63-546	53.8	24.8	45.2	43.1	-1.4	2.8	26.4	36.7
GU 63-548	57.0	31.0	43.1	42.0	-2.6	5.1	34.5	35.5

AEROFOIL	ZERO LIFT INCIDENCE (deg)	LIFT CURVE SLOPE (/deg)	LOW DRAG RANGE OF LIFT COEFFICIENT LOWER LIMIT	DESIGN	UPPER LIMIT	AERODYNAMIC CENTRE POSN. (percent c) x	y	PITCHING MOMENT COEF.
GU 63-322	-0.8	0.117	0.12	0.23	0.35	25.7	0.3	-0.018
GU 63-324	-0.3	0.123	0.00	0.25	0.49	26.1	-0.2	-0.014
GU 63-326	0.4	0.129	-0.13	0.26	0.65	26.5	-0.9	-0.010
GU 63-328	1.3	0.135	-0.27	0.27	0.81	27.0	-1.9	-0.006
GU 63-342	-1.8	0.117	0.35	0.47	0.58	25.7	0.8	-0.037
GU 63-344	-1.1	0.123	0.25	0.49	0.74	26.2	0.3	-0.028
GU 63-346	-0.2	0.129	0.13	0.52	0.90	26.7	-0.5	-0.020
GU 63-348	0.9	0.135	0.00	0.54	1.08	27.2	-1.5	-0.011
GU 63-362	-2.8	0.117	0.58	0.70	0.82	25.7	1.4	-0.055
GU 63-364	-1.9	0.123	0.49	0.74	0.98	26.3	0.8	-0.043
GU 63-366	-0.9	0.129	0.39	0.77	1.15	26.8	0.0	-0.030
GU 63-368	0.3	0.134	0.27	0.80	1.34	27.4	-1.0	-0.017
GU 63-382	-3.8	0.117	0.82	0.93	1.05	25.7	1.9	-0.074
GU 63-384	-2.8	0.123	0.74	0.98	1.22	26.3	1.4	-0.057
GU 63-386	-1.7	0.128	0.64	1.02	1.40	26.9	0.6	-0.041
GU 63-388	-0.4	0.134	0.53	1.07	1.59	27.6	-0.4	-0.023
GU 63-422	-0.9	0.118	0.12	0.24	0.35	26.0	0.3	-0.022
GU 63-424	-0.4	0.124	0.00	0.25	0.50	26.5	-0.2	-0.018
GU 63-426	0.3	0.131	-0.13	0.26	0.66	27.1	-0.9	-0.014
GU 63-428	1.2	0.138	-0.28	0.28	0.83	27.8	-1.9	-0.010
GU 63-442	-2.0	0.118	0.35	0.47	0.59	26.0	0.8	-0.044
GU 63-444	-1.3	0.124	0.25	0.50	0.74	26.6	0.3	-0.036
GU 63-446	-0.4	0.131	0.13	0.52	0.91	27.3	-0.5	-0.027
GU 63-448	0.8	0.137	0.00	0.55	1.10	28.1	-1.6	-0.018
GU 63-462	-3.1	0.118	0.59	0.70	0.82	26.0	1.3	-0.066
GU 63-464	-2.2	0.124	0.50	0.74	0.99	26.7	0.8	-0.054
GU 63-466	-1.2	0.131	0.39	0.78	1.17	27.5	-0.1	-0.041
GU 63-468	0.0	0.137	0.27	0.82	1.36	28.3	-1.1	-0.028
GU 63-482	-4.2	0.118	0.82	0.94	1.06	26.0	1.8	-0.088
GU 63-484	-3.2	0.124	0.74	0.99	1.23	26.8	1.4	-0.072
GU 63-486	-2.1	0.130	0.65	1.04	1.42	27.6	0.6	-0.055
GU 63-488	-0.7	0.136	0.54	1.09	1.62	28.5	-0.5	-0.038
GU 63-522	-1.0	0.118	0.12	0.24	0.35	26.3	0.2	-0.025
GU 63-524	-0.5	0.126	0.00	0.25	0.50	27.1	-0.3	-0.021
GU 63-526	0.3	0.133	-0.13	0.27	0.66	27.9	-1.0	-0.017
GU 63-528	1.2	0.141	-0.28	0.28	0.84	28.9	-2.1	-0.012
GU 63-542	-2.2	0.118	0.35	0.47	0.59	26.3	0.6	-0.051
GU 63-544	-1.5	0.126	0.25	0.50	0.75	27.2	0.1	-0.043
GU 63-546	-0.5	0.133	0.13	0.53	0.93	28.1	-0.7	-0.035
GU 63-548	0.6	0.140	0.00	0.56	1.12	29.1	-1.6	-0.026

AEROFOIL	THICKNESS AT 0.05c (percent of max.)	T.E. ANGLE (deg)	EXTENT OF FAV. PRESSURE GRAD. (percent c) TOP	BOTTOM	MAX.CAMBER (per cent chord)	POSITION (percent chord)	MAX. THICKNESS (per cent chord)	POSITION (percent chord)
GU 63-562	46.8	10.2	50.0	45.2	4.2	45.4	10.0	39.8
GU 63-564	49.9	17.9	48.0	43.7	3.2	47.5	18.4	38.3
GU 63-566	52.9	24.8	46.0	42.5	2.2	48.2	26.3	36.9
GU 63-568	54.6	31.0	43.9	41.6	-2.1	5.9	34.3	35.7
GU 63-582	47.7	10.0	50.7	44.3	5.6	46.2	9.8	40.3
GU 63-584	50.0	17.9	48.7	43.0	4.5	47.1	18.2	38.5
GU 63-586	51.9	24.8	46.8	41.9	3.3	47.6	26.1	37.2
GU 63-588	51.7	31.1	44.7	41.2	1.9	49.1	34.0	36.0
GU 63-622	43.9	12.9	58.4	56.9	1.3	50.9	10.8	43.1
GU 63-624	48.3	22.6	56.4	55.1	0.8	56.8	19.7	41.9
GU 63-626	52.4	31.1	54.5	53.6	-1.6	2.4	28.3	40.8
GU 63-628	56.1	38.9	52.6	52.5	-2.7	4.2	37.1	39.6
GU 63-642	44.3	12.9	59.1	56.2	2.7	49.9	10.7	43.2
GU 63-644	47.8	22.6	57.2	54.4	2.1	56.0	19.6	42.0
GU 63-646	51.7	31.1	55.3	53.0	-1.5	3.0	28.3	40.9
GU 63-648	54.7	38.9	53.4	52.1	-2.7	5.1	37.1	39.9
GU 63-662	44.8	12.8	59.8	55.4	4.1	49.4	10.6	43.4
GU 63-664	47.8	22.5	57.9	53.7	3.3	56.8	19.5	42.2
GU 63-666	50.8	31.1	56.1	52.4	2.4	56.2	28.1	41.1
GU 63-668	52.6	39.0	54.2	51.5	-2.3	5.9	36.9	40.0
GU 63-682	45.6	12.7	60.5	54.6	5.6	49.1	10.3	43.8
GU 63-684	47.8	22.5	58.7	53.0	4.5	57.6	19.3	42.4
GU 63-686	49.9	31.1	56.9	51.8	3.5	56.2	27.9	41.3
GU 63-688	49.9	39.0	55.0	50.9	2.3	56.5	36.6	40.3
GU 63-722	42.2	16.9	68.4	67.1	1.3	57.9	11.3	46.4
GU 63-724	46.3	29.6	66.7	65.5	0.9	64.4	20.7	45.6
GU 63-726	50.4	40.8	65.1	64.2	-1.7	2.3	30.1	44.7
GU 63-728	54.0	51.1	63.5	63.3	-2.8	4.2	39.8	43.9
GU 63-742	42.6	16.9	69.1	66.5	2.6	53.1	11.2	46.6
GU 63-744	46.2	29.6	67.4	64.9	2.0	60.4	20.7	45.8
GU 63-746	49.8	40.8	65.9	63.6	-1.6	3.0	30.1	44.9
GU 63-748	52.7	51.1	64.3	62.7	-2.8	5.2	39.8	44.2
GU 63-762	43.0	16.8	69.7	65.9	4.0	52.6	11.1	46.8
GU 63-764	46.0	29.5	68.2	64.2	3.2	58.5	20.6	45.9
GU 63-766	48.9	40.8	66.7	62.9	2.5	66.0	29.9	45.0
GU 63-768	50.7	51.2	65.1	62.1	-2.4	5.9	39.4	44.3
GU 63-782	43.7	16.7	70.4	65.2	5.4	52.3	10.9	47.0
GU 63-784	46.0	29.5	68.9	63.5	4.5	58.7	20.4	46.1
GU 63-786	48.0	40.8	67.5	62.3	3.7	65.2	29.7	45.3
GU 63-788	48.3	51.3	66.0	61.4	2.8	66.2	39.1	44.5

AEROFOIL	ZERO LIFT INCIDENCE (deg)	LIFT CURVE SLOPE (/deg)	LOW DRAG RANGE OF LIFT COEFFICIENT LOWER LIMIT	DESIGN	UPPER LIMIT	AERODYNAMIC CENTRE POSN. (percent c) x	y	PITCHING MOMENT COEF
GU 63-562	-3.4	0.118	0.59	0.71	0.83	26.3	1.1	-0.078
GU 63-564	-2.5	0.125	0.50	0.75	1.00	27.3	0.6	-0.065
GU 63-566	-1.5	0.133	0.40	0.79	1.19	28.2	-0.2	-0.052
GU 63-568	-0.2	0.140	0.28	0.84	1.39	29.3	-1.2	-0.038
GU 63-582	-4.6	0.118	0.83	0.94	1.06	26.3	1.6	-0.104
GU 63-584	-3.6	0.125	0.75	1.00	1.25	27.3	1.1	-0.087
GU 63-586	-2.5	0.132	0.66	1.05	1.45	28.4	0.4	-0.070
GU 63-588	-1.1	0.139	0.56	1.11	1.66	29.6	-0.6	-0.053
GU 63-622	-1.1	0.119	0.12	0.24	0.36	26.6	0.2	-0.030
GU 63-624	-0.6	0.127	0.00	0.25	0.51	27.8	-0.3	-0.026
GU 63-626	0.1	0.135	-0.14	0.27	0.68	29.0	-1.0	-0.022
GU 63-628	1.1	0.144	-0.29	0.29	0.86	30.2	-2.1	-0.018
GU 63-642	-2.4	0.119	0.36	0.48	0.59	26.6	0.6	-0.061
GU 63-644	-1.7	0.127	0.25	0.51	0.76	27.9	0.0	-0.054
GU 63-646	-0.8	0.135	0.14	0.54	0.94	29.1	-0.7	-0.045
GU 63-648	0.4	0.143	0.00	0.57	1.14	30.4	-1.8	-0.036
GU 63-662	-3.7	0.119	0.59	0.71	0.83	26.7	0.9	-0.092
GU 63-664	-2.9	0.127	0.51	0.76	1.01	28.0	0.5	-0.080
GU 63-666	-1.9	0.135	0.40	0.81	1.21	29.3	-0.3	-0.068
GU 63-668	-0.6	0.143	0.29	0.86	1.42	30.7	-1.3	-0.053
GU 63-682	-5.0	0.119	0.83	0.95	1.07	26.7	1.3	-0.123
GU 63-684	-4.1	0.127	0.76	1.01	1.26	28.1	0.9	-0.107
GU 63-686	-3.0	0.135	0.67	1.07	1.47	29.5	0.2	-0.091
GU 63-688	-1.6	0.142	0.57	1.14	1.70	30.9	-0.7	-0.072
GU 63-722	-1.3	0.120	0.12	0.24	0.36	27.0	0.0	-0.036
GU 63-724	-0.8	0.129	0.00	0.26	0.51	28.5	-0.5	-0.033
GU 63-726	-0.0	0.138	-0.14	0.28	0.69	30.1	-1.3	-0.030
GU 63-728	1.0	0.148	-0.30	0.30	0.89	31.8	-2.2	-0.024
GU 63-742	-2.7	0.120	0.36	0.48	0.60	27.0	0.3	-0.072
GU 63-744	-2.0	0.129	0.26	0.51	0.77	28.6	-0.2	-0.066
GU 63-746	-1.1	0.138	0.14	0.55	0.96	30.3	-1.0	-0.059
GU 63-748	0.1	0.147	0.00	0.59	1.18	32.0	-2.0	-0.049
GU 63-762	-4.1	0.120	0.60	0.72	0.84	27.1	0.6	-0.107
GU 63-764	-3.3	0.128	0.51	0.77	1.02	28.8	0.1	-0.098
GU 63-766	-2.3	0.137	0.41	0.82	1.23	30.5	-0.6	-0.087
GU 63-768	-1.0	0.147	0.29	0.88	1.46	32.2	-1.6	-0.073
GU 63-782	-5.5	0.120	0.84	0.96	1.07	27.2	0.9	-0.143
GU 63-784	-4.7	0.128	0.77	1.02	1.28	28.9	0.5	-0.130
GU 63-786	-3.5	0.137	0.69	1.09	1.50	30.6	-0.2	-0.116
GU 63-788	-2.1	0.146	0.59	1.17	1.75	32.5	-1.3	-0.099

AEROFOIL	THICKNESS AT 0.05c (percent of max.)	T.E. ANGLE (deg)	EXTENT OF FAV. PRESSURE GRAD. (percent c)		MAX. CAMBER		MAX. THICKNESS	
			TOP	BOTTOM	(per cent chord)	POSITION (percent chord)	(per cent chord)	POSITION (percent chord)
GU 65-322	51.4	8.8	29.1	27.4	1.2	36.0	9.0	30.5
GU 65-324	56.3	15.2	27.4	26.1	-0.7	1.1	16.2	29.0
GU 65-326	60.9	20.8	25.6	24.9	-1.5	2.4	23.0	27.5
GU 65-328	65.0	25.9	23.8	23.9	-2.5	4.2	29.6	26.1
GU 65-342	51.4	8.6	30.0	26.4	2.5	35.2	8.9	30.8
GU 65-344	55.9	15.1	28.1	25.4	1.6	41.3	16.2	29.2
GU 65-346	59.8	20.7	26.3	24.5	-1.3	3.1	22.9	27.7
GU 65-348	62.8	25.9	24.4	23.8	-2.4	5.2	29.5	26.4
GU 65-362	52.1	8.4	30.7	25.3	3.8	34.9	8.8	31.2
GU 65-364	55.5	14.9	28.9	24.6	2.8	36.2	16.0	29.5
GU 65-366	58.6	20.6	27.0	24.0	1.5	39.8	22.7	28.0
GU 65-368	60.0	25.8	25.2	23.6	-1.9	6.1	29.2	26.7
GU 65-382	52.9	8.1	31.5	24.2	5.2	34.8	8.6	31.7
GU 65-384	55.5	14.7	29.6	23.8	4.0	35.6	15.8	29.8
GU 65-386	57.2	20.4	27.8	23.5	2.5	40.3	22.4	28.3
GU 65-388	56.4	25.7	25.9	23.4	-1.2	7.0	28.9	27.0
GU 65-422	48.0	10.2	38.8	37.1	1.2	43.2	9.8	35.7
GU 65-424	52.7	17.7	36.9	35.6	-0.7	1.1	17.6	34.2
GU 65-426	57.2	24.3	35.0	34.2	-1.6	2.4	25.1	32.7
GU 65-428	61.1	30.3	33.0	33.1	-2.6	4.2	32.6	31.2
GU 65-442	48.1	10.1	39.6	36.2	2.6	43.9	9.6	35.8
GU 65-444	52.3	17.6	37.7	34.9	1.8	41.9	17.5	34.3
GU 65-446	56.2	24.2	35.7	33.8	-1.4	3.0	25.0	32.9
GU 65-448	59.2	30.3	33.7	32.9	-2.5	5.2	32.4	31.6
GU 65-462	48.9	9.9	40.4	35.2	4.0	39.9	9.5	36.4
GU 65-464	52.1	17.5	38.4	34.1	3.0	42.5	17.4	34.4
GU 65-466	55.1	24.1	36.5	33.2	1.8	44.4	24.8	33.0
GU 65-468	56.6	30.2	34.5	32.5	-2.0	6.0	32.0	31.7
GU 65-482	49.8	9.6	41.1	34.2	5.5	39.8	9.3	37.3
GU 65-484	52.2	17.3	39.2	33.3	4.3	43.2	17.2	34.8
GU 65-486	53.9	24.0	37.2	32.6	3.0	41.3	24.6	33.2
GU 65-488	53.5	30.1	35.3	32.2	1.5	44.7	31.7	31.9
GU 65-522	45.7	12.1	48.6	47.0	1.3	47.3	10.4	39.9
GU 65-524	50.0	21.1	46.7	45.4	0.8	49.4	18.9	38.7
GU 65-526	54.4	29.1	44.8	44.0	-1.6	2.4	27.1	37.4
GU 65-528	58.2	36.3	42.8	42.8	-2.7	4.2	35.3	36.0
GU 65-542	45.7	12.0	49.4	46.2	2.7	45.9	10.2	40.0
GU 65-544	49.6	21.1	47.5	44.7	2.0	47.8	18.7	38.8
GU 65-546	53.3	29.0	45.5	43.4	-1.4	2.8	26.8	37.4
GU 65-548	56.5	36.3	43.5	42.4	-2.6	5.1	35.1	36.3

AEROFOIL	ZERO LIFT INCIDENCE (deg)	LIFT CURVE SLOPE (/deg)	LOW DRAG RANGE OF LIFT COEFFICIENT LOWER LIMIT	DESIGN	UPPER LIMIT	AERODYNAMIC CENTRE POSN. (percent c) x	y	PITCHING MOMENT COEF.
GU 65-322	-0.8	0.117	0.12	0.23	0.35	25.8	0.3	-0.018
GU 65-324	-0.3	0.124	0.00	0.25	0.49	26.3	-0.2	-0.014
GU 65-326	0.4	0.130	-0.13	0.26	0.65	26.7	-1.0	-0.010
GU 65-328	1.3	0.136	-0.27	0.27	0.82	27.3	-1.9	-0.006
GU 65-342	-1.8	0.117	0.35	0.47	0.59	25.8	0.8	-0.037
GU 65-344	-1.1	0.124	0.25	0.49	0.74	26.3	0.3	-0.028
GU 65-346	-0.2	0.130	0.13	0.52	0.91	26.9	-0.5	-0.020
GU 65-348	0.9	0.136	0.00	0.54	1.08	27.5	-1.5	-0.011
GU 65-362	-2.8	0.117	0.59	0.70	0.82	25.8	1.4	-0.055
GU 65-364	-1.9	0.123	0.49	0.74	0.98	26.4	0.8	-0.043
GU 65-366	-0.9	0.129	0.39	0.77	1.16	27.1	-0.0	-0.030
GU 65-368	0.3	0.135	0.27	0.81	1.34	27.8	-1.0	-0.017
GU 65-382	-3.8	0.117	0.82	0.94	1.05	25.8	1.9	-0.074
GU 65-384	-2.8	0.123	0.74	0.98	1.23	26.5	1.4	-0.058
GU 65-386	-1.7	0.129	0.64	1.03	1.41	27.2	0.6	-0.041
GU 65-388	-0.4	0.135	0.54	1.07	1.60	27.9	-0.4	-0.024
GU 65-422	-0.9	0.118	0.12	0.24	0.35	26.1	0.3	-0.022
GU 65-424	-0.4	0.125	0.00	0.25	0.50	26.7	-0.2	-0.018
GU 65-426	0.3	0.132	-0.13	0.26	0.66	27.4	-0.9	-0.014
GU 65-428	1.3	0.139	-0.28	0.28	0.83	28.2	-1.9	-0.010
GU 65-442	-2.0	0.118	0.35	0.47	0.59	26.1	0.8	-0.044
GU 65-444	-1.3	0.125	0.25	0.50	0.75	26.8	0.3	-0.036
GU 65-446	-0.4	0.132	0.13	0.53	0.92	27.6	-0.5	-0.028
GU 65-448	0.8	0.138	0.00	0.55	1.10	28.4	-1.6	-0.018
GU 65-462	-3.1	0.118	0.59	0.71	0.82	26.1	1.3	-0.066
GU 65-464	-2.2	0.125	0.50	0.75	0.99	26.9	0.8	-0.054
GU 65-466	-1.2	0.131	0.39	0.79	1.18	27.7	-0.0	-0.041
GU 65-468	0.1	0.138	0.28	0.83	1.37	28.6	-1.1	-0.028
GU 65-482	-4.2	0.118	0.82	0.94	1.06	26.1	1.8	-0.088
GU 65-484	-3.2	0.125	0.75	0.99	1.24	26.9	1.4	-0.072
GU 65-486	-2.1	0.131	0.65	1.04	1.43	27.8	0.6	-0.055
GU 65-488	-0.7	0.137	0.55	1.09	1.63	28.8	-0.5	-0.038
GU 65-522	-1.0	0.118	0.12	0.24	0.35	26.4	0.2	-0.025
GU 65-524	-0.5	0.126	0.00	0.25	0.50	27.3	-0.3	-0.021
GU 65-526	0.3	0.134	-0.13	0.27	0.67	28.2	-1.0	-0.017
GU 65-528	1.3	0.142	-0.28	0.28	0.85	29.2	-2.0	-0.012
GU 65-542	-2.2	0.118	0.35	0.47	0.59	26.4	0.6	-0.051
GU 65-544	-1.5	0.126	0.25	0.50	0.75	27.3	0.1	-0.044
GU 65-546	-0.5	0.134	0.13	0.53	0.93	28.4	-0.7	-0.035
GU 65-548	0.6	0.141	0.00	0.56	1.13	29.5	-1.7	-0.026

AEROFOIL	THICKNESS AT 0.05c (percent of max.)	T.E. ANGLE (deg)	EXTENT OF FAV. PRESSURE GRAD. (percent c) TOP	BOTTOM	MAX.CAMBER (per cent chord)	POSITION (percent chord)	MAX. THICKNESS (per cent chord)	POSITION (percent chord)
GU 65-562	46.4	11.9	50.1	45.3	4.2	45.5	10.1	40.4
GU 65-564	49.5	21.0	48.2	43.9	3.2	47.6	18.6	38.9
GU 65-566	52.4	28.9	46.3	42.8	2.2	48.4	26.6	37.6
GU 65-568	54.1	36.3	44.3	42.1	-2.1	6.0	34.9	36.4
GU 65-582	47.3	11.7	50.8	44.4	5.6	46.3	9.9	40.9
GU 65-584	49.6	20.8	49.0	43.2	4.5	47.2	18.4	39.2
GU 65-586	51.4	28.8	47.1	42.2	3.3	47.8	26.5	37.8
GU 65-588	51.2	36.2	45.1	41.6	1.9	49.6	34.6	36.7
GU 65-622	43.8	14.9	58.5	57.1	1.3	51.0	10.9	43.7
GU 65-624	47.9	26.0	56.7	55.4	0.8	57.0	20.0	42.6
GU 65-626	51.9	35.8	54.9	54.0	-1.6	2.4	28.7	41.6
GU 65-628	55.7	44.8	53.1	53.0	-2.8	4.2	37.7	40.4
GU 65-642	44.0	14.8	59.2	56.3	2.7	49.9	10.8	43.8
GU 65-644	47.5	25.9	57.5	54.7	2.1	56.3	19.8	42.7
GU 65-646	51.3	35.7	55.7	53.5	-1.5	3.0	28.7	41.7
GU 65-648	54.2	44.7	53.9	52.6	-2.7	5.2	37.7	40.7
GU 65-662	44.4	14.7	59.9	55.6	4.1	49.4	10.6	44.0
GU 65-664	47.4	25.8	58.2	54.0	3.3	57.1	19.7	42.9
GU 65-666	50.4	35.7	56.5	52.8	2.4	56.6	28.5	41.8
GU 65-668	52.1	44.7	54.7	52.0	-2.3	6.0	37.4	40.9
GU 65-682	45.2	14.5	60.6	54.8	5.6	49.1	10.4	44.4
GU 65-684	47.4	25.7	59.0	53.3	4.5	57.9	19.5	43.1
GU 65-686	49.4	35.6	57.3	52.2	3.5	56.5	28.3	42.0
GU 65-688	49.4	44.7	55.6	51.5	2.3	57.1	37.2	41.1
GU 65-722	42.0	18.9	68.6	67.3	1.3	58.1	11.3	47.0
GU 65-724	46.0	33.1	67.1	65.8	0.9	64.2	20.9	46.3
GU 65-726	50.0	45.6	65.6	64.7	-1.7	2.3	30.5	45.5
GU 65-728	53.6	57.2	64.1	64.0	-2.9	4.3	40.4	44.8
GU 65-742	42.4	18.8	69.2	66.7	2.6	53.2	11.3	47.1
GU 65-744	45.9	33.0	67.8	65.2	2.0	60.7	20.9	46.4
GU 65-746	49.4	45.6	66.4	64.1	-1.6	3.0	30.5	45.7
GU 65-748	52.3	57.2	64.9	63.4	-2.8	5.2	40.3	45.0
GU 65-762	42.8	18.8	69.9	66.0	4.0	52.7	11.1	47.3
GU 65-764	45.7	33.0	68.5	64.5	3.3	58.8	20.8	46.5
GU 65-766	48.6	45.6	67.2	63.4	2.5	66.3	30.3	45.8
GU 65-768	50.3	57.2	65.8	62.8	-2.5	6.0	40.1	45.2
GU 65-782	43.5	18.6	70.5	65.4	5.4	52.3	10.9	47.6
GU 65-784	45.6	32.9	69.3	63.8	4.5	59.0	20.6	46.8
GU 65-786	47.7	45.5	68.0	62.7	3.6	65.3	30.0	46.0
GU 65-788	47.9	57.2	66.7	62.1	2.7	66.8	39.7	45.3

AEROFOIL	ZERO LIFT INCIDENCE (deg)	LIFT CURVE SLOPE (/deg)	LOW DRAG RANGE OF LIFT COEFFICIENT LOWER LIMIT	DESIGN	UPPER LIMIT	AERODYNAMIC CENTRE POSN. (percent c) x	y	PITCHING MOMENT COEF.
GU 65-562	-3.4	0.119	0.59	0.71	0.83	26.4	1.1	-0.078
GU 65-564	-2.5	0.126	0.50	0.75	1.00	27.5	0.6	-0.066
GU 65-566	-1.5	0.133	0.40	0.80	1.19	28.5	-0.2	-0.053
GU 65-568	-0.2	0.141	0.28	0.84	1.40	29.7	-1.2	-0.038
GU 65-582	-4.6	0.119	0.83	0.95	1.06	26.4	1.6	-0.104
GU 65-584	-3.6	0.126	0.75	1.00	1.25	27.5	1.1	-0.088
GU 65-586	-2.5	0.133	0.66	1.06	1.45	28.7	0.4	-0.071
GU 65-588	-1.1	0.140	0.56	1.12	1.67	29.9	-0.6	-0.052
GU 65-622	-1.1	0.119	0.12	0.24	0.36	26.7	0.2	-0.030
GU 65-624	-0.6	0.128	0.00	0.25	0.51	28.0	-0.3	-0.026
GU 65-626	0.1	0.136	-0.14	0.27	0.68	29.2	-1.1	-0.022
GU 65-628	1.2	0.145	-0.29	0.29	0.87	30.6	-2.1	-0.017
GU 65-642	-2.4	0.119	0.36	0.48	0.59	26.7	0.5	-0.061
GU 65-644	-1.7	0.127	0.25	0.51	0.76	28.0	0.0	-0.054
GU 65-646	-0.8	0.136	0.14	0.54	0.95	29.4	-0.7	-0.045
GU 65-648	0.4	0.145	0.00	0.58	1.15	30.8	-1.8	-0.037
GU 65-662	-3.7	0.119	0.60	0.71	0.83	26.8	0.9	-0.092
GU 65-664	-2.9	0.127	0.51	0.76	1.02	28.2	0.5	-0.081
GU 65-666	-1.9	0.136	0.41	0.81	1.21	29.6	-0.3	-0.068
GU 65-668	-0.5	0.144	0.29	0.86	1.43	31.1	-1.3	-0.054
GU 65-682	-5.0	0.119	0.83	0.95	1.07	26.8	1.3	-0.123
GU 65-684	-4.1	0.127	0.76	1.01	1.27	28.3	0.9	-0.108
GU 65-686	-3.0	0.135	0.68	1.08	1.48	29.7	0.2	-0.091
GU 65-688	-1.6	0.144	0.57	1.14	1.71	31.3	-0.7	-0.073
GU 65-722	-1.3	0.120	0.12	0.24	0.36	27.0	0.0	-0.036
GU 65-724	-0.7	0.129	0.00	0.26	0.52	28.7	-0.5	-0.033
GU 65-726	0.0	0.139	-0.14	0.28	0.69	30.4	-1.3	-0.030
GU 65-728	1.1	0.149	-0.30	0.30	0.89	32.2	-2.2	-0.024
GU 65-742	-2.7	0.120	0.36	0.48	0.60	27.1	0.3	-0.072
GU 65-744	-2.0	0.129	0.26	0.52	0.77	28.8	-0.2	-0.066
GU 65-746	-1.1	0.139	0.14	0.55	0.97	30.5	-1.0	-0.059
GU 65-748	0.1	0.149	0.00	0.59	1.19	32.4	-2.1	-0.051
GU 65-762	-4.1	0.120	0.60	0.72	0.84	27.2	0.6	-0.107
GU 65-764	-3.3	0.129	0.52	0.77	1.03	28.9	0.1	-0.098
GU 65-766	-2.3	0.138	0.41	0.83	1.24	30.7	-0.6	-0.088
GU 65-768	-0.9	0.148	0.30	0.89	1.47	32.7	-1.7	-0.075
GU 65-782	-5.5	0.120	0.84	0.96	1.08	27.2	0.9	-0.143
GU 65-784	-4.7	0.129	0.77	1.03	1.28	29.0	0.5	-0.131
GU 65-786	-3.5	0.138	0.69	1.10	1.51	30.9	-0.2	-0.117
GU 65-788	-2.1	0.148	0.59	1.18	1.76	32.8	-1.3	-0.100

APPENDIX IV

ALGOL 60 Procedures used in the Computation.

Contents: 1. Description of Procedures

2. ALGOL 60 text (procedures *dwbydz* and *RM2112*)

3. Index to array elements *features* of *RM2112*

4. Index to failure exits of *RM2112*

1. *Description of Procedures.*

As explained in paragraph 2 of the main text, the procedure *RM2112* provides a general computational method for the evaluation of the co-ordinates and other features of an aerofoil designed by the Lighthill method, and calls on a procedure *dwbydz* (which is one of its formal parameters) to supply the information relevant to the specific aerofoil to be designed. In the extract on page 71, the procedure *dwbydz* is an example of this latter routine, whose particular purpose is to supply information relevant to the GU-series of aerofoils. The computational plan of the ALGOL Text is summarised below in terms of the block structure, and line numbers.

LINE 1	**real procedure** *dwbydz*, heading and full descriptive **comment**.
LINE 79	**begin** body of *dwbydz*, with entries —1, 0, 1 and 2 designated by value of parameter *entry*.
LINE 84	**real procedure** EF, calculating functions $E(x)$, $F(x)$ referred to in equations (7) and (10) of Appendix I.
LINE 119	**real procedure** *S*, calculating function $S(x)$ referred to in equation (17) of Appendix I.
LINE 143	**real procedure** *FGO*, calculating functions f_0 and g_0 of equation (4), Appendix I.
LINE 161	**real procedure** *FG1*, calculating functions f_1 and g_1 of equation (5), Appendix I.
LINE 175	**real procedure** *FG2*, calculating functions f_2 and g_2 of equation (6), Appendix I.
LINE 191	**begin** entries 1 and 2 of *dwbydz* to evaluate (entry 1) the surface velocity at zero lift, and (entry 2) the surface slope.
LINE 199	**end**
LINE 203	**begin** entry 0 of *dwbydz*, an initialising entry which sets up constants used in entries 1 and 2, so as to satisfy the equations (24) to (27) of Appendix I.
LINE 288	**end**
LINE 291	**begin** entry -1, recording extent of constant pressure region in array *data*.
LINE 305	**end**
LINE 306	**end** of *dwbydz*
LINE 307	**procedure** *RM 2112*, heading and full descriptive **comment**.
LINE 413	**begin** body of *RM 2112*, a 'straight through' calculation.
LINE 418	**procedure** *rootfind*. A general purpose rootfinding technique (by *regula falsi*) with convergence discrimination.

LINE 503 **real procedure** *Hermite*. Provides the Hermitian interpolate at a point of a given set of co-ordinates.

LINE 533 **integer procedure** *ifind*. A general purpose bisection routine used in searching or rootfinding.

LINE 550 **procedure** *TX*. Interpolates a value of θ for a prescribed aerofoil abscissa, x.

LINE 572 **begin** calculation of profile ordinates and abscissa, using procedure *dwbydz* and numerical quadrature.

LINE 579 **procedure** *paralint*. A general purpose technique for the parallel numerical quadrature of a number of functions of the same variable, using Simpson's rule, with automatic adjustment of the interval of integration to provide stipulated accuracy, and with a slot permitting the recording of partial results.

LINE 671 **procedure** *integran*. Sets up the integrands of the various integrals by calls of *dwbydz* for use by *paralint*.

LINE 713 **procedure** *record*. The actual procedure slotted into *paralint* to record the values of x, y, θ, etc. as calculated for intermediate values of θ.

LINE 723 *START*: initialise constants and goto *INTEGRATE*.

LINE 727 *OVERSIZE*: adjust accuracy criterion *eps*.

LINE 730 *INTEGRATE*: call *paralint*, but goto *OVERSIZE* if array size inadequate for recording all intermediate results (*via* procedure *record*).

LINE 732 Record results in array *features*, and other variables for later use.

LINE 247 **end** calculation of profile ordinates.

LINE 748 **begin** change of axis to coincide with aerofoil chord line.

LINE 768 *ANGLE*: Region of leading edge discriminated.

LINE 775 *rootfind* used to isolate leading edge, so as to satisfy equation (6) of Appendix II.

LINE 782 convert x, y co-ordinates to new axis system.

LINE 806 **end** conversion of axis system.

LINE 807 **begin** evaluating geometric features of aerofoil section.

LINE 812 **real procedure** *rfind*. A rootfinding technique (analogous to *ifind*) by bisection.

LINE 831 **real procedure** *grad*. Uses *TX* to find the slope of the aerofoil at given abscissa on top or bottom surface.

LINE 850 **real procedure** *ord*. Uses *TX* to find the ordinate of the aerofoil at given abscissa on top or bottom surface.

LINE 859 Find position of maximum thickness.

LINE 861 Find maximum thickness.

LINE 871 **begin** location of maximum camber position.

LINE 891 **end.**

LINE 892 Find maximum camber.

LINE 895 **end** calculation of geometric features.

LINE 896 **begin** A.O.B.

LINE 902 make entry -1 to procedure *dwbydz*.

LINE 908 evaluate *fix*.

LINE 909 **if** fix < 0 **then**

LINE 910 **begin** replacement of abscissae by values in array *xval*

LINE 919 Check ordering of values of elements of *xval*

LINE 936 **begin** interpolation of values of θ corresponding to new abscissae

LINE 939 **end**

LINE 941 **begin** interpolation of ordinates at new values of θ.

LINE 949 **end**

LINE 950 insert leading edge and trailing edge values

LINE 966 **begin** rearrangement of arrays *x*, *y*, *theta*, and calculation (using *dwbydz*) of velocity and surface slope, at new abscissae values.

LINE 980 **end**

LINE 981 **end** adjustments to new abscissae (if *fix* is positive).

LINE 982 Convert elements of array *theta* to degrees, and **goto** *OU7*

LINE 984 **end** A.O.B.

LINE 985 *F*: Form failure index, convert *theta* to degrees, and **goto** *EXIT* (this label reached in event of a failure)

LINE 989 **end** body of *RM 2112*.

Note that, in *RM 2112*, several of the stages of the calculation are short circuited if the aerofoil is symmetric, which is recorded by a **true** value of variable *sym* assigned on the basis of information supplied by the initial call (LINE 724) at entry 0 of *dwbydz*.

2. *Algol* 60 *Test*.

The following pages (71–90) are reproduced from the flexowriter copy of a paper tape hardware representation of the procedures *dwbydz* and *RM 2112*. Lines are numbered in **end** comments, and there are 50 lines to a page.

In recent work, it has been found that the evaluation of the integral (5) in Appendix II—which is needed only as a corroborative check—can be unduly troublesome, due to the behaviour of q_0 in the vicinity of the trailing-edge stagnation point. It is now preferred to insert a factor $2\sin^2(\theta/2)$ into the integrand, which leaves the value of the definite integral theoretically unchanged. In the procedure *RM2112* as supplied here, this is achieved by altering the assignment to $y[3]$ on line 682 to $c \times ck \times (s+s) \times y[9]$, and by deleting the assignment (to $y[3]$) on line 711. Further, the simple boolean expression $a = 0$ on line 171 should be replaced by $a \leqslant 0$.

A version of the procedures in the FORTRAN language has now been developed; a listing is available from the author.

```
real procedure dwbydz(entry,data,index,value,FAIL);
  value entry,value;  integer entry,index;
  array data;  real value;  label FAIL;
  comment this is an example of an actual procedure
    corresponding to the formal of the same
    identifier used by RM2112. Its special purpose
    is to enable computation by RM2112 of the shape
    of the GU-series of aerofoils;
  comment different functions are to be performed
    by the body of this procedure according to the
    value of <entry>, which will be equal to -1,0,1,or 2;
  comment entry=0. Here <value> has been assigned
    equal to pi. This is an initialising entry,
    enabling the setting up of own constants, or
    other preliminary business. On exit, the
    funtion designator must be given the value of
    the angle subtended by the trailing edge (in
    radians), and <index> assigned zero if the
    aerofoil is symmetric, else non-zero (if it is
    cambered);
  comment entry=1. Here <value> is to be
    interpreted as theta(the angular coordinate of
    the transform point on the unit circle). The
    function designator must be assigned the value
    of ln(q0/abs(cos(theta/2))) for any value
    0<theta<2×pi, where q0 is the aerofoil zero
    lift speed relative to that of the free stream.
    If the trailing edge is cusped (i.e. dwbydz=0
    at entry 0) there will be an entry with theta
    (= value) =0. If the aerofoil is symmetric,
    there will be no entries with theta>pi;
  comment entry=2. Here <value> is to be
    interpreted as theta, as for entry 1. The
    function designator must be assigned the value
    of (ki-[theta]/2) where [theta] is the
    principle part of theta, such that
    abs[theta]≤pi. Thus the function designator is
    a continuous function of theta (except at sharp
    corners of the aerofoil) and is to be less than
    pi/2 in absolute value, signed so that it is
    (normally) negative at the top surface trailing
    edge (theta=0) and positive at the bottom
    surface trailing edge (theta=2×pi);
  comment entry=-1. An interrogative entry made by
    RM2112 immediately prior to evaluation of the
    actual parameter corresponding to its formal
    parameter <fix>. If dwbydz is assigned zero (or
    negative), no special action is taken by RM2112
```

```
  (which proceeds to the evaluation of <fix>).
  However, if dwbydz is assigned a positive
  value, this value will be interpreted by RM2112
  (upon return ) as a value of theta, for which a
  value of the aerofoil abscissa is required
  (expressed as a fraction of the chord). This is
  evaluated by RM2112, and then dwbydz
  re-entered, with entry=-1, and with this
  abscissa assigned to <value>. The process is
  repeated until a zero value is assigned to the
  function designator <dwbydz>. The purpose of
  such entries may be to record information in
  array <data>;
comment data. The actual array corresponding to
  this formal is the same as that corresponding
  to the formal parameter <data> of RM2112. It
  may serve to supply information(e.g. at
  entry0), or record information (e.g. at entry
  -1). It is not used by RM2112;
comment FAIL. An exit to the actual label
  corresponding to this formal will cause RM2112
  to transfer control to the actual label
  corresponding to its formal parameter <EXIT>.
  On such exits, a positive value should be
  assigned to <index>, for diagnostic purposes,
  which will be packed into the value of the
  actual parameter corresponding to the formal
  parameter <fail> of RM2112 - see the separate
  description of failure exits;
begin
own real D1,D2,D3,D4,D5,D6,bby2,ub,sigma,ta0,a0,
  gby2,pg,mg,ug,tmby2,muby2,pi,beta;
own integer k;
boolean F;
real procedure EF(E,x);  value E,x;  boolean E;  real x;
  comment evaluates if E then E(x) else F(x);
  comment uses non local variable pi;
  begin
  real p,s,t,q;
  if x>0 then p:=pi else
    begin
    p:=-pi;  x:=-x
    end LINE 92,  ;
  if x<1.0 then s:=0 else
    begin
    s:=0.5×p;  p:=-p;  x:=1.0/x
    end LINE 96,  ;
  if x<0.385 then
    begin
    if x=0 then EF:=s else
```

```
        begin
        t:=ln((1.0+x)/(1.0-x));  q:=t×t;
        EF:=((if E then 1.0 else 1.0-ln(x))
          -q×(0.05555555556-q×(0.00388888889-
          q×(2.9289494₁₀-4-q×(2.333186₁₀-5-
          q×(1.93964₁₀-6-q×(1.6641₁₀-7-q×(1.462₁₀-8-
          q×1.31₁₀-9))))))))×t/p+s;
       end  LINE 107,  expansion about zero;
     end  LINE 108,
     else if x=1.0 then EF:=0.25×p+s else
     begin
     t:=ln(x);  q:=t×t;
     EF:=(ln(if E then -2.0/t else (x+x-2.0)
       /(1.0+x)/t)+1.0+q×(0.02777777778-
       q×(0.00097222222-q×(4.881582₁₀-5-
       q×(2.91648₁₀-6-q×(1.9396₁₀-7-q×(1.387₁₀-8-
       q×(1.04₁₀-9-q×0.8₁₀-10))))))))×t/p+p×0.25+s
    end  LINE 117,  expansion about unity
  end  LINE 118,  EF;
real procedure S(x);  value x;  real x;
  comment evaluates function defined as the
    series whose nth. term is (2/pi)×(-1)
    ↑n×tan(x/2)↑(2n+1)/(2n+1)↑2 summed from n=0 upwards;
  comment uses non-local variables pi;
  begin
  real p,q,f;
  p:=pi+pi;  x:=x-entier(0.5+x/p)×p;
  if x>0 then p:=pi else
    begin
    p:=-pi;  x:=-x
    end  LINE 130,  ;
  if x+x≤pi then f:=0 else
    begin
    f:=ln((1.0-cos(x))/sin(x));  x:=pi-x;
    end  LINE 134,  ;
  q:=x×x;
  S:=(x+x×q×(0.05555555556+q×(0.00388888889+
    q×(2.92894936₁₀-4+q×(2.33318636₁₀-5+
    q×(1.9396405₁₀-6+q×(1.6641134₁₀-7+q×(1.461551₁₀-
    8+q×(1.3067₁₀-9+q×(1.1846₁₀-10+q×(1.086₁₀-11+
    q×(1.005₁₀-12+q×(9.36₁₀-14+q×(8.79₁₀-15+q×8.29₁₀-
    16))))))))))))))/p+f
  end  LINE 142,  S;
real procedure FG0(F,t,b,c);  value F,t,b,c;
  boolean F;  real t,b,c;
  comment with t=theta, b=beta/2 and
    c=1-cos(beta), evaluates if F then
    f0(theta,beta) else g0(theta,beta);
  comment uses non-local variable pi;
  begin
```

```
   real ct,u,p;
   real procedure lm(x,y);  value x,y;  real x,y;
     lm:=if x>0 then ln(x)×y else if x≠0 then
       ln(-x)×y else 0;
   ct:=1.0-cos(t);  u:=t/(pi+pi);  u:=u-entier(u+0.5);
   p:=u×pi;
   FG0:=if F then
     c×u+(if p>b then (if p>0 then -0.5×c else
     ct-0.5×c) else if p>0 then 0.5×c-ct else 0.5×c) else
     (sin(t)×b-lm(sin(p),ct)+lm(sin(p-b),ct-c))/pi;
   end  LINE 160,  FG0;
real procedure FG1(F,theta,tan,a);
   value F,theta,tan,a;  boolean F;  real theta,tan,a;
   comment with tan=tan(alpha) and a=alpha,evaluates if F
     then f1(theta,alpha) else g1(theta,alpha);
   comment uses non-local variable pi, and procedure EF;
   begin
   theta:=theta×0.5;  theta:=theta-entier(0.5+theta/pi)×pi;
   if F then FG1:=ln(cos(abs(theta)-a)×2.0) else
     begin
     a:=cos(theta);
     FG1:=if a=0 then 0 else
       theta-EF(false,tan×sin(theta)/a);
     end  LINE 173,
   end  LINE 174,  FG1;
real procedure FG2(F,theta,tan,m);
   value F,theta,tan,m;  boolean F;  real theta,tan,m;
   comment with m=mu/2 and tan=tan(mu/2),
     evaluates if F then f2(theta,mu) else g2(theta,mu);
   comment uses non-local variable pi, and procedure EF;
   begin
   real t;
   t:=theta×0.5;  t:=t-entier(0.5+t/pi)×pi;
   FG2:=if F then
     (if abs(t)≥m then 0 else if t=0 then -80.0
     else ln(abs(sin(t)/cos(t)/tan))) else
     if t=0 then
     (if theta<0 then -0.5 else 0.5)×pi else
     -EF(true,cos(t)/sin(t)×tan)
   end  LINE 189,  FG2;
if entry>0 then
   begin
   F:=entry=1;
   dwbydz:=FG0(F,value,bby2,ub)×D1+FG0(F,value,
     -bby2,ub)×D2-FG1(F,value-sigma,ta0,a0)+(if F
     then D6 else 0)+(if gby2=0 then 0 else
     FG0(F,value+pg,gby2,ug)×D3+FG0(F,value+mg,
     -gby2,ug)×D4)+(if D5=0 then 0 else
     FG2(F,value,tmby2,muby2)×D5)
   end  LINE 199,  normal entry evaluating
```

```
    velocity distribution according to equation
    (23) of Appendix1
  else if entry=0 then
  begin
  comment initialises own constants from
    information supplied by data. data[1]
    =0.5×(1+cos(beta)),data[2]=0.5×sigma(deg),
    data[3]=alpha0(deg), data[4]=G and
    data[5]=0.5×(1-cos(mu));
  real lta,b1,sb,cb,b0,S34,two,one,pt5,rad;
  two:=2.0;  one:=1.0;  pt5:=0.5;  pi:=value;
  rad:=180.0/value;
    begin
    real s,c,t;
    a0:=data[3]/rad;  s:=sin(a0);  c:=cos(a0);
    if s≤0 or c≤0 then
      begin
      index:=3;  goto FAIL
      end  LINE 218,  ;
    ta0:=s/c;  lta:=ln(ta0)×two;
    b1:=(lta×c-pi×s)×(s+s)+pi;  t:=one-data[1];  ub:=t+t;
    cb:=one-ub;
    if t≤0 or data[1]≤0 then
      begin
      index:=1;  goto FAIL;
      end  LINE 225,  ;
    bby2:=arctan(sqrt(t/data[1]));  beta:=bby2+bby2;
    sb:=sin(beta);  b0:=beta-sb×cb;
    end  LINE 228,  ;
  if data[4]=0 then
    begin
    if data[2]=0 then gby2:=sigm;=D6:=S34:=0 else
GFAIL:  begin
      index:=4;  goto FAIL;
      end  LINE 234,
    end  LINE 235,
    else if data[4]<0 then goto GFAIL else
    begin
    real hc,g,sg,s,c,i,d34;
    g:=data[4]×a0;  gby2:=g×pt5;  s:=sin(gby2)×two;
    hc:=cos(gby2);  ug:=pt5×s×s;  c:=g×(one-ug);
    sg:=s×hc;  i:=pt5/sg;  d34:=i/ta0;
    b1:=b1-(pt5-i×c)/ta0;
    if data[2]=0 then sigma:=S34:=0 else
      if data[2]>0 then
      begin
      real i,cs;
      sigma:=two×data[2]/rad;  cs:=cos(sigma);  i:=g×hc/s;
      b1:=(cs×i+data [1])/b1;  S34:=sin (sigma)/b1/s/s;
      b1:=(i+cs×data[1])/b1;
```

```
              end  LINE 250,
              else
  SIGFAIL:    begin
              index:=2;  goto FAIL
              end  LINE 254,  ;
            mg:=pi-g-sigma;
            if mg<beta then goto SIGFAIL;
            pg:=pi+g-sigma;  D3:=S34+d34;  D4:=S34-d34;
            D6:=(d34+d34)×(sg-c);  S34:=ug×S34/ub;
            end  LINE 259,  ;
          b1:=(b1-pi)/b0;  D1:=b1-S34;  D2:=-b1-S34;  D5:=0;
          if data[5]=0 then dwbydz:=0 else
            if data[5]<0 then
 MUFAIL:    begin
            index:=5;  goto FAIL
            end  LINE 265,
            else
            begin
            real mu,t;
            integer i;
            tmby2:=sqrt(data[5]/(one-data[5]));
            muby2:=arctan(tmby2);  mu:=muby2+muby2;
            t:=(mu+mu)/b0;
            if mu>beta then goto MUFAIL;
            D5:=(dwbydz(2,data,i,-mu,FAIL)-dwbydz(2,data,
              i,mu,FAIL)-mu)/((FG0(false,mu,bby2,ub)
              -FG0(false,-mu,bby2,ub))×(t+t)+pi×pt5);
            if D5<0 then
              begin
              index:=6;  goto FAIL
              end  LINE 280,  ;
            t:=t×D5;  D1:=D1+t;  D2:=D2-t;  dwbydz:=t:=D5×pi;
            D6:=D6-S(mu)×(t+t)
            end  LINE 283,  calculating trailing edge
              angle by equation(29) of Appendix1;
          index:=if sigma=0 then 0 else 1;  k:=0;
          D6:=ln(two)+S(a0+a0)-a0×lta/pi-((D1-D2)
            ×(sb-beta×cb)+D6)/(pi+pi);
          end  LINE 288,  entry0, satisfying
            equations(24) to (27) of Appendix1
          else
          begin
          comment record extent of constant pressure
            region on top and bottom surfaces in data[6]
            and[7] respectively;
          switch E:=L1,L2,L3;
          k:=k+1;  goto E[k];
    L1:   dwbydz:=beta;  goto RTN;
    L2:   data[6]:=value×100.0;
          if sigma≠0 then
```

```
        begin
        dwbydz:=pi+pi-beta;  goto RTN
        end  LINE 302,  ;
 L3:  data[7]:=value×100.0;  dwbydz:=0;
RTN:
      end  LINE 305,  entry negative;
    end  LINE 306,  dwbydz;
  procedure RM2112(eps,size,x,y,theta,ki,qs,fix,xval,
    features,dwbydz,data,fail,EXIT);  value eps;
    real eps;  integer size,fix,fail;
    array x,y,theta,ki,qs,xval,features,data;
    real procedure dwbydz;  label EXIT;
    comment the purpose of this procedure is the
      evaluation of the coordinates of an aerofoil
      with a velocity distribution prescribed as a
      function of theta ( the angular coordinate on
      the circle to which the aerofoil transforms
      uniformally) together with other information,
      according to the Lighthill method of R and
      M2112. The significance of the actual
      parameters corresponding to the formal
      parameters is indicated below;
    comment eps. An accuracy tolerance, used in the
      integration process;
    comment size. The actual parameter corresponding
      to this formal must be a variable. On entry,
      its value is taken as n(say), the upper bound
      of subscript for which the arrays x,y,theta,ki
      and qs are defined. On exit, its value will be
      assigned equal to m(say) the upper limit of
      subscript for which these arrays have been
      assigned meaningful values (see below). The
      entry value determines the size of working
      areas requisitioned by the procedure body and
      must leave about a third of the working storage
      available for this purpose. However, too small
      a value of n will limit the accuracy with which
      the calculation may be performed, irrespective
      of the value of eps;
    comment arrays x,y,theta,ki and qs. The actual
      arrays corresponding to these formals must be
      defined for subscript limits [1:n],- see <size>
      above. Entry values are immaterial. Actual
      elements x[k],y[k]are assigned values
      corresponding to the kth evaluated point for
      k=1(1)m, where m is defined by the exit value
      of parameter <size>. The origin is taken at the
      leading edge, and the upper surface trailing
      edge at (1,0). The value of theta[k] is
      assigned the angular coordinate ( in degrees)
```

```
  of the kth point in the convention
  0≤theta≤2×pi, with theta=0 at the top surface
  trailing edge. The surface slope (in radians)
  is assigned to ki[k]=arctan(dy/dx), with the
  convention -pi/2<ki<pi/2 on the top surface and
  pi/2<ki<3×pi/2 on the bottom. qs[k] contains
  the associated value of abs(q/cos
  (theta/2-alpha)), where q is the surface speed
  measured relative to that of the free stream at
  an incidence alpha above zero lift;
comment fix. This parameter is evaluated just
  prior to exit from the procedure. Ifit is zero
  or negative, the current values of theta[k] are
  converted from radians to degrees and the
  procedure exits. In this condition, the arrays
  x,y, etc will have been evaluated at points
  corresponding generally to integer values of
  theta in degrees, at intervals determined by
  the accuracy tolerance (eps). If the actual
  parameter corresponding to fix is evaluated as
  positive, and equal to p (say), it will be
  taken that the actual array elements
  corresponding to the formal elements
  xval[1],....xval[p] contain abscissae at which
  values of these arrays x,y etc are required in
  preference to those currently assigned. The
  conversion is made by the procedure and the
  xval values copied to the elements x[k],
  repeating for both top and bottom surfaces ( if
  the aerofoil is assymmetric), updating <size>
  accordingly.Evidently p must be less than n+2
  for a cambered aerofoil, and less than n for a
  symmetric section. If the actual parameter
  corresponding to fix is a function designator,
  then ( for example) there is an opportunity for
  both forms of representation to be recorded, or
  for the values of xval to be modified in the
  light of the data accesible from the parameters
  of this procedure;
comment array xval. If the evaluation of <fix>
  provides a value p>0, then xval must be defined
  for subscript limits [1:p], else this array is
  not used, -see <fix> above. If used, then it is
  necessary that 1≥xval[k]>xval[k+1]≥0 for k=1(1)p;
comment array features. The actual array
  corresponding to this formal must be defined
  for subscript limits [1:16 ]. Entry values
  immaterial. Its elements are assigned values of
  certain geometric and aerodynamic properties of
  the aerofoil-see appended list;
```

```
comment dwbydz. This procedure is described in
   comment attached to the appended actual
   procedure with this identifier;
comment array data. Intended solely for use by
   the actual procedure corresponding to dwbydz;
comment fail. The actual parameter corresponding
   to this formal must be a variable. In the event
   of an exit via label EXIT, an assignment to
   <fail> is made for diagnostic purposes;
comment label EXIT. Any failure causes this label
   to be evaluated, and control transferred to the
   designation, with an assignment made to <fail>.
   A list of failure exits is appended;
begin
integer count,LE,i,arraylim;
real pi,rad,c,hp,twopi,az,cs,sn,xac,yac,cm;
boolean sym;
array Dx,Dy[1:size];
procedure rootfind(x1,y1,x2,y2,x,y,eps,FAIL);
  value x1,y1,x2,y2,eps;
  real x1,y1,x2,y2,x,y,eps;  label FAIL;
  comment finds( correct within accuracy eps) a
    zero of the expression evaluated by a call on
    the actual parameter corresponding to y,
    which is supposed to be a function of the
    actual parameter corresponding to x,
    monotonic in the interval (x1,x2), and having
    the values y1,y2 at x1,x2 respectively, where
    y1 and y2 are preferably of opposite sign.
    Successive approximations to the root, by
    Regula falsi, are assigned to the parameter
    x, and the procedure exits to label FAIL if
    these do not converge;
  comment actual parameter corresponding to x
    must be a variable;
  begin
  real d,t;
  integer j,p,n;
  d:=x2-x1;  p:=if sign(d)=sign(y2-y1) then 1 else -1;
  if sign(y1)≠sign(y2) then j:=0 else if y2≠0 then
    begin
    n:=20;  j:=if sign(y2)=p then -1 else 1
    end  LINE 442,  marking by j direction of x
      in which root bound is undefined
    else if d≠0 then goto FAIL else
    begin
    x:=x2;  goto RTN
    end  LINE 447,  ;
  if abs(y1)>abs(y2) then
    begin
```

```
          t:=x2;
          if d<0 then x2:=x1
          end  LINE 452,
          else
          begin
          t:=y1;  y1:=y2;  y2:=t;  t:=x1;  d:=-d;
          if d>0 then x1:=x2
          end  LINE 457,  ;
       comment t is currently best estimate of root
          and y2 its residual. Where defined, x2 and x1
          are upper and lower bounds;
LOOP:  if y1=y2 then goto FAIL else d:=d×y2/(y1-y2);
       if sign(y2)=p then
          begin
          if j≠0 then
            begin
            if j>0 then j:=0 else
              begin
              if n≠0 then n:=n-1 else goto FAIL;
              goto if d>0 then UB else AX
              end  LINE 470,  no lower bound found yet;
            end  LINE 471,  finding if value of t
              provides the undefined bound;
          x2:=t
          end  LINE 474,  record upper estimate of root
          else
          begin
          if j≠0 then
            begin
            if j<0 then j:=0 else
              begin
              if n≠0 then n:=n-1 else goto FAIL;
              goto if d<0 then LB else AX
              end  LINE 483,  no upper bound found yet
            end  LINE 484,  finding if value of t
              provides the undefined bound;
          x1:=t
          end  LINE 487,  record lower estimate of root;
       if d>0 then
  UB:     begin
          if t+d>x2 then goto FAIL
          end  LINE 491,  test new upper estimate
          else
  LB:     begin
          if t+d<x1 then goto FAIL
          end  LINE 495,  test new lower estimate;
  AX:  x:=t:=t+d;
       if abs(d)>eps then
          begin
          y1:=y2;  y2:=y;  goto LOOP
```

```
      end  LINE 500,  process unconverged;
RTN:
    end  LINE 502,  rootfind by Regula falsi;
  real procedure Hermite(x0,n,m,x,y,Dy);
    value x0,n,m;  real x0;  integer n,m;  array x,y,Dy;
    comment given a set of coordinates (x[k],y[k])
      and corresponding slopes dy/dx=Dy[k], for
      k=n(1)m, this function designator is assigned
      the Hermitian interpolate of the ordinate y
      at the given abscissa x=x0. The values
      x[n],...x[m] should preferably be
      monotonically increasing or decreasing;
    comment actual arrays corresponding to the
      formal arrays x,y,Dy must be defined for
      subscript limits [n:m]. Failure occurs if any
      two values of x[k] are identical or if m<n;
    begin
    integer i,j;
    real r,s,t,a,h,d;
    array p[n:m];
    s:=0;
    for j := n step 1 until m do p[j]:=x0-x[j];
    for j := n step 1 until m do
      begin
      a:=0;  h:=1.0;  r:=p[j];  t:=y[j];
      for i := n step 1 until m do if i≠j then
        begin
        d:=r-p[i];  h:=h×p[i]/d;  a:=a+t/d
        end  LINE 528,  ;
      s:=s+((Dy[j]+a+a)×r+t)×h×h;
      end  LINE 530,  ;
    Hermite:=s;
    end  LINE 532,  Hermite;
  integer procedure ifind(a,b,m,bool);  value a,b;
    integer a,b,m;  boolean bool;
    comment supposing bool is an expression
      depending on m, such that it is true for
      a≤m≤j, say, and false for j<m<b, this
      function designator is assigned the value of j;
    comment actual parameter corresponding to m
      must be a variable;
    begin
    integer k;
    for k := (a+b)÷2 while k≠a do
      begin
      m:=k;
      if bool then a:=k else b:=k;
      end  LINE 547,  ;
    ifind:=a;
    end  LINE 549,  ifind;
```

```
procedure TX(top,x0,value,element);
  value top,x0;  boolean top;  real x0,value;
  integer element;
  comment finds theta value corresponding to
    given abscissa x0 on top ( or bottom)
    surface, assigning to <element> the largest
    value of k such that theta[k]≤value;
  comment uses non locals LE, count and eps,
    arrays x, theta, Dx and procedures ifind ,
    Hermite and rootfind. Exit to label FX if the
    value cannot be interpolated;
  begin
  integer j,k;
  real t;
  element:=k:=if top then
    ifind(1,LE,k,x[k]>x0) else ifind(LE,count,k,x[k]<x0);
  j:=k+1;
  rootfind(theta[k],x[k]-x0,theta[j],x[j]-x0,t,
    Hermite(t,k,j,theta,x,Dx)-x0,eps×
    abs((theta[k]-theta[j])/(x[k]-x[j])),FX);
  value:=t;
  end  LINE 571,  TX;
  begin
  comment calculates profile ordinates and
    abscissa with no lift line parallel to
    x-axis, and origin at trailing edge;
  real tau,endpt;
  integer k;
  array a[1:11];
  procedure paralint(n,assign,a,b,eps,h,I,m,record);
    value n,a,b,eps,h,m;  integer n,m;  array I;
    real a,b,eps,h;  procedure assign,record;
    comment The primary purpose is to integrate
      the functions represented by (say)
      f[1],...f[n] with respect to (say) t from
      t=a to t=b. For this purpose the actual
      procedure assign(f,t)must evaluate the
      array elements f[1],...f[m] where m≥n.
      Integration is by Simpsons rule with
      variable step length = h/2↑p, where p is
      adjusted to the least integer value
      compatible with the accuracy criterion eps.
      A secondary purpose is to provide access to
      the intermediate values of the n integral
      values I[1],...I[n] after each step of
      integration (and initially), by a call in
      the body on the actual procedure record,
      with an actual parameter list (I,y,x), thus
      providing the integrals from t=a to the
      current value t=x, and also a copy of the m
```

```
       function values previously evaluated for
       this value of independent variable. At exit
       from the body, I will have been assigned
       values appropriate to t=b, so that if these
       are the only results required the body of
       the actual procedure <record> can be empty.
       At entry, appropriate values are assigned
       to the function values and the array I is
       assigned zero;
     comment The actual array corresponding to the
       formal array y must be defined for
       subscript limits [1:m], and to I for [1:n].
       The headings of the actual procedures
       should have formal parameter parts as
       above, with t called by value and specified
       real, and f specified array, for <assign>,
       and all parameters called by value with x
       specified real, and I and y array , for <record>;
     begin
     if m<n then m:=n;
     if n>0 then
       begin
       integer k,c;
       boolean last;
       real t,d,delta,xe;
       array e,f0[1:n],y,f1[1:m];
       for k := 1 step 1 until n do I[k]:=0;
       assign(y,a); record(I,y,a);
       if b=a then goto FINISHED;
       eps:=abs(eps); delta:=eps/8.0; last:=false; c:=0;
       if h=0 then goto COMPLETE else
         h:=sign(b-a)×abs(0.5×h);
NEXT:  if b-a>h×2.1 eqv h>0 then xe:=a+h+h else
         begin
         if last then goto FINISHED else
           begin
           c:=0;
COMPLETE:  h:=(b-a)×0.5; last:=true; xe:=b;
           end LINE 638, ;
         end LINE 639, ;
       for k := 1 step 1 until n do f0[k]:=y[k];
       assign(y,xe);
HALVE: assign(f1,a+h); d:=0;
       for k := 1 step 1 until n do
         begin
         t:=e[k]:=(f0[k]+y[k])×0.25; t:=abs(t+t-f1[k]);
         if t>d then d:=t;
         end LINE 647, ;
       d:=d×h;
       if d≥eps then
```

```
          begin
          xe:=a+h;  c:=c+c;  last:=false;  h:=0.5×h;
          for k := 1 step 1 until m do y[k]:=f1[k];
          goto HALVE;
          end  LINE 654,   ;
        t:=h/0.75;
        for k := 1 step 1 until n do
          I[k]:=I[k]+(e[k]+f1[k])×t;
        record(I,y,xe);  a:=xe;
        if d>delta then c:=c+1 else
          begin
          k:=c÷2;
          if c=k+k then c:=c+1 else
            begin
            c:=k+1;  h:=h+h
            end  LINE 665,   ;
          end  LINE 666,   ;
        goto NEXT;
FINISHED:
        end  LINE 669,
      end  LINE 670,  paralint;
    procedure integran(y,theta);  value theta;
      real theta;  array y;
      comment uses non local i,endpt,sym,tau,pi and
        twopi, procedure dwbydz, array data and label F;
      if theta≠endpt then
      begin
      real ki,e,h,s,c,ck;
      h:=0.5×theta;  s:=-sin(h);  y[10]:=s×s;
      y[9]:=exp(dwbydz(1,data,i,theta,F));
      y[7]:=dwbydz(2,data,i,theta,F);  ki:=y[11]:=y[7]+h;
      ck:=cos(ki);  e:=s/y[9];  y[8]:=ck×e;  c:=cos(h)×s;
      y[1]:=y[8]-c;  y[2]:=sin(ki)×e;  y[3]:=c×ck/e;
      y[4]:=cos(theta)×c×ki-h×y[1];
      if not sym then
        begin
        y[5]:=c×c×y[7];  y[6]:=h×y[2];
        end  LINE 687,   ;
      comment y[1],y[2] and y[3] are the integrands
        of equations (4), (3b) and (5) respectively
        of Appendix2, y[5] is proportional to
        integrand of (12) and y[4] and y[6] are
        related to integrands occurring in (11);
      end  LINE 693,
      else
      begin
      own real y70,y90;
      integer k;
      for k := 1 step 1 until 10 do y[k]:=0;
      if endpt=0 then
```

```
          begin
          endpt:=twopi;
          y70:=y[11]:=y[7]:=if sym then -0.5×tau else
            dwbydz(2,data,i,0,F);
          y90:=y[9]:=if tau≠0 then 0 else
            exp(dwbydz(1,data,i,0,F));
          end  LINE 706,  at theta zero
          else
          begin
          y[7]:=y70+tau;  y[11]:=y[7]+pi;  y[9]:=y90;
          end  LINE 710,  at theta = twopi;
        y[3]:=cos(y[7])×y90
        end  LINE 712,  integran;
      procedure record(I,f,t);  value t;  array I,f;  real t;
        comment uses non locals count,size and label
          OVERSIZE, and arrays x,y,theta,ki,qs,Dx, and Dy;
        if count=arraylim then goto OVERSIZE else
        begin
        integer k;
        k:=count:=count+1;  theta[k]:=t;  x[k]:=I[1]-f[10];
        y[k]:=I[2];  ki[k]:=f[11];  qs[k]:=f[9];  Dx[k]:=f[8];
        Dy[k]:=f[2];
        end  LINE 722,  record;
START:    arraylim:=size; fail:=k:=size:=0;
      pi:=arctan(1.0)×4.0;  twopi:=pi+pi; hp:=0.5×pi;
      rad:=180.0/pi;  tau:=dwbydz(0,data,i,pi,F); sym:=i=0;
      goto if eps≤0 or arraylim<10 then EXIT else INTEGRATE;
OVERSIZE:  k:=k+1;
      eps:=((if sym then pi else twopi)/theta[count])
        ↑3×eps×2.0;
INTEGRATE:  count:=0; endpt:=0;
      paralint(if sym then 4 else 7,integran,endpt,if
        sym then pi else twopi,eps,8.0/rad,a,11,record);
      if sym then
        begin
        features[15]:=(a[3]-pi)×2.0;  features[16]:=0;
        eps:=abs(a[2]);  xac:=a[4]/hp+0.25
        end  LINE 737,
        else
        begin
        features[15]:=a[3]-twopi;  features[16]:=a[7];
        eps:=sqrt(a[1]↑2+a[2]↑2);  cm:=-2.0×a[5];
        yac:=(cm-a[6])/pi;  xac:=a[4]/pi-0.75;
        end  LINE 743,  ;
      for k := 1 step 1 until 12 do features[k]:=0;
      size:=count;  features[7]:=tau×rad;
      end  LINE 747,  xac, yac and cm assigned;
      begin
      comment change axes to pass through leading edge;
```

```
        integer k;
        fail:=100;
        if sym then
          begin
          LE:=count;  c:=-x[LE];  az:=0;
          features[3]:=xac×100.0/c;
          for k := 1 step 1 until count do
            begin
            y[k]:=y[k]/c;  x[k]:=1.0+x[k]/c;  Dx[k]:=Dx[k]/c;
            Dy[k]:=Dy[k]/c
            end  LINE 760,
          end  LINE 761,
          else
          begin
          integer j;
          real k1,k2,t,xt,yt;
          j:=ifind(2,count,k,x[k]↑2+y[k]↑2>x[k-1]↑2+y[k-1]↑2);
          k2:=0;
ANGLE:    k1:=ki[j]-arctan(y[j]/x[j])-hp;
          if k1>0 then
            begin
            k2:=k1;  j:=j-1;  goto ANGLE
            end  LINE 772,  ;
          LE:=j+1;
          if k2=0 then k2:=ki[LE]-arctan(y[LE]/x[LE])-hp;
          rootfind(theta[j],k1,theta[LE],k2,t,dwbydz(2,
            data,i,t,F)-arctan(Hermite(t,j,LE,theta,y,
            Dy)/Hermite(t,j,LE,theta,x,Dx))-hp+0.5×t,
            eps×(theta[LE]-theta[j])/(k2-k1),EXIT);
          az:=hp-dwbydz(2,data,i,t,F)-0.5×t;  cs:=cos(az);
          c:=-Hermite(t,j,LE,theta,x,Dx)/cs;  sn:=sin(az)/c;
          cs:=cs/c;  j:=-1;  size:=count:=count+1;
          for k := count step -1 until 1 do
            if k=LE then j:=0 else
            begin
            xt:=x[k+j];  yt:=y[k+j];  x[k]:=1.0+xt×cs-yt×sn;
            y[k]:=yt×cs+xt×sn;  ki[k]:=ki[k+j]+az;  xt:=Dx[k+j];
            yt:=Dy[k+j];  Dx[k]:=xt×cs-yt×sn;
            Dy[k]:=yt×cs+xt×sn;
            if j≠0 then
              begin
              theta[k]:=theta[k+j];  qs[k]:=qs[k+j];
              end  LINE 792,
            end  LINE 793,  ;
          features[3]:=(1.0+xac×cs-yac×sn)×100.0;
          features[4]:=(yac×cs+xac×sn)×100.0;
          features[5]:=cm/(c×c);  features[1]:=az×rad;
          x[LE]:=y[LE]:=Dx[LE]:=0;  ki[LE]:=hp;  theta[LE]:=t;
          fail:=200;  qs[LE]:=exp(dwbydz(1,data,i,t,F));
          Dy[LE]:=-sin(0.5×t)/qs[LE]/c
```

```
  end  LINE 800,   ;
features[2]:=twopi/c/rad;  features[12]:=eps:=eps/c;
comment variables LE,c,cs = cos(alphaz)/c, and
  sn=sin(alphaz)/c have been assigned with c
  equal to a quarter of the value defined in
  the Appendix 2;
end  LINE 806,   ;
begin
comment find geometric features-thickness at
  0.05c, and position and size of max thickness
  and camber;
real x0,t,t5,b5;
real procedure rfind (a,b,x,eps,bool);
  value a,b,eps;  real a,b,x,eps;  boolean bool;
  comment supposing bool is a function of x
    such that it is true for a≤x≤y, say, and
    false for y≤x≤b,this function designator is
    assigned the value of y correct to within
    an accuracy eps;
  comment actual parameter corresponding to x
    must be a variable;
  begin
  real t;
  b:=b-a;  eps:=abs(eps)×0.5;
  for b := b×0.5 while b>eps do
    begin
    t:=x:=a+b;
    if bool then a:=t;
    end  LINE 828,   ;
  rfind:=a
  end  LINE 830,  rfind;
real procedure grad(cam,x0);  value cam,x0;
  boolean cam;  real x0;
  comment uses non local i, array data,
    procedures TX and dwbydz, and exits to
    label F in event of failure;
  begin
  integer k;
  real kt,t;
  TX(true,x0,t,k);  kt:=dwbydz(2,data,i,t,F)+0.5×t;
  if sym then
      grad:=if cam then 0 else kt+kt
    else
    begin
    TX(false,x0,t,k);
    grad:=(if cam then dwbydz(2,data,i,t,F)
      +0.5×t-pi+az+az else pi-0.5×t-dwbydz(2,
      data,i,t,F))+kt;
    end  LINE 848,   ;
  end  LINE 849,  grad;
```

```
real procedure ord(top,x0);  value top,x0;
  boolean top;  real x0;
  comment uses non local arrays theta,y,Dy and
    procedures TX and Hermite;
  begin
  integer k;
  real t;
  TX(top,x0,t,k);  ord:=Hermite(t,k,k+1,theta,y,Dy);
  end  LINE 858,  ord;
fail:=300;  x0:=rfind(0,1.0,x0,eps,grad(false,x0)>0);
features[8]:=x0×100.0;
if sym then
  begin
  t:=ord(true,x0);  features[6]:=ord(true,0.05)/t;
  features[9]:=200.0×t
  end  LINE 865,
  else
  begin
  t:=ord(true,x0)-ord(false,x0);  t5:=ord(true,0.05);
  b5:=ord(false,0.05);  features[6]:=(t5-b5)/t;
  features[9]:=100.0×t;
    begin
    integer k,j;
    real m;
    boolean up;
    up:=true;  m:=0;
    for k := count-1 step -1 until 2 do
      if abs(k-LE)<1.5 then up:=false else
      begin
      t:=ord(up,x[k])+y[k];
      if abs(t)>abs(m) then
        begin
        m:=t;  j:=k
        end  LINE 883,
      end  LINE 884,  ;
    TX(j>LE,x[j],t,k);
    up:=dwbydz(2,data,i,t,F)+0.5×t+az+ki[j]>pi eqv m>0;
    x0:=rfind(x[if up then j else if j>LE then
      k+1 else k],x[if not up then j else if
      j>LE then k else k+1],x0,eps,grad(true,x0)>0 eqv
      m>0)
    end  LINE 891,  locating max camber;
  features[11]:=(ord(true,x0)+ord(false,x0))×50.0;
  features[10]:=x0×100.0;
  end  LINE 894,
end  LINE 895,  ;
begin
comment interogate dwbydz by entry=-1, and
  interogate <fix>, then convert theta to degrees;
integer k,xk;
```

```
real t;
fail:=400;
for t := dwbydz(-1,data,i,t,F) while t>0 do
  begin
  k:=ifind(1,count,k,theta[k]<t);
  if k=count then k:=k-1;
  t:=Hermite(t,k,k+1,theta,x,Dx)
  end  LINE 907,  returning to dwbydz with abscissae;
xk:=fix;
if xk>0 then
  begin
  comment replace abscissae by tabulated values
    in <xval>;
  integer n,m,j,newcount,NCP1;
  real bte,gle;
  if xval[1]<x[1] then n:=1 else
    begin
    n:=2;  bte:=ki[count];
    end  LINE 918,  ;
  for j := 2 step 1 until xk do
    if xval[j]>xval[j-1] or xval[j]<0 or
    xval[j]>1.0 then
    begin
    fail:=600+j;  goto FX;
    end  LINE 924,  ;
  if xval[xk]>0 then m:=xk else
    begin
    m:=xk-1;  gle:=qs[LE];
    end  LINE 928,  ;
  newcount:=if sym then xk else xk+m;
  if newcount>arraylim then
    begin
    fail:=600;  goto FX;
    end  LINE 933,  ;
  NCP1:=newcount+1;  fail:=500;
  for j := n step 1 until m do
    begin
    TX(true,xval[j],ki[j],k);
    if not sym then TX(false,xval[j],ki[NCP1-j],k)
    end  LINE 939,  ki now contains new theta values;
  for j := n step 1 until m do
    begin
    t:=ki[j];  k:=ifind(1,LE,k,theta[k]<t);
    Dx[j]:=Hermite(t,k,k+1,theta,y,Dy);
    if not sym then
      begin
      t:=ki[NCP1-j];  k:=ifind(LE,count,k,theta[k]<t);
      Dx[NCP1-j]:=Hermite(t,k,k+1,theta,y,Dy);
      end  LINE 948,
    end  LINE 949,  ;
```

```
        if not sym and n≠1 then
          begin
          x[newcount]:=x[count];  y[newcount]:=y[count];
          theta[newcount]:=twopi;  qs[newcount]:=qs[count];
          ki[newcount]:=bte
          end  LINE 955,  ;
        if m≠xk then
          begin
          if sym then
            begin
            x[xk]:=x[LE];  y[xk]:=y[LE];
            end  LINE 961,
            else x[xk]:=y[xk]:=0;
          theta[xk]:=theta[LE];  qs[xk]:=gle;  ki[xk]:=hp
          end  LINE 964,  ;
        size:=count:=newcount;
          begin
          procedure COPY (P);  procedure P;
            begin
            for j := n step 1 until m do P(j);
            if not sym then
              for j := n step 1 until m do P(NCP1-j)
            end  LINE 972,  COPY;
          procedure P(k);  value k;  integer k;
            begin
            x[k]:=xval[j];  y[k]:=Dx[k];  theta[k]:=t:=ki[k];
            qs[k]:=exp(dwbydz(1,data,i,t,F));
            ki[k]:=dwbydz(2,data,i,t,F)+0.5×t+az;
            end  LINE 978,  ;
          COPY (P);
          end  LINE 980,
        end  LINE 981,  if fix not zero;
      for k := 1 step 1 until count do theta[k]:=theta[k]×rad;
      goto OUT;
      end  LINE 984,  ;
 F:  fail:=fail+1;
FX:  for i := 1 step 1 until count do theta[i]:=theta[i]×rad;
     goto EXIT;
OUT:
     end  LINE 989,  RM2112;
```

3. *Index to Array Elements 'features' of RM2112.*

Subscript value.

1	Zero-lift incidence (degrees)
2	Lift-curve slope (per degree)
3	x-co-ordinate of aerodynamic centre (% chord from leading edge)
4	y-co-ordinate of aerodynamic centre (% chord above chordline)
5	C_{M_0}
6	thickness at 5% of chord from leading edge/maximum thickness
7	trailing-edge angle (degrees)
8	maximum thickness position (% chord from leading edge)
9	maximum thickness (% chord)
10	maximum camber position (% chord from leading edge)
11	maximum camber (% chord)
12	error in trailing-edge closure condition (fraction of chord)
13	number of re-starts with increased value of *eps.*
14	value of *eps*, possibly increased on restart due to storage limitation
15	error in integral of equation (5), Appendix II
16	integral of χ with respect to θ from 0 to 360°.

4. *Index to Failure Exits of RM2112.*

Indicated below is the state of the information assigned to the actual parameters corresponding to the formals

size, x, y, theta, ki, qs, features

when control is passed to the actual label corresponding to *EXIT*, and the reason for failure, as determined by the actual value corresponding to the formal parameter *fail.*

This latter is an integer equal (say) to $100 \times n+m$, (where $0 \leqslant m < 100$). The failures with $m \neq 0$ and $n < 6$ are these associated with failure number m in the procedure *dwbydz*, and so the cause depends on the procedure body supplied. None occurs in the version of *dwbydz* herewith, except at entry 0 (when $n = 0$ and $m \neq 0$). With the exception of the trivial failure $n = m = 0$ (due to a non-positive value of *eps* on entry), the failures with $m = 0$ all originate from the body of *RM2112*, and in particular from its local procedure, *rootfind.* Such failures should not occur, but where they cannot be ascribed to machine error, the most likely cause is a small irregularity in the shape of the aerofoil in the region where interpolation of the co-ordinates is being attempted (which involves the iterative solution of a transcendental equation). A remedy will usually be found in altering the value of *eps.*

Failures (with $m \neq 0$) in dwbydz.

$n = 0$. Failure during initialising entry or in formation of wing co-ordinates. All array values undefined.

$n = 1$. Failure during determination of co-ordinates of leading-edge. State of arrays as for $n = 1$, $m = 0$ (*see* below).

$n = 2$. Failure during determination of the velocity at the leading-edge. The arrays *x*, *y*, *theta*, *ki* and *qs* and the variable *size*, have now their values as at a normal exit with *fix* $= 0$, except that *qs* and *ki* are incorrect at $x = y = 0$.

$n = 3$. Failure at entry 2 during evaluation of *fea$^e\lambda$res*. State of arrays as for $n = 3, m = 0$ (*see* below).

$n = 4$. Failure at entry -1. State of arrays as at a normal exit with *fix* $= 0$.

$n = 5$. Failure during determination of *qs* or *ki* values at new abscissae, which are consequently undefined. All other arrays and variable *size*, as at normal exit (with abscissae values as prescribed by *xval*).

Failures (with $m = 0$) in RM2112.

$n = 0$. non-positive *eps* or inadequate entry value of *size*.

$n = 1$. Failure during determination of co-ordinates of leading edge. The arrays *x*, *y*, *theta*, *ki* and *qs* have been assigned, as well as the variable *size*, but the co-ordinate system is that referred to the trailing-edge as origin, with the *x*-axis parallel to the free stream direction for zero lift.

$n = 3$. Failure during formation of array *features*, which has unassigned values appearing as zeros. Other arrays have values as for normal exit with *fix* $= 0$.

$n = 5$. Failure in locating ordinates for values of array *xval*. Values of *ki* are rubbish, but all others are as at a normal exit with *fix* $= 0$.

Failure $n \geqslant 6$. Interpret *m* as the value of *fail* minus 600. Then this failure is caused because the value of *xval* $[m]$ is unacceptable (either *xval* $[m] >$ *xval* $[m-1]$ or *xval* $[m] < 0$ or *xval* $[m] > 1$). State of arrays as at a normal exit with *fix* $= 0$. Failure $n = 6$, $m = 0$ implies that the number of elements of *xval*, prescribed by the value of *fix*, is too large for the results to be accommodated in the arrays *x*, *y*, *theta*, etc.

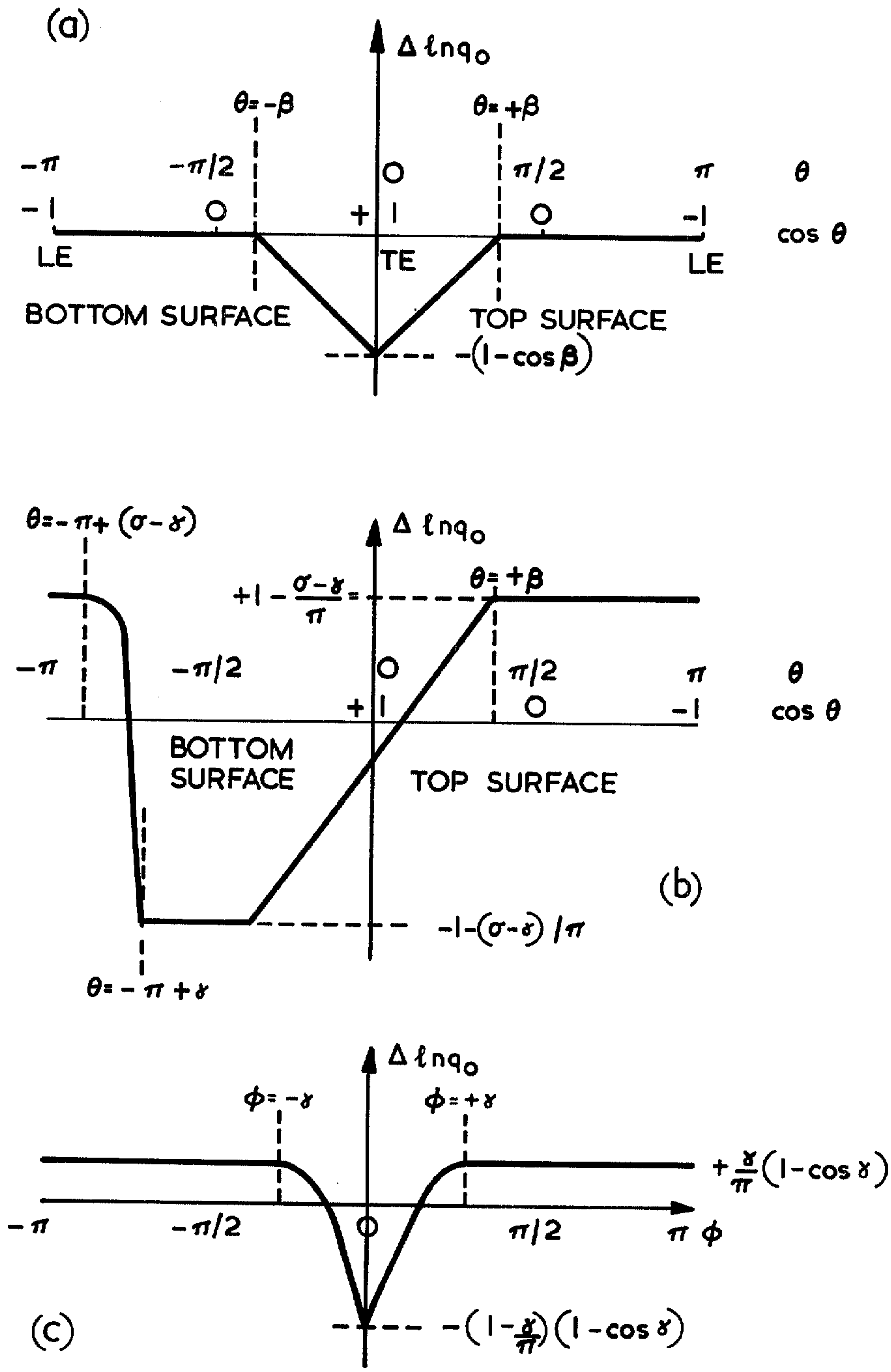

FIG. 1. Diagramatic representations of incremental velocity distributions.

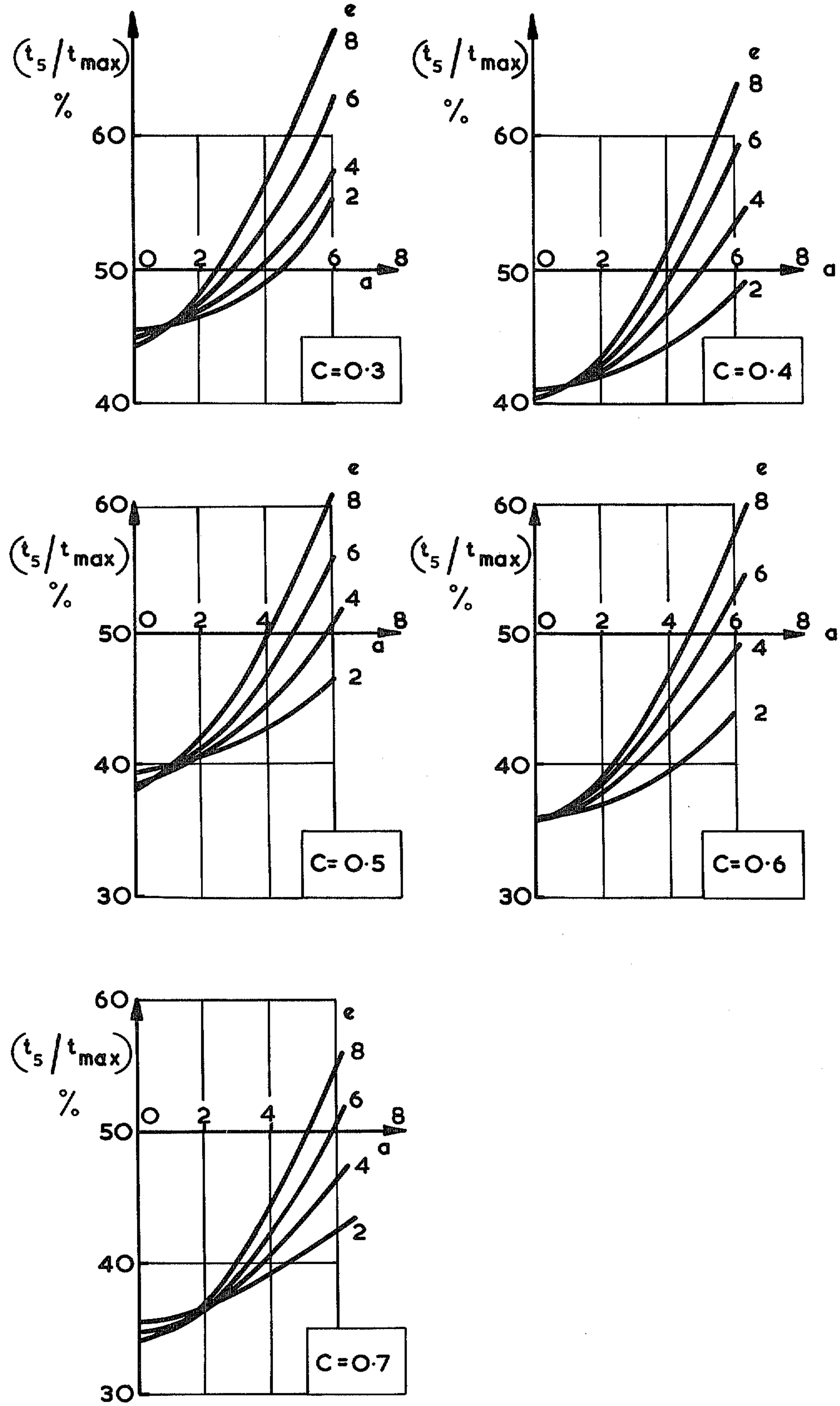

FIG. 2. Effect of aerofoil parameters on leading-edge thickness. (Aerofoil identifier *GU* **a3-c0e**).

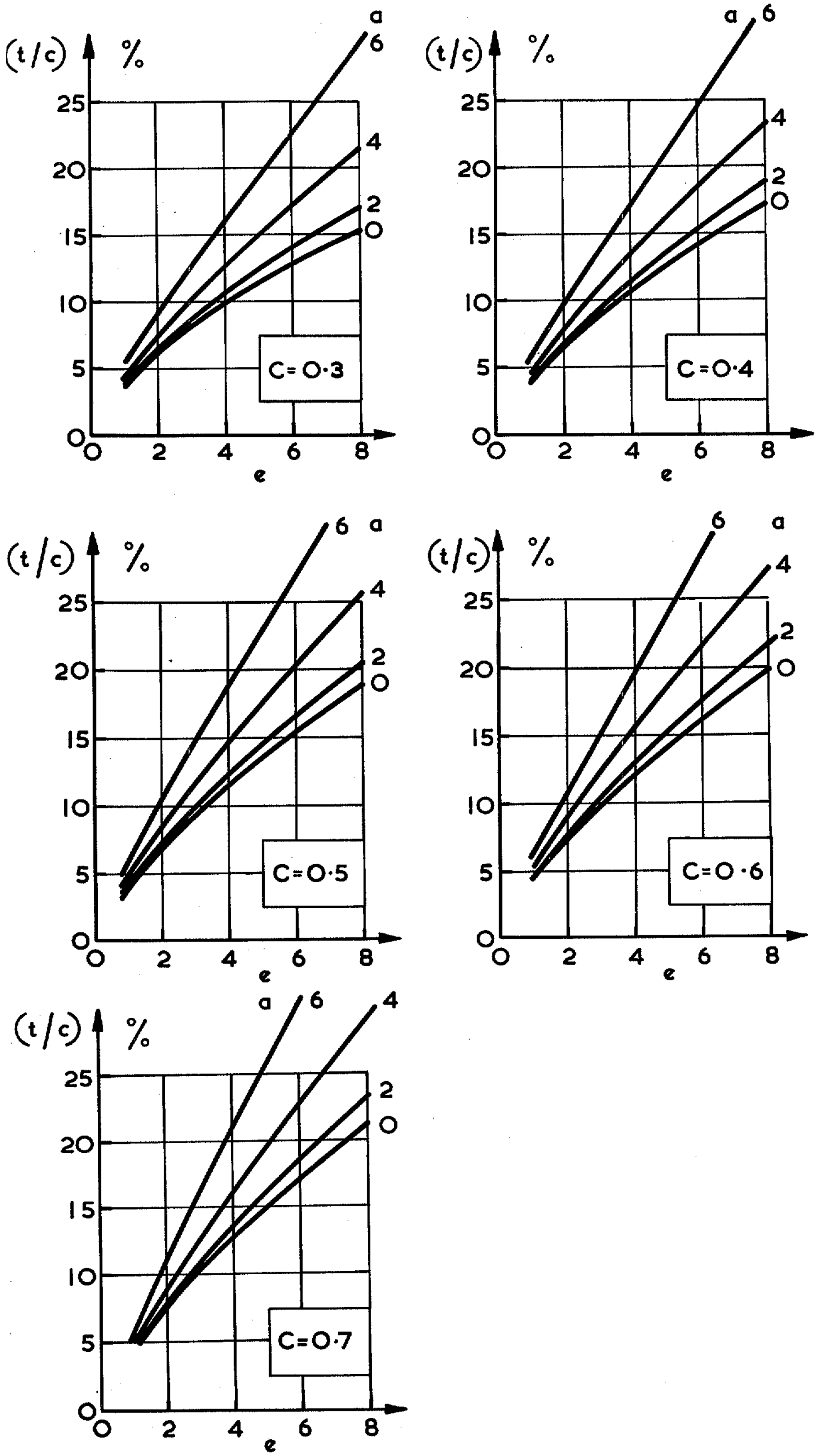

FIG. 3. Effect of aerofoil parameters on maximum thickness.
(Aerofoil identifier *GU* **a3-c0e**)

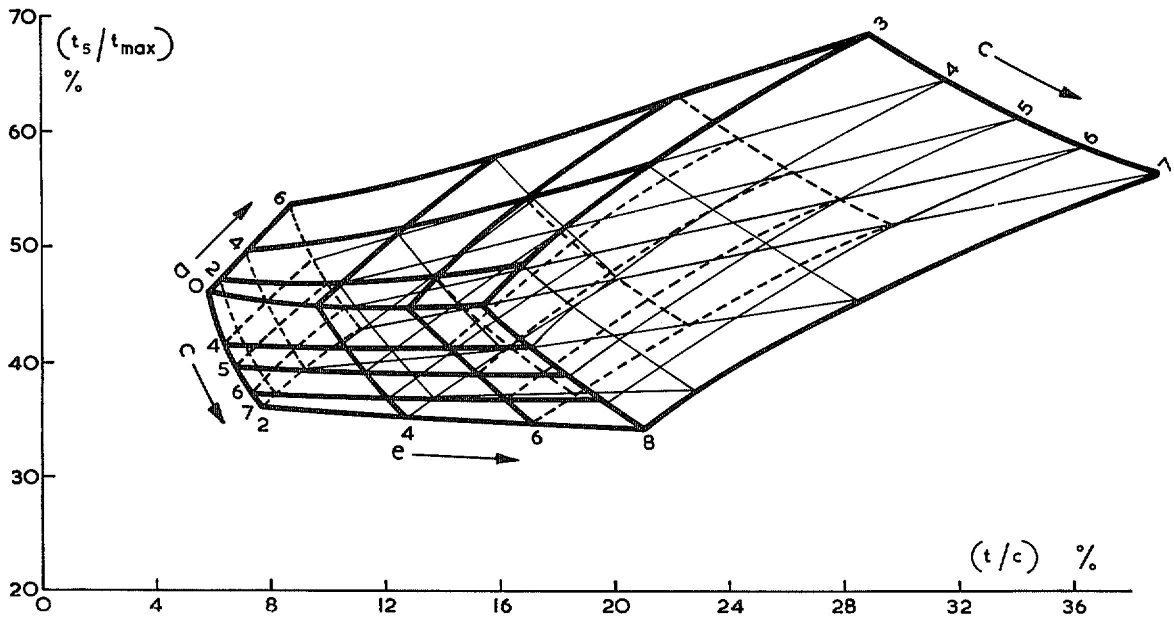

FIG. 4. Effect of aerofoil parameters on maximum and leading-edge thickness. (Aerofoil identifier *GU* a3-c0e)

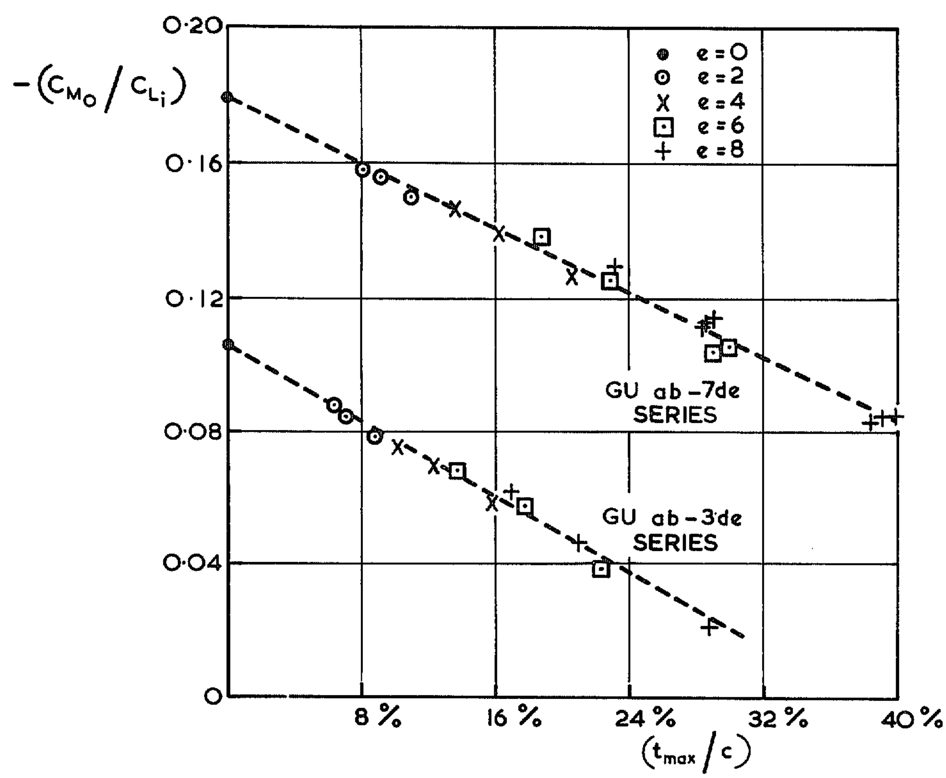

FIG. 5. Correlation of zero-lift pitching moment, variation with thickness/chord ratio.

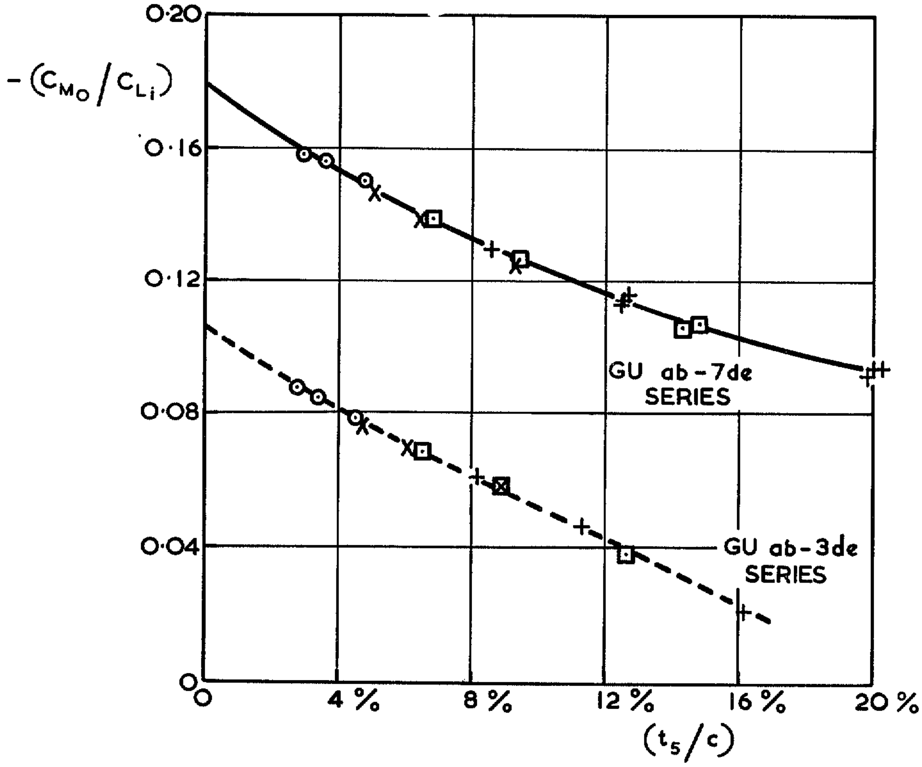

FIG. 6. Correlation of zero-lift pitching moment variation with leading edge thickness.

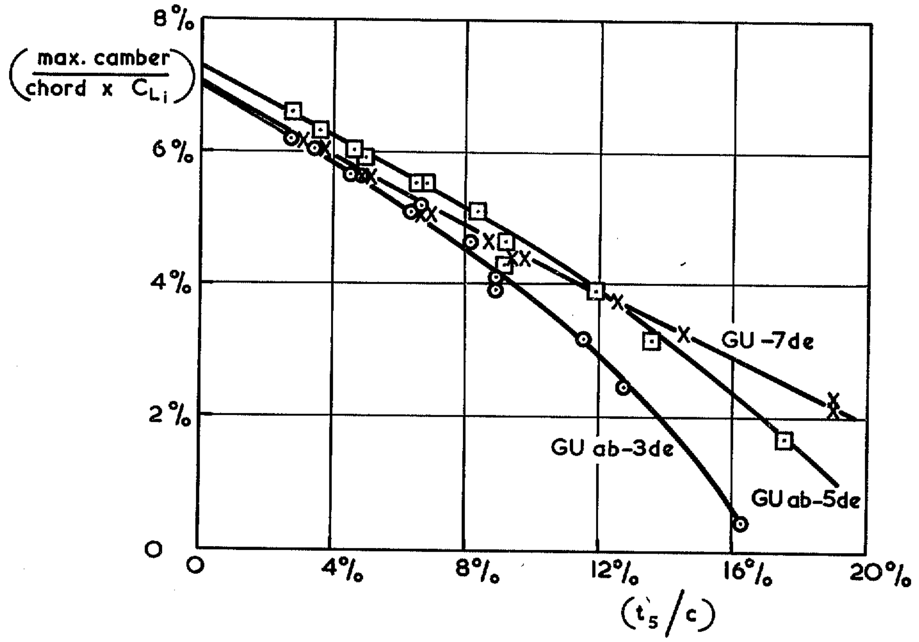

FIG. 7. Correlation of maximum geometric camber variation with leading-edge thickness.

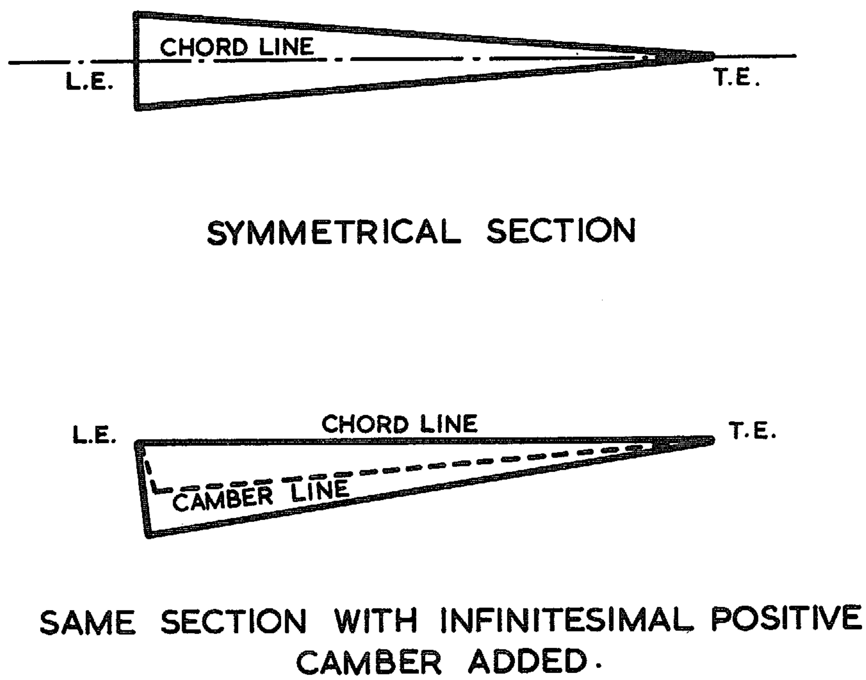

FIG. 8. Illustrating anomalous negative camber due to a blunt leading edge.

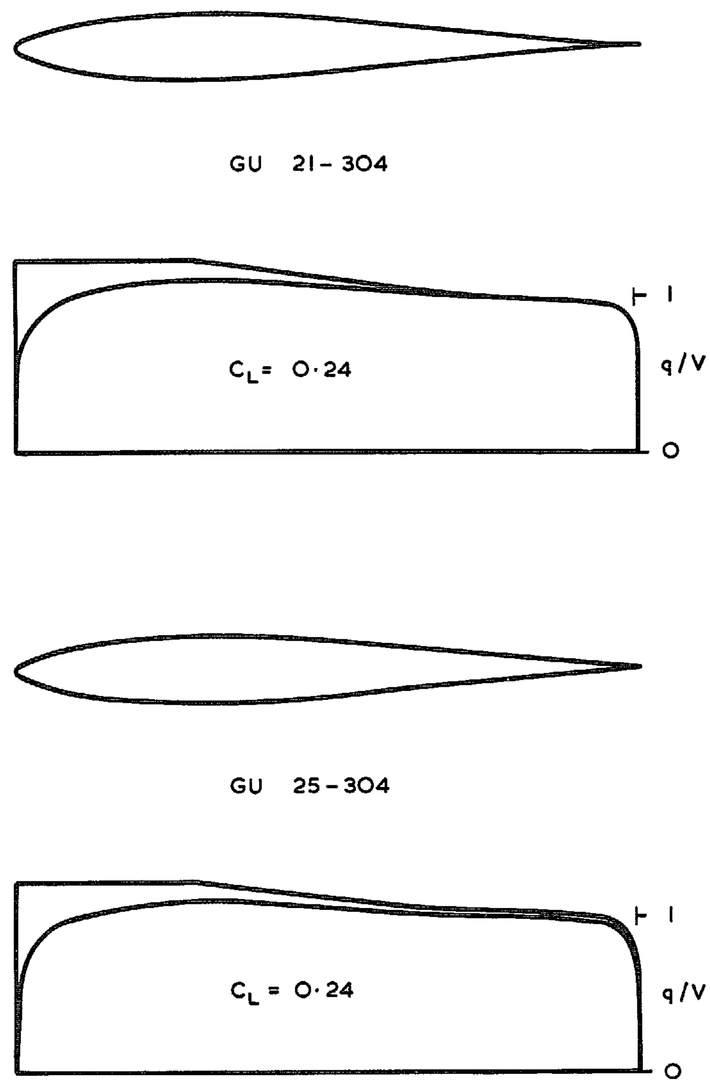

FIG. 9. Effect of variation of the trailing edge angle.

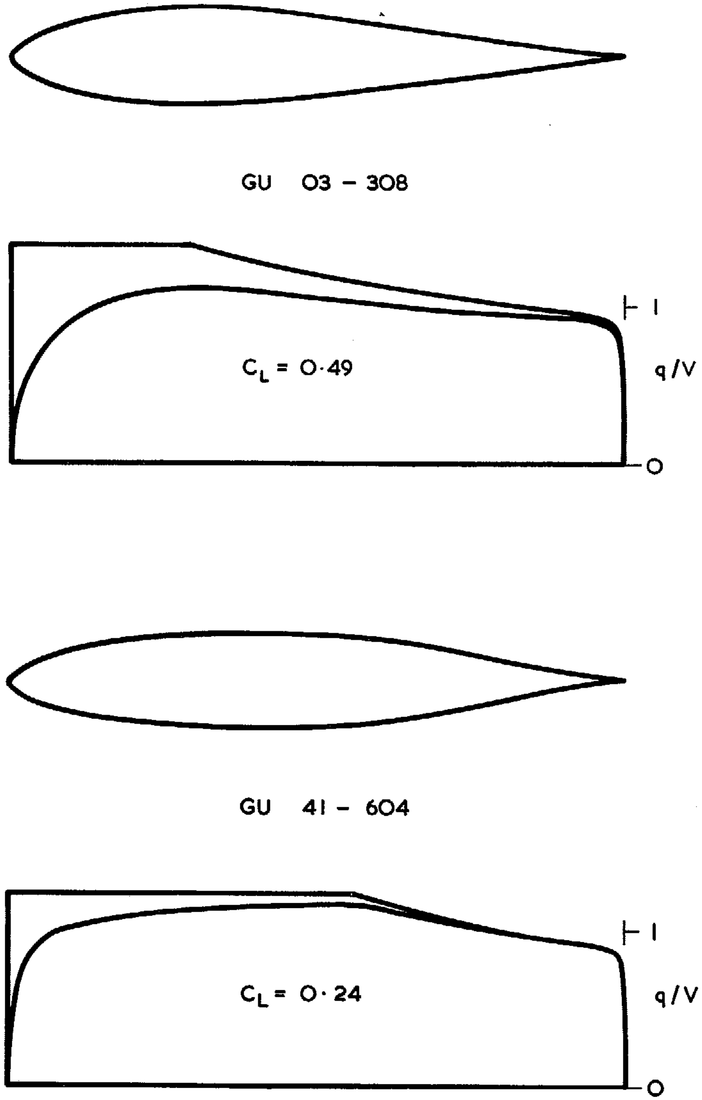

FIG. 10. Low drag range of incidence traded against increased extent of favourable pressure gradient.

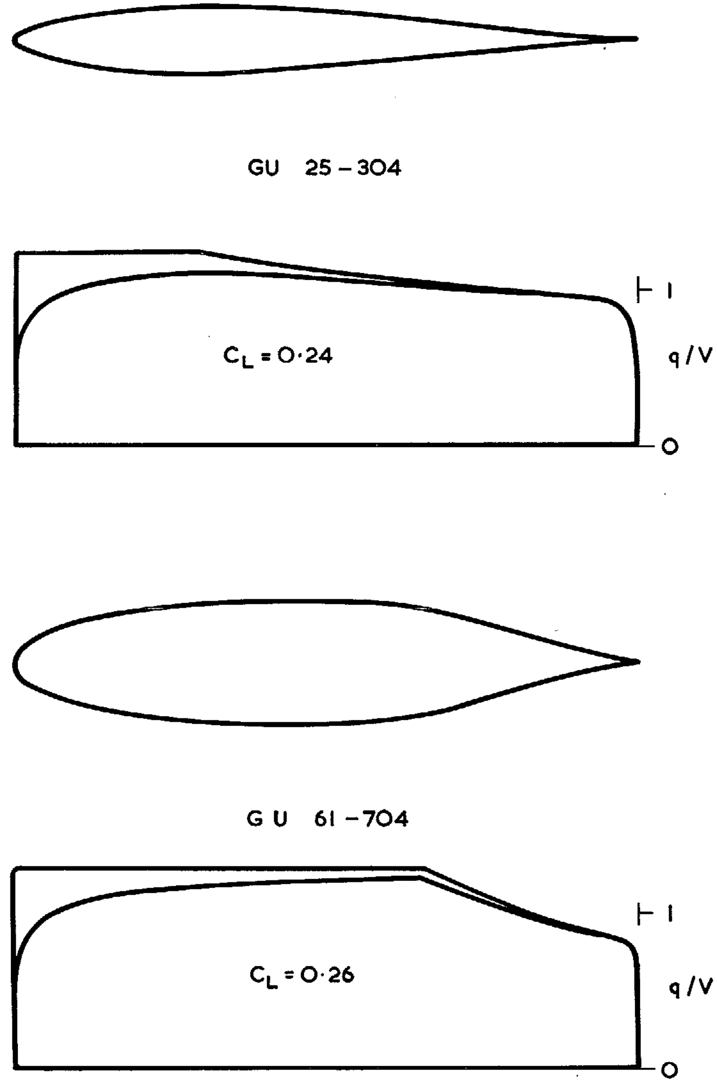

FIG. 11. Increase of thickness to extend the region of favourable pressure gradient.

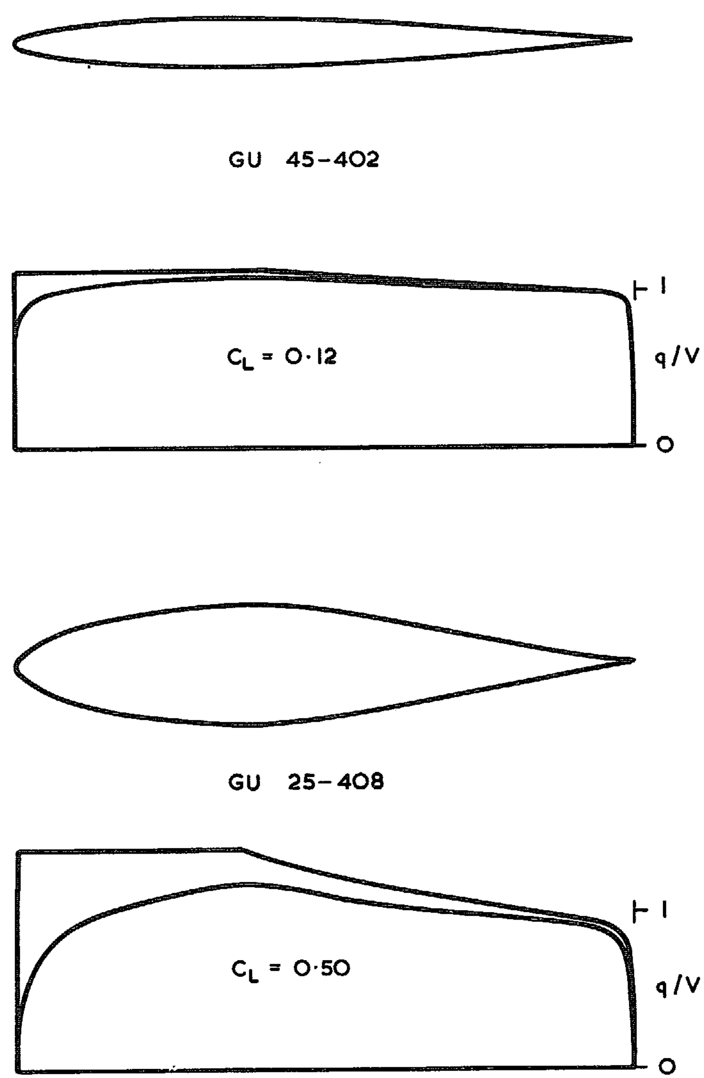

FIG. 12. Increase of thickness to increase the low drag range of incidence.

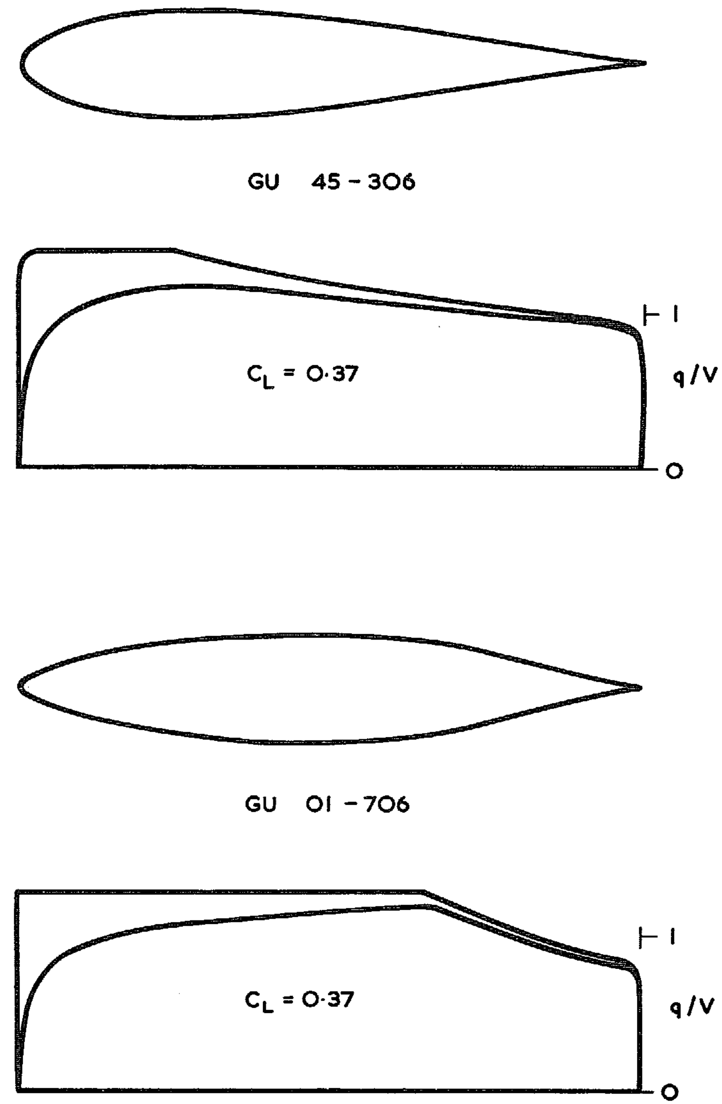

FIG. 13. Reduction of leading edge thickness to extend the region of favourable pressure gradient.

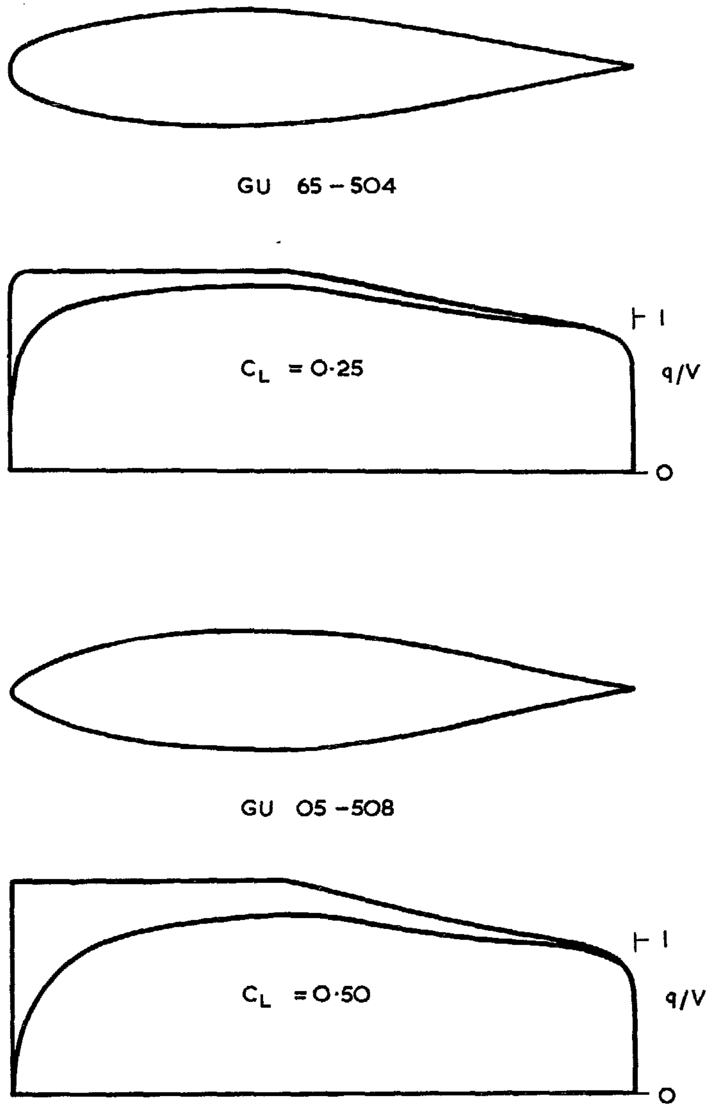

FIG. 14. Reduction of leading edge thickness to increase the low drag range of incidence.

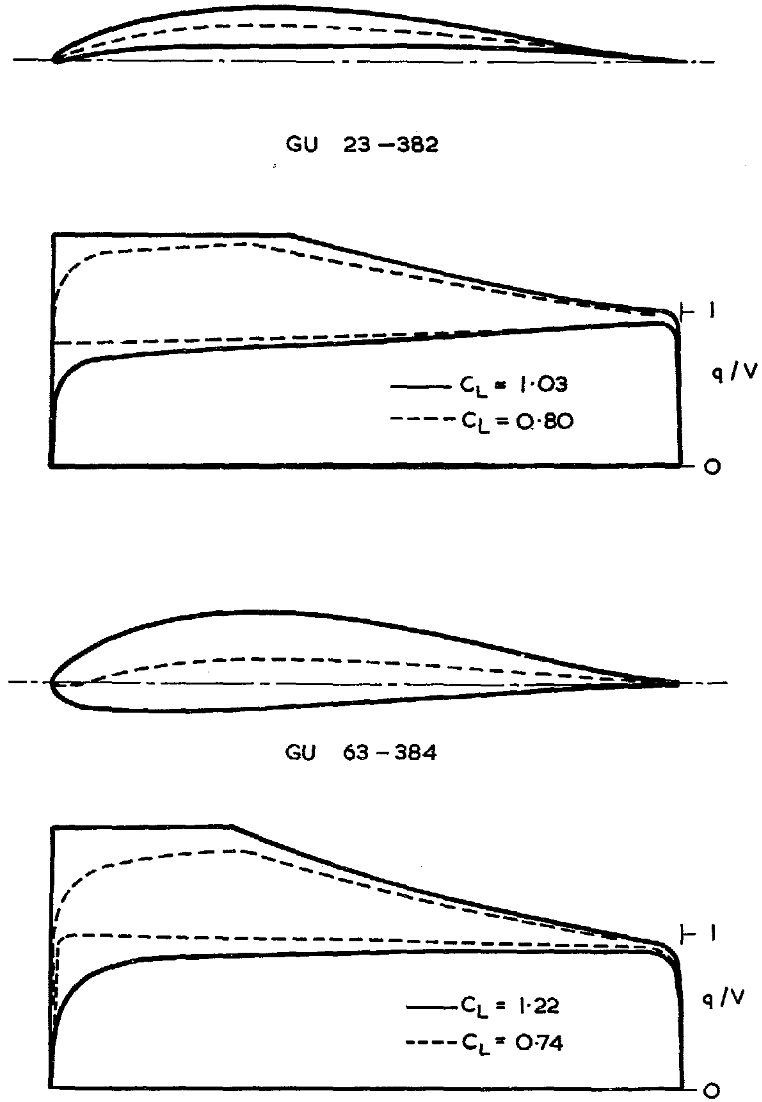

FIG. 15. The effect of thickness on camber. (*GU* a3-38e *series*)

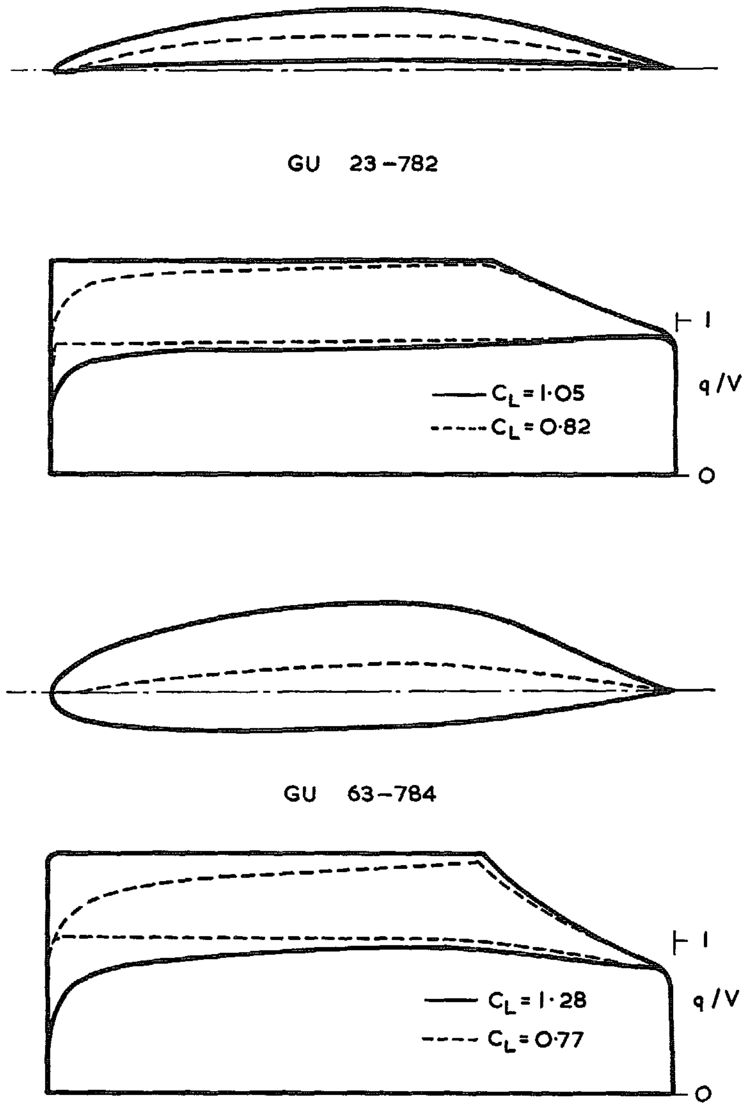

FIG. 16. The effect of thickness upon camber. (*GU* a3-78e *series*)

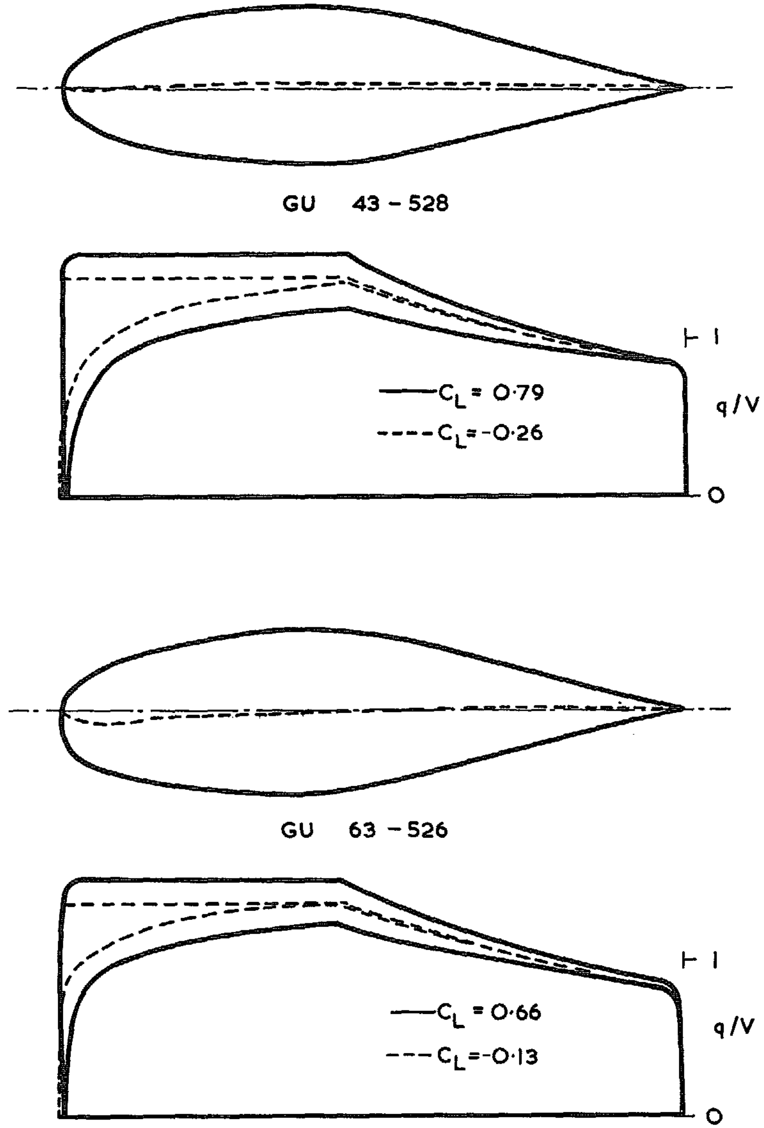

FIG. 17. Anomalous negative camber on thick nosed sections.

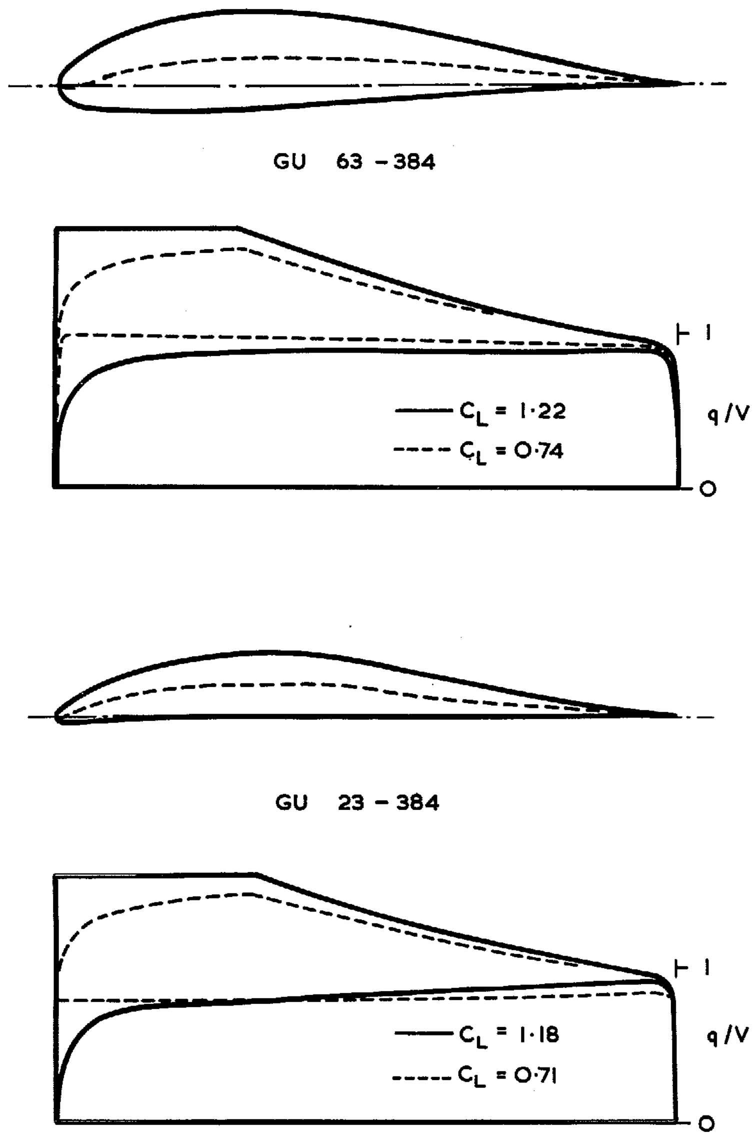

FIG. 18. Full chord bottom surface favourable pressure gradient due to reduction in thickness by parameter **a**.

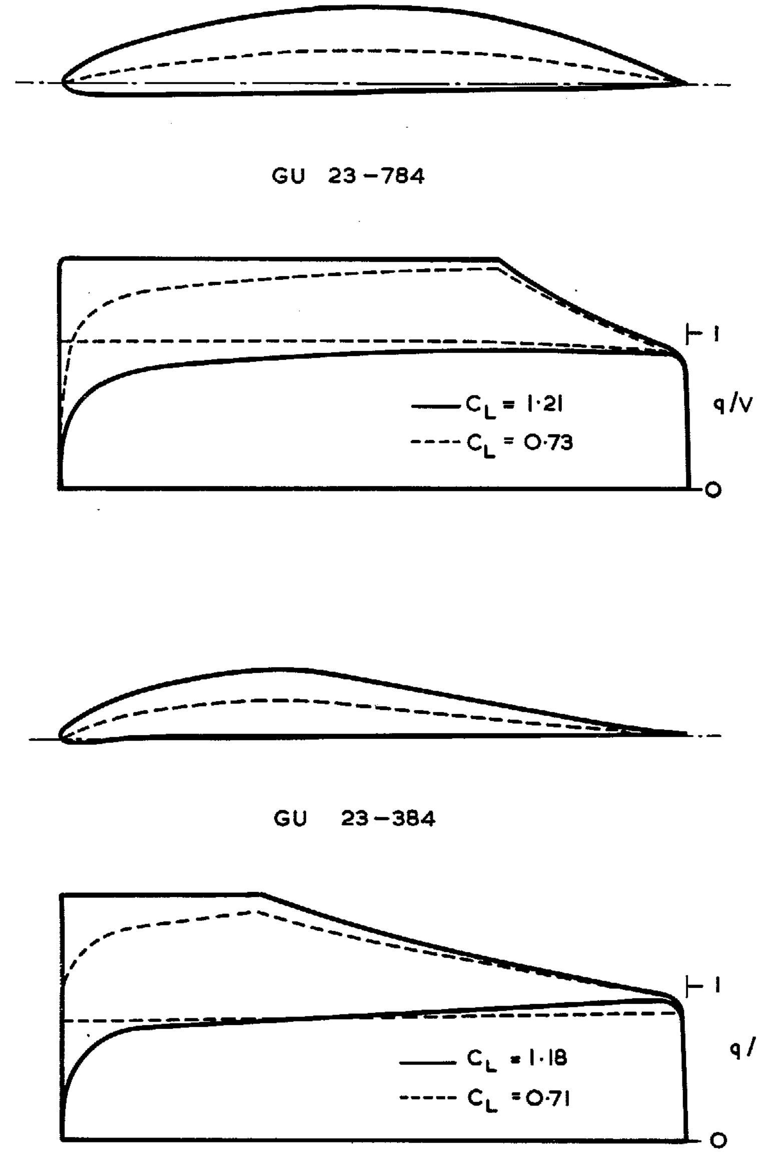

FIG. 19. Full chord bottom surface favourable pressure gradient due to decrease of top surface extent (parameter **c**).

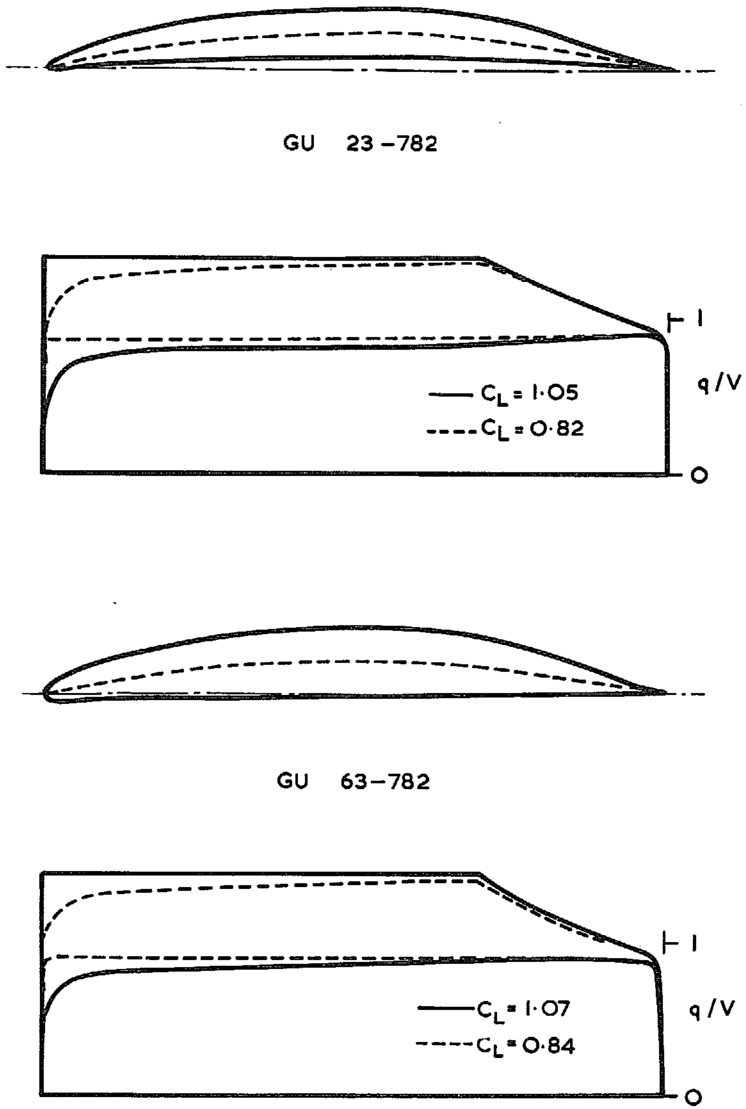

FIG. 20. Full chord bottom surface favourable pressure gradient due to reduction of low drag range (parameter e).

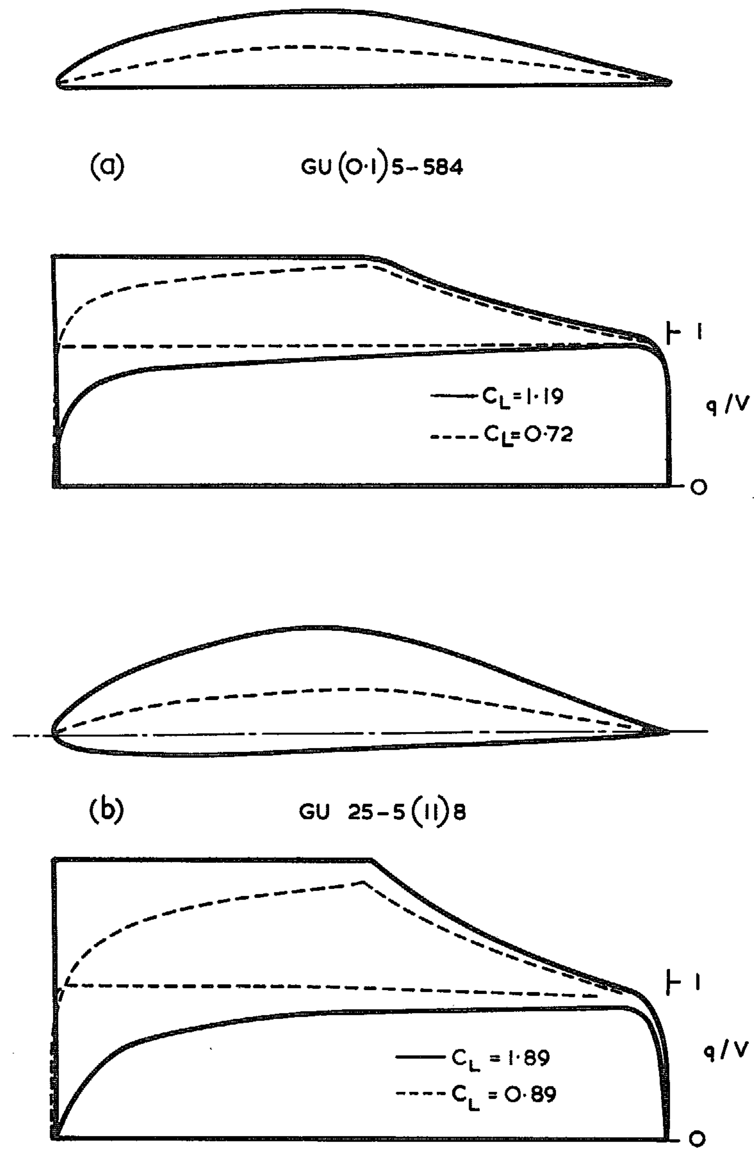

FIG. 21.

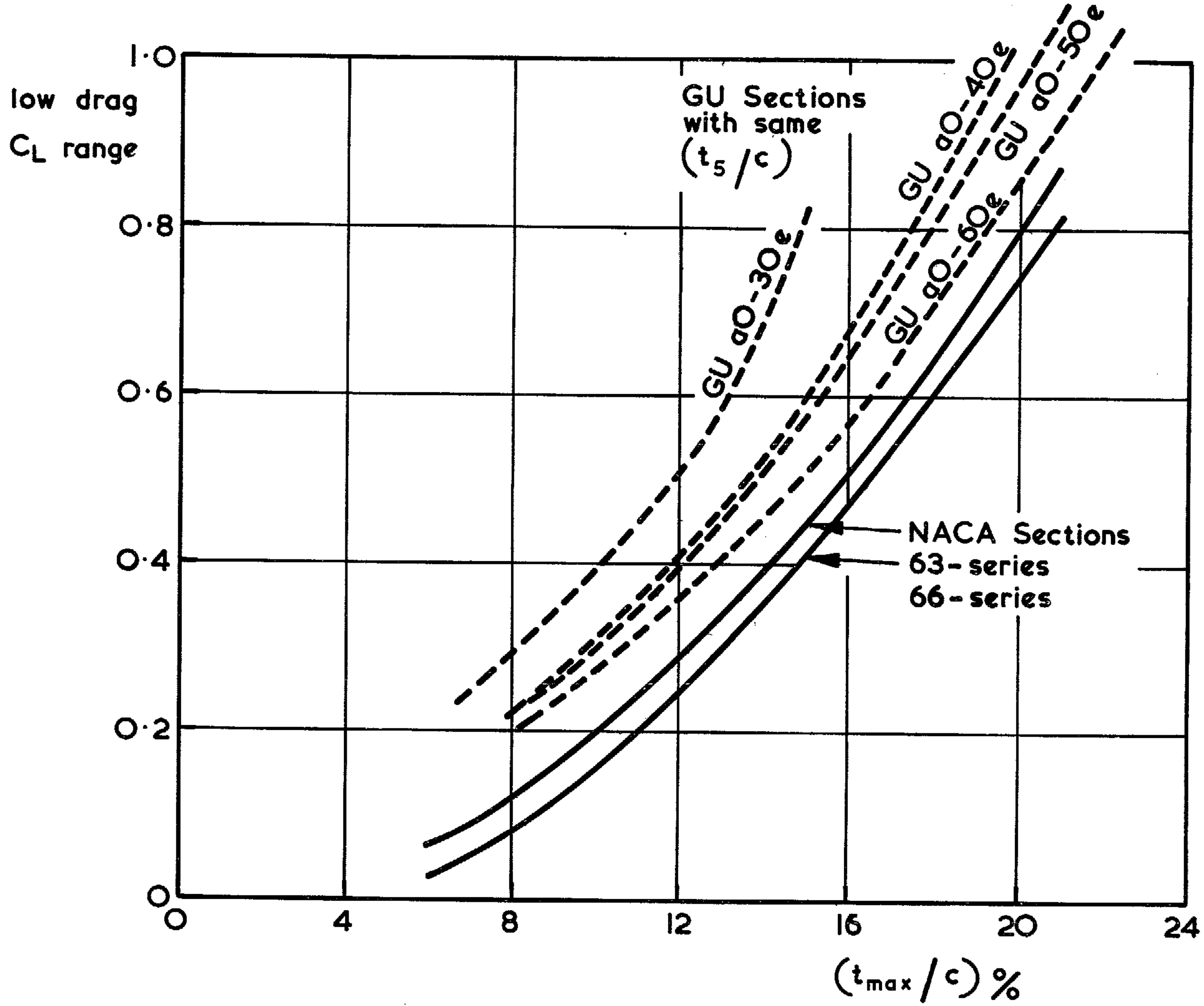

FIG. 22. Comparison of low drag range of NACA 6-series aerofoils and comparable sections of the *GU* series.

Printed in Wales for Her Majesty's Stationery Office by Allens Printers (Wales) Limited.
Dd. 501372 K.5

Published by
HER MAJESTY'S STATIONERY OFFICE

To be purchased from
49 High Holborn, London WC1V 6HB
13a Castle Street, Edinburgh EH2 3AR
109 St Mary Street, Cardiff CF1 1JW
Brazennose Street, Manchester M60 8AS
50 Fairfax Street, Bristol BS1 3DE
258 Broad Street, Birmingham B1 2HE
7 Linenhall Street, Belfast BT2 8AY
or through booksellers

R. & M. No. 3618
SBN 11 470253 5*